

**EXPRESSION ANALYSIS OF THE NILE TILAPIA FERTILITY GENES AND  
IMPROVEMENT OF MEDAKA STEM CELL CULTURE**

**NARAYANI BHAT**

(M.Sc. University of Mysore, India)

**A THESIS SUBMITTED**

**FOR THE DEGREE OF DOCTOR OF PHILOSOPHY**

**DEPARTMENT OF BIOLOGICAL SCIENCES**

**NATIONAL UNIVERSITY OF SINGAPORE**

**2014**

## ***DECLARATION***

I hereby declare that this thesis is my original work and it has been entirely written by me.

I have duly acknowledged all the sources of information which have been used in the thesis.

This thesis has not been submitted for any degree in any university previously.

A handwritten signature in black ink, appearing to read 'Narayani Bhat', is written over a horizontal line.

---

**Narayani Bhat**

27 November 2014

## *Acknowledgements*

I would like to convey my gratitude to my supervisor A/P Hong Yunhan for giving the opportunity to carry out research under his guidance, for his encouragement, for sharing invaluable knowledge and technical expertise. I extend my thanks to Prof. Meisheng Yi for his mentorship in cell culture aspects.

I would also like to thank Madam Deng Jiaorong and Mr. Zeng Qinghua for medaka breeding and maintenance. I thank Mok Meng Huang, Michelle for the help in FACS.

My thanks go to my labmates and seniors for their kind help and the happy environment they brought to the lab.

I would like to thank the National University of Singapore for the scholarship and Department of Biological Sciences for facilities and safe working atmosphere.

Finally, I would like to thank my loving parents, friends for their continuous moral support and also like to express my thanks to my beloved husband who has always been my strength.

### ***Publications***

1. **Bhat, N** and Hong, Y. Cloning and expression of *boule* and *dazl* in the Nile tilapia (*Oreochromis niloticus*). *Gene* 540 (2), 140-145 (2014)
2. Li, Z., **Bhat, N.**, Dwarakanath, M., Wang, D., Hong, N., Yi, M., Ge, R. and Hong, Y. Medaka cleavage embryos are capable of generating ES-like cell cultures, *Int. J. Biol. Sci.* 7(4), 418-425 (2011)
3. Wang, D., Dwarakanath, M., Wang, T., **Bhat, N.**, Hong, N., Li, Z., Wang, L., Yan, Y., Liu, R. And Hong, Y. Identification of Pluripotency Genes in the Fish Medaka, *Int. J. Biol. Sci.* 7(4), 440-451 (2011)

### ***Conferences***

1. ***“6<sup>th</sup> Science Conclave” IIT Allahabad, India 2013***

Participant from ASIAN group of researchers from Biological Science

2. ***“16<sup>th</sup> Biological Sciences Graduate Congress” Bangkok, Thailand 2012***

Oral presentation: Early Embryonic Primary cultures to study cell fate decision in vitro in Medaka: (Silver medal award for the presentation)

3. ***“International conference on Structural Biology and Functional Genomics” Singapore 2011***

Poster Title: Medaka Cleavage Embryos are capable of generating ES-like cell cultures

**Table of contents**

Title	Page
Declaration	i
Acknowledgements	ii
Publications	iii
Conferences	iii
Table of contents	iv-vi
List of figures and tables	vi-viii
Abbreviations	viii-ix
<b>Summary</b>	1-2
<b>Background:</b> Germ cell specification and gametogenesis	3-6
<b>1 Cloning and expression of <i>boule</i> and <i>dazl</i> in the Nile tilapia</b>	
<b>1.1 Introduction</b>	
1.1.1 History of DAZ family genes	6-7
1.1.2 Species and stage-specific expression of DAZ family genes	7-8
1.1.3 Germ cell-specific gene <i>vasa</i>	8
1.1.4 The Nile tilapia	8-9
1.1.5 Scope of the study	9-10
1.1.6 Limitations	10
<b>1.2 Materials and methods</b>	
1.2.1 Fish and chemicals	10-11
1.2.2 RNA isolation and cDNA synthesis	11
1.2.3 Polymerase Chain Reaction (PCR)	12
1.2.4 Agarose gel electrophoresis	12
1.2.5 Purification of DNA from agarose gel	12-13
1.2.6 T-A Cloning	13
1.2.7 Preparation of competent cells	13-14
1.2.8 Transformation	14
1.2.9 Isolation of plasmid DNA	14-15
1.2.10 Sequence confirmation	15
1.2.11 Bioinformatics analysis	15
1.2.12 Restriction endonuclease (RE) digestion of DNA	15
1.2.13 Probe synthesis	15-16
1.2.14 Chemical <i>in situ</i> hybridization (CISH)	16-17
1.2.15 Fluorescent <i>in situ</i> hybridization (FISH)	17-18
1.2.16 Microscopy and image analysis	18
<b>1.3 Results</b>	
1.3.1 Identification of tilapia <i>boule</i> and <i>dazl</i> genes	18-19
1.3.2 Cloning of tilapia <i>vasa</i>	19-23
1.3.3 Gonad- specific expression	23-25
1.3.4 Expression of <i>vasa</i> RNA in gonads	
1.3.4a Expression of <i>vasa</i> RNA in ovary	24-25
1.3.4b Expression of <i>vasa</i> RNA in testis	25-26

1.3.5	Germ cell-specific expression of <i>boule</i> in ovary	26-27
1.3.6	Germ cell-specific expression of <i>dazl</i> in ovary	27-28
1.3.7	Germ cell-specific expression of <i>boule</i> in testis	29
1.3.8	Germ cell-specific expression of <i>dazl</i> in testis	29-31
1.3.9	Localization of <i>vasa</i> with <i>boule</i> and <i>dazl</i> in gonads	
1.3.9a	Localization of <i>vasa</i> and <i>boule</i>	31-33
1.3.9b	Localization of <i>vasa</i> and <i>dazl</i>	33-35
1.3.10	Localization of <i>boule</i> and <i>dazl</i> RNAs in ovary	35-36
1.3.11	Localization of <i>boule</i> and <i>dazl</i> RNAs in testis	36-37
<b>2</b>	<b>Improvement of medaka stem cell and PGC culture</b>	
<b>2.1</b>	<b>Introduction</b>	
2.1.1	Embryonic stem cells (ES)	38-39
2.1.2	Medaka haploid ES (hES) cells	40-41
2.1.3	Primordial germ cells (PGC) of medaka	42
2.1.4	Germ cell identity	42-44
2.1.5	Transcriptional and translational regulation in PGCs	44
2.1.6	Importance of PGCs	44-45
2.1.7	Challenges in PGC culture	45
2.1.8	Apoptosis inhibitors	45-48
2.1.9	Y-27632 and stem cell culture	48-49
2.1.10	Significance	49
2.1.11	Limitations of the study	49
<b>2.2</b>	<b>Materials and methods</b>	
2.2.1	Fish strains and maintenance	49-50
2.2.2	Medaka haploid stem cell line	50
2.2.3	Media components	50-51
2.2.3a	Preparation of medaka embryo extract	51
2.2.3b	Preparation of fish serum	51
2.2.3c	Preparation of cell culture plates	51-52
2.2.3d	Components of embryonic stem cell media	52
2.2.4	Cryopreservation of hES cells	53
2.2.5	Cell recovery	53
2.2.6	Cell count-trypan blue vital staining	53-54
2.2.7	Live-dead staining and Annexin V- FITC assay	54
2.2.8	Cell attachment upon recovery and proliferation assay	54
2.2.9	Clonal expansion	54-55
2.2.10	Embryo staging and preparation for primary culture	55
2.2.11	Blastomere cryopreservation with Y-27632	56-57
2.2.12	Media formulation for PGC culture	57
2.2.13	Primordial germ cell culture	57
2.2.14	Observation and imaging	58
2.2.15	Statistical analysis	58
<b>2.3</b>	<b>Results</b>	
2.3.1	Y-27632 enhances thawing efficiency of hES cells	58-59
2.3.2	Y-27632 reduces floating cells	59-60

2.3.3	Y-27632 retains normal cell morphology	60
2.3.4	Y-27632 enhances post recovery cell survival	60-62
2.3.5	Y-27632 improves cell attachment and proliferation	63-64
2.3.6	Y-27632 enhances clonal expansion	64
2.3.7	Y-27632 improves thaw-survival of medaka blastomeres	65
2.3.8	ESM2 maintains PGCs in culture	65-66
2.3.9	Midblastula cells are capable of survival and PGC formation	66
2.3.10	Y-27632 improves early attachment of blastomeres in culture	67-68
2.3.11	Apoptosis inhibitors improve PGC number in culture	68-73
2.3.12	Y-27632 is the most potent enhancer of PGC number	74
2.3.13	Y-27632, apoptosis inhibitors and growth factors in PGC culture	74-79
<b>3</b>	<b>Discussion</b>	79-89
<b>4</b>	<b>Conclusions</b>	90-91
	References	92-96
	Web pages	96
	Appendix	97-105

*List of figures and tables*

Number	Figure title	Page
1	Stages of gametogenesis	8
2	The Nile tilapia	9
3	Nucleotide and amino acid sequences of tilapia (A) <i>boule</i> (B) <i>dazl</i> (C) <i>vasa</i> .	20
4	Tilapia (A) <i>Boule</i> and (B) <i>Dazl</i> alignment with other organisms	21
5	Tilapia <i>Vasa</i> alignment with other organisms	22
6	Phylogenetic tree of <i>Boule</i> and <i>Dazl</i> proteins	23
7	RT-PCR of tilapia <i>boule</i> , <i>dazl</i> and <i>vasa</i>	24
8	Ovarian and testicular expression of <i>vasa</i> RNA	25
9	Localization of <i>boule</i> and <i>dazl</i> RNA in ovary by CISH	27
10	Localization of <i>boule</i> and <i>dazl</i> RNA in ovary by FISH	28
11	Localization of <i>boule</i> and <i>dazl</i> RNA in testis by CISH	29
12	Localization of <i>boule</i> and <i>dazl</i> RNA in testis by FISH	30
13	Expression of <i>vasa</i> and <i>boule</i> in ovary	32
14	Expression of <i>vasa</i> and <i>boule</i> in testis	33
15	Expression of <i>vasa</i> and <i>dazl</i> in ovary	34
16	Expression of <i>vasa</i> and <i>dazl</i> in testis	35
17	Expression of <i>boule</i> and <i>dazl</i> in ovary	36
18	Expression of <i>boule</i> and <i>dazl</i> in testis	37
19	Procedure of medaka hES cell derivation	41
20	Structure of Y-27632, ROCK inhibitor	46
21	Cryopreservation of medaka hES cells	52
22	Medaka maintenance in continuous water flow system	55
23	Flow chart illustration of PGC culture	57
24	Effect of Y-27632 on survival of cryopreserved medaka hES cells	59
25	Floating cell count at 5h post recovery	60

26	Annexin V-FITC assay soon after recovery	61
27	Annexin V-FITC assay at 72 h post recovery	62
28	Proliferation efficiency of medaka hES cells	64
29	Effect of Y-27632 on medaka blastomere cryopreservation	65
30	Blastomere attachment at 12 hpc in different treatment groups	68
31	Effect of Y-27632 and proliferation, differentiation inhibitors on PGC culture	70
32	Phase contrast images of PGCs	71
33	Effect of Y-27632 and other inhibitors on PGCs and Phase contrast images of PGCs	72
34	Effect of Y-27632 and growth factors and Phase contrast images of PGCs	73
35	Effect of Y-27632 with other inhibitors on PGC culture	75
36	Phase contrast images of PGCs	76
37	Phase contrast images of PGC	77
38	Effect of Y-27632 with growth factors on PGC culture	79
41	Phase contrast images of PGCs	79
42	Schematic representation of <i>boule</i> and <i>dazl</i> RNA expression during gametogenesis in tilapia	85
<b>Table description</b>		
1	Blastomere cryopreservation with and without ROCK inhibitor	55
2	Inhibitors and growth factors used in PGC culture	56
3	Blastomere culture in different test groups and media composition	56-57
<b>Appendix</b>		
1	Table S1 Primers used for gene cloning and probe synthesis	96
2	Figure S2 <i>vasa</i> RNA expression in ovary	96
3	Figure S3 Proliferation of hES cells	97
4	Figure S4 Clonal expansion of cryopreserved medaka hES cells	98
5	Figure S5 Effects of Y-27632 and apoptosis inhibitors on PGC culture (images of PGCs)	99
6	Figure S6. Effect of Y-27632 and other apoptosis inhibitors on PGC culture (images of PGCs.)	100
7	Figure S7. Effect of Y-27632 and growth factors on PGC culture. (images of PGCs)	101
8	Figure S8. Effect of Y-27632 with other apoptosis inhibitors on PGC culture. (images of PGCs)	102
9	Figure S9. Effect of Y-27632 with other apoptosis inhibitors on PGC culture. (images of PGCs)	103
10	Figure S10. Effect of Y-27632 with growth factors on PGC culture (images of PGCs)	104
11	S11. NCBI links of proteins used for comparison and phylogenetic analysis	105



## Abbreviations

---

AP	Alkaline phosphatase
BCIP	5-bromo, 4-chloro, 3-indolylphosphate
BMP	Bone Morphogenetic Protein
Bp	Base pairs
BSA	Bovine serum albumin
bFGF	Basic fibroblast growth factor
BMP4	Bone morphogenetic protein 4
dpc or hpc	Day(s) or hour(s) post culture
dpf or hpf	Day(s) or hour(s) post fertilization
dpth	Day(s) post thawing
cDNA	DNA complementary to RNA
DEPC	Diethyl pyrocarbonate
DIG	Digoxygenin
DNA	Deoxyribonucleic acid
dNTP	deoxyribonucleotide triphosphate
DTT	Dithiothreitol
EDTA	Ethylene diamine tetraacetic acid
ERM	Embryo rearing medium
ES cell	embryonic stem cell
FBS	Fetal bovine serum
ESM4	Embryonic stem cell medium 4
FGF	Fibroblast growth factor
FBS	Fetal bovine serum
FS	Fish serum from rainbow trout
GFP	Green fluorescent protein
GSK3- $\beta$	Glycogen Synthase Kinase 3 $\beta$
h	Hour
hpf	hours post fertilization
HRP	Horseradish peroxidase
ISH	<i>in situ</i> hybridization
kb	kilobase
LB	Luria-Bertani medium
LiCl	Lithium Chloride
MBE	Mid blastula embryo
MEE	Medaka embryo extract
MES1	Medaka embryonic stem cell line 1
min	Minutes
mRNA	messenger RNA
NBT	nitro blue tetrazolium chloride

nt	nucleotide
OI	<i>Oryzias latipes</i>
ORF	Open reading frame
PBS	Phosphate buffered saline
PCR	Polymerase chain reaction
PGC	Primordial germ cell
PFA	Paraformaldehyde
POD	Peroxidase enzyme
PTK	Proteinase K
PTW	PBS with 0.1% Tween-20
RNA	Ribonucleic acid
RT-PCR	Reverse Transcriptase Polymerase Chain Reaction
SDS	Sodium dodecylsulfate
s	seconds
SSC	Saline-sodium citrate
TAE	tris-acetate EDTA
TSA	Tyramide signal amplification
TEMED	N,N,N',N'-tetramethylethylene diamine
W	Tryptophan
YSL	Yolk syncytial layer

## Summary

Sexual reproduction involves sex differentiation and production of male and female gametes in the adult gonad. The precursors of gamete are primordial germ cells (PGCs), which are formed early during embryogenesis and subsequently migrate into the gonad. PGCs are considered as germ stem cells capable of self-renewal and differentiation during gametogenesis, leading to the production of sperm in the male gonad testis and eggs in the female gonad ovary. Germ cells are thus responsible for germline transmission and species continuum. Followed by PGC formation, gametogenesis takes place where Deleted in Azoospermia (DAZ) family of RNA binding proteins play an important role. Since the genes *boule* and *dazl* which are members of DAZ family show varied expression pattern in diverse organisms, it is important to study their specific or shared role during gametogenesis.

The first part of this thesis was aimed at the partial cloning and expression analysis of germ genes *boule* and *dazl* in the Nile tilapia (*Oreochromis niloticus*), an important aquaculture fish. Molecular cloning and sequence analysis led to the identification of tilapia *boule* and *dazl* cDNA. The predicted partial Boule contains a conserved RRM motif and Dazl has the C-terminal sequence. On a phylogenetic tree, tilapia Boule and Dazl are in separate clades of their homologs from other species, indicating their divergence during early vertebrate evolution. An RT-PCR analysis revealed bisexual gonad-specific expression of both *boule* and *dazl*. Chromogenic and fluorescent *in situ* hybridization (CISH and FISH) analyses revealed germ cell-specific expression of *boule* and *dazl* RNAs in both the sex. In the ovary, *boule* RNA expression increased from oogonia to pre-vitellogenic oocytes and decreased in oocytes as vitellogenesis progressed. The *dazl* RNA expression was present throughout oogenesis with strong expression in early stages and weak expression in stage III and IV. In the testis, *boule* RNA existed throughout spermatogenesis except sperm. Expression was gradually increased as the spermatogenesis progressed but significantly

reduced in sperm, making it barely visible. The *dazl* RNA was expressed throughout spermatogenesis and unlike *boule*, it was present in sperm. Germ cell-specific expression of *vasa*, the most conserved germ gene in the animal kingdom, was also observed in both the sex of tilapia. These data demonstrate that *boule*, *dazl* and *vasa* are germ cell markers in tilapia and bisexual, stage-specific germline expression patterns of these germ genes are conserved in diverse teleost fish species.

The second project focused on improvement of procedures for derivation and maintenance of stem cells and germ cell cultures from medaka (*Oryzias latipes*), a unique fish model for stem cell research. Specific attention was given to the maintenance of medaka haploid embryonic stem cell (hES) lines because the percentage of hES cells in these lines tends to decrease during subculture and repetitive cryopreservation-thawing procedures. To this end, the ROCK inhibitor Y-27632 was tested for its effect on hES cell cryopreservation. Y-27632 selectively inhibits p160-Rho-associated coiled-coil kinase (ROCK) and is known as the most potent inhibitor of apoptosis. Y-27632 significantly increased the survival rate of cryopreserved haploid ES cells and blastomeres via reducing the number of Annexin V-positive apoptotic cells. It also increased the survival rate of PGCs in primary cell culture from dissociated blastula cells. Hence, it is demonstrated in this study that Y-27632 is effective to improve the maintenance of medaka hES cells and derivation of new cell cultures including PGCs via inhibition of cell apoptosis.

## **Background**

### **Germ cell specification and gametogenesis**

Fusion of male and female gametes results in the formation of embryo by multiple divisions of blastomeres. During embryogenesis, few cells are destined to become Primordial germ cells (PGC) and migrate to the future gonad area in the resulting embryo. These cells either become male or female gametes depending on the sex of the embryo. The production of haploid gametes in the adult is known as gametogenesis and is pivotal for fertility in sexually reproducing organisms. Any abnormality during gamete formation leads to infertility (Wylie, 1999). However, gametogenesis is not as simple as defined and involves many intricate molecular events during the process to become fertile gametes. Decisive processes like arresting mitosis or entering meiosis to form sex-specific gametes depends on critical balance of gene expressions and somatic signals (Kimble and Page, 2007; Eirin-Lopez and Ausio, 2011). Cells in the early developmental stage are able to become any cell type upon stimulus. As the early development with division of blastomeres progresses, specificity to become particular cell type also increases. PGCs are the most important cell types which carry genetic information to next generation. Following section deals with the formation, features and importance of PGCs.

Upon the specification germ cells confront two major cell-fate decisions as they move from an immature state into the world of sexuality. One decision is to enter a germline-specific cell cycle called meiosis, and the other is commitment to differentiate as sperm or egg (Kimble and Page, 2007). PGCs of many different species share intrinsic qualities that differentiate them from somatic cells often long before the somatic gonads are formed. However, there is long-discussed debate as to how germ cells may be identified and when the germline is specified (Extavour and Akam, 2003).

There are two theories to explain the germline segregation in metazoans, preformation and epigenesis. During preformation, for example in *Drosophila*, RNAs and proteins are synthesized and transported through cytoplasmic bridges to the oocyte. They localize to the posterior of the ooplasm known as germ plasm or germline determinant. During early embryogenesis, cells which inherit the germ plasm become the primordial germ cells. In epigenesis, maternally deposited germ plasm is absent as observed in mice. Instead, PGC determination takes place after the segregation of embryonic and extraembryonic tissues. A subpopulation of the pluripotent epiblast cells expresses 'germline competence genes'. These cells are able to interpret the inductive signals that arrive from neighboring tissues and differentiate into PGCs (Extavour and Akam, 2003). In mammals, germ cells are specified at a very early stage of development from the post-implantation epiblast cells following blastocyst implantation. The inner cell mass (ICM) of blastocysts is the source of epiblast cells as well as embryonic stem cells (ESCs). In mice, precursors of the primordial germ cells (PGCs) are specified in the extreme proximal region of the epiblast adjacent to the extra-embryonic ectoderm (ExE) (Irie et al., 2014). In primates, passive translocation of PGCs takes place from the mesenchyme that surrounds the gut to the prospective gonad through the intercalary expansion of mesenchymal tissue which contains PGCs (Aeckerle et al., 2014). In marmoset and humans, the process of early germ cell differentiation takes place over a relatively prolonged period of time and is asynchronous resulting in the presence of germ cells at several stages of differentiation within individual seminiferous cords during fetal and early postnatal life. In addition, proliferation occurs in a variable proportion of germ cells throughout perinatal life (Mitchell et al., 2008).

Germ cell-specification in fish models was mainly studied in teleosts and the work mainly relied on light and electron microscopy. The germ cells in teleosts are easily identifiable by their large size and electron dense nuage-like structures. Using these criteria the earliest time point they

can be identified is during somatogenesis (Hamaguchi, 1982; Gevers et al., 1992; Herpin et al., 2007). From past two decades a tiny teleost fish medaka, popularly known as Japanese killifish is emerging as a successful vertebrate model for developmental genetics research. Medaka is an excellent teleost model to study PGC with the advantages of clear embryology, fast developmental stages and hardness for laboratory use.

In addition to understand PGC formation, it is of immense importance to study the genes involved in the formation of sex-specific gametes in individual sex. DAZ family genes are one of the molecular conservational evidences in this aspect. So far DAZ family is extensively studied and its evolution across the animal kingdom is of great interest. Among vertebrates, teleost fishes are excellent and most feasible models to study one of the most complicated processes like gametogenesis. Expression patterns of these genes have been analyzed in several teleost fish species, some of them are laboratory models and some are economically important aquaculture species. One such aquaculture fish which is the second most consumed food species worldwide is the Nile tilapia. Expression analysis of DAZ family in this fish provides additional evidence on the conservation and evolution of these germ genes in teleosts.

This study covers two aspects of germ cell biology. The first focus is on gametogenesis where germ cell-specific genes are cloned and their expression pattern is analyzed in a teleost fish Nile tilapia. Expression pattern analysis of germ genes in this fish allows us to study different gametogenic stages and identification of new germ cell markers. The second part is focused on the aspect of stem cells and germ stem cells where medaka haploid Embryonic Stem cell culture and PGC culture from freshly dissociated blastula cells were shown in the presence of apoptosis inhibitor Y-27632.

## **Part 1: Cloning and expression of fertility genes in the Nile tilapia**

### **1.1 Introduction**

#### **1.1.1 History of DAZ family genes**

As explained in the previous section, gametes are the carriers of genetic information to the next generation thereby help in species continuum. During embryogenesis, a group of cells specialize to become germ cell precursors because of maternally inherited mRNAs in the embryo. Once the specialized germ cells reach gonad gametogenesis begins. Gametogenesis involves several sex-specific gene expression events. The expression of genes is regulated in transcriptional as well as post-transcriptional levels. The post-transcriptional regulation is a critical step for the formation of sperm and oocytes. In this post-transcriptional regulation, RNA-binding proteins play pivotal role in splicing, mRNA localization and the translational regulation of mRNA (Venables and Eperon, 1999; de Moor and Richter, 2001). The DAZ genes are one such family of genes which are important fertility components in all animals, including humans (Vangompel and Xu, 2011). The DAZ family represents one of the few lines of evidence for evolutionary conservation of gametogenesis at the molecular level (Xu et al., 2001). They encode potential RNA binding proteins that are expressed exclusively in prenatal and postnatal germ cells and are strong candidates for human fertility factors (Wylie, 1999). DAZ family genes include *boule*, *daz* and *dazl* which encode RNA binding proteins containing a conserved RNA recognition motif (RRM) plus one or two multiple repeats of DAZ motif (Yen, 2004). The human *Daz* gene was first identified on the Y chromosome as the founder member of DAZ family (Reijo et al., 1996; Saxena et al., 1996; Xu et al., 2001). *Daz* is essential for male fertility as deletion of *Daz* cluster leads to azoospermia and oligospermia. The *Daz* is limited to certain primates, whereas the autosomal *Dazl* (*Daz-like*) homolog has been found in mouse (Cooke et al., 1996). The autosomal *Dazl* on chromosome 3 (ENSG00000092345) was proposed to be the ancestor of the *Daz* cluster via its duplication and transposition to the Y chromosome during the



evolution of primates (Reijo et al., 1996; Saxena et al., 1996; Seboun et al., 1997). The *dazl* gene was found in all major groups of non-mammalian vertebrates including chicken (Elis et al., 2008), *Xenopus* (Houston et al., 1998), axolotl (Johnson et al., 2001), zebrafish (Maegawa et al., 1999), gibel carp (Peng et al., 2009) and medaka (Xu et al., 2007). The *boule* was identified as the third member of DAZ family in *Drosophila* (Cheng et al., 1998) and then in the nematode (*Caenorhabditis elegans*), in which it was initially called *daz-1* (Otori et al., 2006). Both *boule* and *dazl* are discovered to be present in vertebrates. Since only *boule* is present in invertebrates, it has been hypothesized to be the ancestor of the DAZ family (Xu et al., 2001). The functional conservation between *dazl* and *boule* was demonstrated by the fact that transgenic expression of the *Xenopus dazl* was capable of rescuing the *boule* meiotic entry phenotype in *Drosophila* (Houston et al., 1998).

### **1.1.2 Stage-specific expression of DAZ family genes**

The DAZ family shows not only conserved germline-specific expression but also species specific variation in sex and stages of gametogenesis (Xu et al., 2001). For example, *boule* is essential for meiosis in female but dispensable in male *C. elegans* (Karashima et al., 2000) and for male germ cell development in *Drosophila* (Cheng et al., 1998). The *boule* expression is unisexual in some species and shows considerable variation in germ cells at different developing stages (Xu et al., 2007; Vangompel and Xu, 2011). In contrast, *dazl* expression is bisexual in diverse species (Xu et al., 2001; Elis et al., 2008). Genes *boule* and *dazl* were identified and their RNA expression patterns were subsequently analyzed in medaka (Kuo et al., 2004; Xu et al., 2009), stickleback (Xu et al., 2007; Xu et al., 2009) and rainbow trout (Li et al., 2011a). In medaka, *boule* and *dazl* are expressed bisexually in both mitotic and meiotic germ cells which were shown by RNA *in situ* hybridization (Xu et al., 2007; Xu et al., 2009). In rainbow trout, *boule* exhibits mitotic and meiotic expression in

males but meiosis-specific expression in females whereas, *dazl* is expressed in mitosis and meiosis of both the sexes (Li et al., 2011a; Li et al., 2011b). This diversity in species-specific, sex and stage-specific expression of *boule* and *dazl* welcomes more study on diverse organisms to understand their evolutionarily conserved role in gametogenesis.

### 1.1.2 Germ cell-specific gene *vasa*

The gene *vasa* is widely acknowledged as an indispensable germline marker. It was originally identified in *Drosophila* as an essential gene for germline development (Hay et al., 1988a; Hay et al., 1988b; Yajima and Wessel, 2011). Since then it had been found in the germline of every organism examined. *Vasa* is typically found within granules located near the nucleus of the germline cell of *Drosophila*, the so-called nuage (Hay et al., 1988a; Hay et al., 1988b). *Vasa* is the founding member of the family of DEAD-box proteins and its consensus sequence L-D-E-A-D-X-(M/L)-L-X-X-G-F shared with other DEAD-box members reflects a unique version of the B-motif of ATP-binding proteins (Linder et al., 1989). The gene *vasa* is expressed as soon as the germ cells are specified during embryogenesis hence is known as early marker for germ cells.

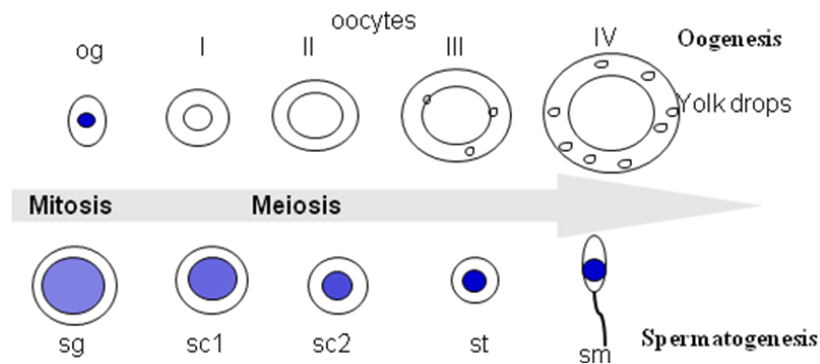


**Figure 1: Stages of gametogenesis.** Various stages of oogenesis and spermatogenesis in fish are shown. og, oogonial; I-IV, stage I-IV oocytes; sg, spermatogonia; sc1 and sc2, spermatogonia 1 and 2; st, spermatid; sm, sperm

### 1.1.3 The Nile tilapia

Present study is aimed at the cloning and expression pattern analysis of *boule* and *dazl* in the fish Nile tilapia (*Oreochromis niloticus*), a member of the family Cichlidae of the order Perciformes. The

order Perciformes represents one of the most divergent fish groups with 1300 species. It belongs to the tribe Tilapiini in the subfamily Pseudocrenilabrinae. The name tilapia is a latinization of *thiape*. The genus Tilapia has lot of popular food fish that are grown in aquacultures worldwide. All Tilapia species are basically from Africa but they are now introduced to many other parts of the world. Tilapiini cichlids readily mate with each other resulting in hybridization. The fast pace of evolution observed in Tilapiini cichlids is because of this nature. Red tilapia chosen in this study is a variety of several different manmade tilapia variants with attractive red coloration. A few examples of red tilapia variants commonly encountered in fish markets and grocery stores are Florida Red, Jamaican Red, Taiwan Red and ND56. Unlike wild tilapia species which tend to be black or grey, these fishes have red and pink colors (Figure 2). Hybrids created by crossing Taiwan Red with Nile tilapia (*Oreochromis niloticus*) are known to grow as fast as the Nile tilapia. Crossing blue tilapia is popular when tilapia is aqua cultured outside the tropics; because the Blue tilapia is one of the most cold tolerant tilapia species we know so far (<http://www.aquaticcommunity.com/tilapia/tilapia.php>).

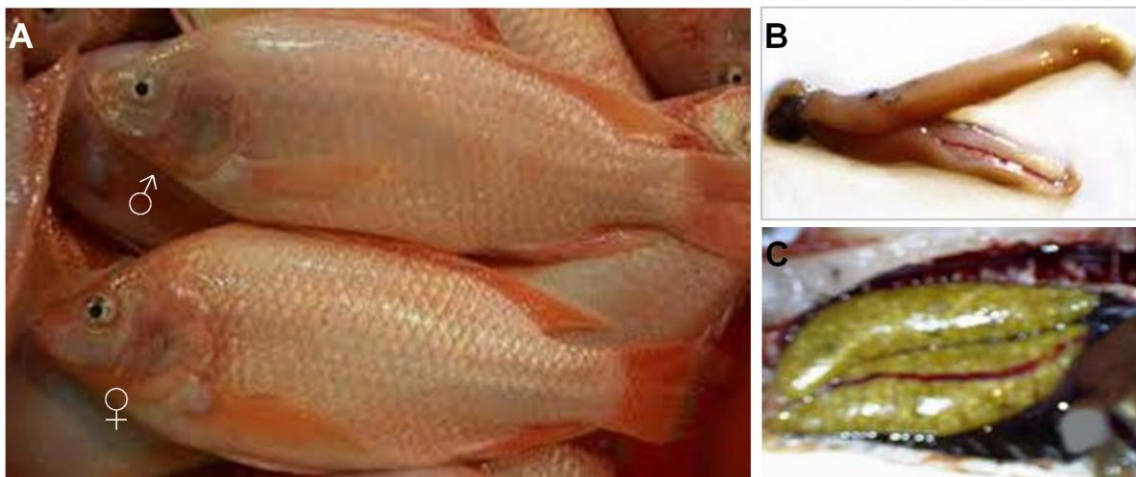


**Figure 2. The Nile tilapia.** Shown are (A) male (♂) and female (♀) adults of red variety together with the male gonad testis (B) and female gonad ovary (C).

#### **1.1.4 Scope of the study**

Analysis of DAZ family in diverse organisms from past few decades revealed their conserved role in gametogenesis. In vertebrates, *boule* and *dazl* showed sex and stage-specific expression. Among the vertebrate models, teleosts attract much attention as they reveal many aspects about early divergence between fish and tetrapod lineage. So far these genes are studied in many teleost fish species including medaka, zebrafish, seabass, and trout which indicate their stage-specific expression pattern and their specific role during gametogenesis. In this study, one of the major economically important food fish is used to study these genes to see whether the germ cell-specific pattern is conserved. Also, so far *vasa* is the only germ gene identified and expression is studied in this fish (Kobayashi et al., 2000). Hence, expression analysis of DAZ family in the Nile tilapia helps in studying the conserved existence of them and identification of new germ cell markers to study gametogenesis in detail. Expression analysis of *boule* and *dazl* throughout the lifespan of Nile tilapia would provide knowledge on its conserved presence in germ cells. Further, perturbation of individual or both genes would help to reveal their specific role in every stage of gametogenesis.

#### **1.1.5 Limitations**

This study shows the expression pattern of germ genes, *boule*, *dazl* and *vasa* by chemical and fluorescent RNA *in situ* hybridization (CISH and FISH) techniques. Adult gonads were used to analyze the expression pattern in the red variety of Nile tilapia.

### **1.2 MATERIALS AND METHODS**

#### **1.2.1 Fish and chemicals**

Work with fish was followed in strict accordance with the recommendations in the Guide for the Care and Use of Laboratory Animals of the National Advisory Committee for Laboratory Animal Research in Singapore and approved by this committee (Permit Number: 067/12). The Nile tilapia

male and female fish were purchased from native fish suppliers in Singapore. Enzymes and chemicals were from Sigma and Promega unless otherwise stated.

### **1.2.2. RNA isolation and cDNA cloning**

Total RNA from tilapia adult tissues were collected by dissection in aseptic conditions using RNase free buffers. Tissues were placed in EP tubes with appropriate amount of Trizol (Invitrogen). Tissues were then homogenized and centrifuged at 6000 rpm for 5 min. Supernatant was collected, 200  $\mu$ l of chloroform was added and centrifuged. 1:3 volume of isopropanol was added to the collected supernatant and centrifuged. The pellet formed was washed twice with 70% ethanol and air-dried. The pellet was then dissolved in DEPC water and subjected to gel electrophoresis to see the presence of RNA as well as measured in spectrophotometer to adjust the concentration to 100 ng/ $\mu$ l. Samples were treated with RNase-free DNase to avoid genomic DNA contamination. Synthesis of cDNA was carried out using M-MLV reverse transcriptase (Invitrogen) kit as described earlier (Xu et al., 2007). Briefly, RT-PCR was performed by two step reaction. First step involved synthesis of first strand cDNA and second step involved amplification of fragments of interest from single strand cDNA as template. First strand cDNA was synthesized from total RNA. A typical reaction was performed in 25  $\mu$ l total volume containing 5  $\mu$ l 5X first strand buffer (250 mM Tris-HCl, pH 8.3, 375 mM KCl, 15 mM MgCl<sub>2</sub>, 50 mM DTT), 1.25  $\mu$ l 10 mM dNTP, 1  $\mu$ l RNase inhibitor (40 U/ $\mu$ l, N251A, Promega, USA), 1  $\mu$ l oligodT primer (1  $\mu$ g/ $\mu$ l), 2  $\mu$ g total RNA and 1  $\mu$ l MMLV reverse transcriptase (200 U/ $\mu$ l, M170B, Promega, USA). Total RNA and oligo dT primer should be pre-mixed, heated to 70 °C and cooled on ice before adding the other components to prevent secondary structure within the template. After incubation at 42 °C for 1 h, the cDNA temple was heated at 70 °C for 5 min. After dilution, the cDNA was used as template for PCR or stored at -80 °C for future use.

### **1.2.3 Polymerase chain reaction (PCR)**

Standard PCR was performed in a 25 µl reaction mix using thermal cycler (Biorad, USA), Geneamp PCR system 9700 (Applied Biosystems, USA) and Mastercycler gradient (Eppendorf, Germany). Each reaction included 2.5 µl 10X PCR buffer (0.2 mM Tris-HCl, pH 8.8, 0.1 M KCl, 0.1 M (NH<sub>4</sub>)<sub>2</sub>SO<sub>4</sub>, 20 mM MgSO<sub>4</sub>, 1% (v/v) Triton X-100), 1 µl of 5 mM dNTP mix, 1 µl of 10 µmol sense primer, 1 µl of 10 µmol antisense primer, 1 µl template, 0.2 µl 5U/µl Taq polymerase. The parameters for standard PCR consisted of first denaturation at 94 °C for 5 min, following 35 cycles of amplification including denaturation at 94 °C for 20 sec, annealing at 55 °C for 30 sec and extension at 72 °C for 1 min and final extension at 72 °C for 10 min.

### **1.2.4 Agarose gel electrophoresis**

DNA electrophoresis was performed using 1% agarose gel for DNA size larger than 1 kb and 1.5% gel for size smaller than 1 kb. The agarose powder was dissolved in 1X TAE (0.04 M Tris-base, 0.02 M acetic acid, 0.01 M EDTA, pH 8.0) by heating in microwave. The melted gel was kept at 60 °C oven to avoid solidification. For gel casting, the melted gel was poured into an appropriate sized tray and a few drops of ethidium bromide (EB)/gel red were added to a final concentration of 0.5 µg/ml with thorough mixing. A voltage of 5 V/cm was applied to run the samples.

### **1.2.5 Purification of DNA fragments from agarose gel**

Gel extraction kit (Qiagen) was used to recover DNA fragments ranging from 100bp to 10kb from agarose gel according to manufacturer's instructions. The procedure consisted of melting of gel containing DNA of interest, binding of DNA to the column, washing and elution. The band was visualized under UV and excised. The excised piece of gel was placed in EP tube and 1-2 volume of diffusion buffer was added and incubated at 55-60 °C for 10-15 min. The melted mixture was centrifuged and supernatant was collected in filter column. 3 volumes of buffer QG was added and

centrifuged. Flow-through was discarded and column was washed with wash buffer. Bound DNA was then eluted with appropriate amount of elution buffer.

### **1.2.6 Cloning of PCR products (T-A cloning)**

To clone the products into plasmid, the pGEM-T easy vector (Promega, USA) was used. The linearized vector contains two 3'T overhangs at the insertion site. The PCR products contain two 3' A overhangs generated by Taq polymerase. With the help of T4 DNA ligase the PCR products were ligated into plasmids to form a circular plasmid for transformation, sequencing. DNA ligation reaction was performed in 20  $\mu$ l volume containing 4  $\mu$ l 5 X ligation buffer (250 mM Tris-HCl, pH 7.6, 50 mM MgCl<sub>2</sub>, 5 mM ATP, 5 mM DTT and 25% (w/v) polyethylene glycol-8000), insert DNA, vector DNA (20ng -200ng ) and 1  $\mu$ l T4 ligase (Invitrogen). The molar ratio of insert to vector DNA was usually 3:1. Ligation mixture was incubated overnight at 4 °C.

### **1.2.7 Preparation of competent cells**

Quality of competent cells is critical for cloning. Normally an efficiency of  $\sim 10^8$  transformed colonies/ $\mu$ g of plasmid is satisfactory for most cloning requirement. The bacterial strain TOP 10 F' (Invitrogen) was used for preparation of competent cells. Two ml of LB broth was incubated with a single fresh colony at 37 °C with 200 rpm overnight. The following morning, 1 ml of culture was inoculated into 100 ml LB with 20 mg MgSO<sub>4</sub> and shaken at 200 rpm at 37 °C until OD<sub>600</sub> reached (about 3 h). The culture was chilled on ice for 15 min and centrifuged at 2,500 g for 15 min at 4 °C. The cell pellets were resuspended in 40 ml Tfb1 (100 mM RbCl, 30 mM Potassium acetate, 50 mM MnCl<sub>2</sub>, 10 mM CaCl<sub>2</sub> and 15% glycerol, pH 5.8). After incubation on ice for 15 min, the cells were spun down and resuspended in 4 ml TfbII (10 mM MOPS, 10 mM RbCl, 75 mM CaCl<sub>2</sub> and 15% glycerol, pH 6.5). After incubation on ice for 20 min, the competent cells were transferred into 1.5 ml EP tubes in 100  $\mu$ l aliquot, fast-frozen in liquid nitrogen and stored at -80 °C.

### **1.2.8 Transformation**

5-10  $\mu\text{l}$  ligation mixture was added into the freshly thawed competent cells and incubated on ice for 30 minutes. Following incubation, the mixture was heated to 42  $^{\circ}\text{C}$  for 60 s in a water bath and cooled immediately on ice for 3 min. After adding 400  $\mu\text{l}$  LB medium, mixture was shaken at 200 rpm in a 37  $^{\circ}\text{C}$  incubator for 1 h. 150  $\mu\text{l}$  mixture was then spread onto LB agar plate (for A-T cloning the plate also containing pre-spread 10  $\mu\text{l}$  1M IPTG and 30  $\mu\text{l}$  50 mg/ml X-gal) supplemented with ampicillin. The plate was left at room temperature for 10 min and incubated at 37  $^{\circ}\text{C}$  inverted overnight.

### **1.2.9 Isolation of plasmid DNA**

Small scale preparation of plasmid DNA was carried out by Kit from Qiagen (USA). The protocol involved several steps including alkaline lysis, binding of plasmid DNA to a silica-based resin and elution in low salt buffer or water. 10  $\mu\text{g}$  of high copy number plasmid DNA can be isolated from 3-5 ml of overnight (12-16 h) bacterial culture in LB medium with appropriate antibiotics. 1 ml of overnight bacteria cultures grown in LB (pH7.4) with 100  $\mu\text{g}$  ampicilin or 50  $\mu\text{g}$  kanamycin were poured into 1.5 ml EP tube and spun down at 8000 rpm in a table centrifuge machine (Eppendorf 5417C, Germany) for 3 min. The pellet was resuspended in 100 $\mu\text{l}$  solution I (15 mM Tris-HCl, 10 mM EDTA, 100  $\mu\text{g}/\text{ml}$  Rnase A) by vortex. 100  $\mu\text{l}$  of freshly prepared Solution II (immediately mixed with equal volume of 2% SDS and 0.4 M NaOH) was added to the bacterial suspension and mixed by gently inverting the tubes four times. This mixture was neutralized by adding 100  $\mu\text{l}$  of solution III (3 M KAC-HAC, pH 5.5), followed by addition of 60  $\mu\text{l}$  chloroform. After being centrifuged at 14,000 rpm for 10 min, 200  $\mu\text{l}$  clear supernatant was transferred to a new tube and mixed with 500 $\mu\text{l}$  ethanol, then centrifuged at 14, 000 rpm for 15 min at 4  $^{\circ}\text{C}$ . The DNA pellet was



drained by careful aspiration of residual ethanol or air dry and eluted with 30  $\mu$ l Mili-Q water or 10 mM Tris-HCl (pH 8.0).

#### **1.2.10 Gene sequencing**

Each sequencing reaction (5  $\mu$ l) consists of 2  $\mu$ l Bigdye mix, 1  $\mu$ l 50~100 ng double strand DNA, 1  $\mu$ l primer (3.2 pmol/ $\mu$ l) and 1  $\mu$ l water. The single primer extension was done in a PCR machine with 25 cycles of 96  $^{\circ}$ C for 10 s, 52  $^{\circ}$ C for 5 s and 60  $^{\circ}$ C for 2 min. After adding 0.5  $\mu$ l of 3M NaOAc (pH 4.6) and 12.5 $\mu$ l 95% ethanol, the reaction products were incubated on ice for 30 min and centrifuged at 4  $^{\circ}$ C for 20 min at 16,000 rpm. The pellet was washed with 500 $\mu$ l of 70% ethanol twice, air dried, dissolved in Hi-Di and sequenced by the automatic sequencer (ABI 3100A, applied Biosystems).

#### **1.2.11 Bioinformatics analysis**

The DNA or protein sequence was analyzed with Bioedit (Ibis Biosciences), DNAMAN (Lynnon Biosoft) and Vector NTI software (Invitrogen). Online sequence analysis was done in NCBI (<http://www.ncbi.nlm.nih.gov/>).

#### **1.2.12 Restriction endonuclease (RE) digestion of DNA**

RE digestion was employed to screen recombinant clones. The REs used in this study were purchased from Promega, New England Biolabs or Fermentas. Digestions were performed at 37  $^{\circ}$ C for 1- 4 h or overnight according to activity of different enzymes with recommended buffers. For the given reaction, the maximum DNA concentration was 300 ng/ $\mu$ l and 5-10 units of enzyme were used to digest 1  $\mu$ g (plasmid) DNA.

#### **1.2.13 Probe synthesis**

Plasmids containing target of interest, pONbol and pONDazl were linearized with SacII and purified. Antisense probes were synthesized with SP6 promoters using DIG (Digoxigenin) labeling kit (Roche) for *boule* and FITC RNA Labeling kit for *dazl*. 10  $\mu$ g of plasmid with cDNA insertion in

pGEM T easy was linearized by enzyme (blunt or 5' overhang should be preferred to avoid snap back effects) to get anti-sense or sense probe. Linearized template was purified by phenol: chloroform extraction and ETOH (ethanol) precipitation. The synthesis reaction was performed at 37 °C for 2 h in a total volume of 20 µl containing 4 µl of 5X transcription buffer, 2 µl of 10 mM NTP mix with Dig-UTP/Fluorescein-UTP (Roche), 1 µg of template DNA, 0.5 µl of RNase inhibitor (40 U/µl) (Promega) and 1 µl of T7 (or Sp6) polymerase. Following the reaction, 1 µl of Turbo DNase (Ambion, USA) was added to digest the DNA template at 37 °C for 15 min. After the digestion the RNA probe was precipitated by adding 30 µl RNase free water and 30 µl Lithium Chloride precipitation solution (7.5 M lithium chloride, 50 mM EDTA, pH 8.0), washed with 70% ethanol, air-dried and dissolved in 25 µl DEPC- treated water. At last the probe was quantified, diluted to a final concentration of 1 ng/µl in hybridization buffer and examined by agarose gel electrophoresis.

#### **1.2.14 Chromogenic *in situ* hybridization (CISH)**

Adult tilapia tissues were fixed in 4% paraformaldehyde (PFA) in phosphate-buffered saline (PBS). They were then transferred to 20% sucrose solution at 4°C. Tissues were frozen after immersing them in tissue freezing medium. Cryosections were taken in Leica Cryostat machine and stored at -20 °C for further hybridization experiments. Slides were air dried or incubated for one h at 37 °C prior to hybridization. Slides were then placed in slide chambers upon pieces of filter papers soaked in 2 X SSCT plus 50% Formamide. Sections on the slides were guarded with a line of liquid blocker surrounding them. A layer of hybridization buffer (50% Formamide, 5 X SSC, 50µg/ml heparin, 0.1% tween, 500µg/ml torula RNA stored at -20 °C) was added and covered with a cover slip (optional). Slide chambers were then covered with thin plastic sheet and incubated at 65°C water bath. After prehybridization step, RNA probes were denatured at 85°C for 10 min and added to the slides and kept overnight at 65°C for incubation. After overnight incubation, slides were washed

twice with 2 X SSCT plus 50% formamide for 30 min, twice with 2 X SSCT for 15 min and twice with 0.2 X SSCT for 30 min. Blocking was carried out for 1 h in PBST containing 10% goat serum at room temperature, the samples were incubated with either the alkaline phosphatase (AP) conjugated anti-DIG-antibody or AP-conjugated anti-FITC-antibody (Sigma) at 1:2000 in the blocking buffer (PBST containing 2% blocking reagent and 10% heat-inactivated fetal bovine serum) for 2 h at room temperature. Following six PBST washes, and pre-incubation in the pre-staining buffer (NTMT; 100 mM NaCl, 50 mM MgCl<sub>2</sub>, 100 mM Tris-Cl, pH9.5, 0.1% Tween-20) for 30 min, the samples were incubated in the staining buffer (0.1 mg/ml NBT/BCIP in NTMT) in darkness at room temperature for 30-60 min or at 4 °C overnight. Color development was microscopically monitored at regular intervals. Nuclear staining was performed using 4'-6 diamidino-2-phenylindole (Dapi; 1 µg/ml) and embedded in 30% glycerol for microscopy (Bhat and Hong, 2014).

### **1.2.15 Fluorescent *in situ* hybridization (FISH)**

To detect low abundance mRNA expression in tissues, tyramide signal amplification (TSA) method was applied to increase the detection sensitivity up to 100-fold, as compared with conventional ISH with chemical substrates such as BCIP/NBT detection. The TSA method utilizes the catalytic activity of horseradish peroxidase (HRP) to generate high-density labeling of a target RNA *in situ* through a mechanism that is highly reactive short-lived tyramide radicals covalently couple to amino acid residues (principally the phenol moiety of protein tyrosine residues) in the vicinity of the HRP–target interaction site with minimal diffusion-related loss of signal localization. Slides were air-dried at 37°C for 30 min. Slides were then placed in slide chambers upon pieces of filter papers soaked in 2 X SSCT+ 50% Formamide. Sections on the slides were guarded with a line of liquid blocker surrounding them. A layer of hybridization buffer (50% Formamide, 5 X SSC, 50 µg/ml heparin,

0.1% tween, 500 µg/ml torula RNA stored at -20 °C) was added and covered with a cover slip (optional). Slide chambers were then covered with thin plastic sheet and incubated at 65 °C water bath. Slides were then incubated with DIG or FITC labeled probes at 65 °C water bath. The slide chambers were wrapped with a thin layer of plastic to avoid the evaporation of probes overnight. Following morning, slides were washed twice with 2 X SSCT plus 50% formamide for 30 min, twice with 2 X SSCT for 15 min and twice with 0.2 X SSCT for 30 min. Blocking was carried out for 1 h in PBST containing 10% goat serum at room temperature. The slides were then incubated with anti-dig POD or anti-fluorescein POD at 4 °C overnight followed by 6 washes for 20 min each with PBS. Slides were then incubated in TSA plus fluorescein solution or TSA plus cy3 solution for signal development for 30 min followed by rinsing in PBS for 3 times for single probe *in situ* experiments. For double color *in situ* experiments, FITC tagged probe was developed first. After the incubation with TSA plus fluorescein solution, 1% H<sub>2</sub>O<sub>2</sub> was dropped directly on to slides and washes with PBS were performed. The slides were then blocked with anti-DIG POD antibody for overnight at 4 °C. Following morning, slides were washed thrice in PBST, thrice with PBS and incubated with TSA plus cy3 at room temperature for 30 min. Slides were then stained with Dapi and mounted with anti-fade reagent.

### **1.2.16 Microscopy and image analysis**

Observation and imaging was carried out using Leica MZFIIII stereo microscope, Zeiss Axiovertinvert, Axiovert upright and confocal laser scanning (Zeiss LSM 710) microscopes with a Zeiss AxioCam M5Rc digital camera (Zeiss Corp) as described in (Xu et al., 2007).

## **Chapter 1.3: Results**

### **1.3.1 Identification of *boule* and *dazl* genes**

BLAST search using medaka sequences against the testis cDNA library of tilapia available at NCBI led to the identification of putative tilapia *boule* and *dazl* sequences. RT-PCR from tilapia gonad

tissues and sequencing of cloned products revealed that they were *boule* and *dazl* homologs in tilapia. The partial *boule* cDNA (GenBank:KF724902) is 808 nt long which includes a 68-nt 5'-untranslated region (UTR) and a 748-nt open reading frame (ORF) coding 246 amino acid residues (Figure 3A). The predicted tilapia Boule shows a maximal identity of 46% and 56% to Boule proteins of medaka and human respectively (Figure 4A).

The partial *dazl* cDNA (GenBank: KF724903) is 478 nt long and contains a 417-nt ORF coding for 111 amino acids (Figure 3B). The predicted tilapia Dazl is 71% and 50% identical to Dazl proteins of medaka and human respectively (Figure 4B). Multiple sequence alignment of cloned tilapia Boule with other organisms showed the conserved positions within the RRM whereas, tilapia Dazl contained downstream sequence to RRM motif (Figure 4A and B). This confirmed that the cloned *boule* and *dazl* are indeed partial sequences of tilapia and are sufficient for further probe synthesis and RNA expression analysis. On a phylogenetic tree, Boule and Dazl proteins are clustered into two separate clades (Figure 6). The branching of Boule and Dazl proteins coincides with the separation of fish and tetrapod lineages which supports the early evolution and divergence of Boule and Dazl before fish and tetrapod separation.

### **1.3.2 Cloning of *vasa***

Tilapia *vasa* is member of DEAD gene family of RNA helicases. A 646 nt long ORF was cloned from gonad cDNA as a standard germ cell marker in adult gonads of tilapia (Figure 3C). The gene *vasa* showed its exclusive expression in the gonads of both the sex whereas no expression was detected in other organs examined. Multiple sequence alignment showed that the cloned tilapia Vasa contains all the conserved domains of DEAD gene family (Figure 5).

**A**

1 GGGGGAGGTCATAGTTCGTGTGAGTGGTGAAGGCTAACCTAACCTAACGGTCGGAGCTTCAGAATAATATGGCTAAGGAAGCGG  
 1 M A K E A  
 85 CGAGCCAAAAGAGCGGGGGCAGTTCCTCCCAAGTGATGTGCTACTTCCAGATGATTATGTGACAGCCTGACAGACCACAGCA  
 28 A S Q K S G G S S S P S D V L L P D D Y A D S L T D H S  
 169 CAACCTTTGGCAACGTGATCCCCAACAGGATTTTGTGCGGGGCACTTGACTACAGGGTTAATGAGCGTGACCTGCGACACATTT  
 56 T T F G N V I P N R I F V G A L D Y R V N E R D L R H I  
 253 TTTCTCAACACGGCACAGTGAAGAGGTGGAGATTGTCTTAGATCATTACAGGAGTGTGCGAGGGATATGGGTTTGTACATTTG  
 84 F S Q H G T V K E V E I V L D H S G V S R G Y G F V T F  
 337 AAACCTCAAGAAGATGCTCTGAAAATCCTCAACAATACTAATGGAGTCACGTTCAAAGACAAGAAGCTCAGTGTGGTCCGGCTT  
 112 E T Q E D A L K I L N N T N G V T F K D K K L S V G P A  
 421 TTCGAAAGCATCAACCTTCAAGTCAAACAAAGAGCACCTTACAGCCAGCTTTGAACCTGCCATGCCTCAGCAAACATCCTATG  
 140 F R K H Q P S S Q T K S T S T A S F E P A M P Q Q T S Y  
 505 GGACCTTCTACTTGACCACAGGCTCCTCCTACACTTACCATAATGGAGTTGCCACTTCCACTGCTCCAACATGACTA  
 168 G T F Y L T T A T G S P Y T Y H N G V A Y F H C S N M T  
 589 GTCCTTCTACCAGTGGCTTCCGCCATCTTCGCCGATGGTCCCCATCCTTATCAGCCTGTGTATGAGCAACCATCCAGTCACC  
 196 S P S Y Q W L P P S S P M V P H P Y Q P V Y E Q P S S H  
 673 ACTACCAGTGCCTCCAAACCAGTATCAGTGAATACCCCCAGNGGNAGATGCCGTCCTATGCAGTCTTGTACCCCCAGCAGT  
 224 H Y Q C V P N Q Y Q W N T P Q X X M P S Y A V L Y P Q Q  
 757 CACAATATGTTTACCTGCCTGCTGATGGAGTTTCTGTTTCAGCCACCTGTGTT  
 252 S Q Y V Y L P A D G V S V Q P P V

**B**

1 GGGATGAAAGAAAGGGTCTCTCGGTTCGATGCCGTCACGCTCTGGTTGGCCCCGCTCCTTGGGTGAATCCCACCAGTACTTCTAC  
 1 M K E R V S R S M P S R L V G P A P W V N P T Q Y F Y  
 85 TGTGCTTGTGCTCACCCATGGGAGGTGGGGTGCCACAACCTTCGCCCATCATAACGGAGGCAACCCATAACATCAGCCATAC  
 29 C A C C S P M G G G V P Q P S P I I N G G N P Y N Q P Y  
 169 TCCTATGCCAACTTTGGAGGGTTCATGATCCCGCAGATGCCAGTGAATTACGCACAGAATGCCATATGCCTATCAGTACACCCCA  
 57 S Y A N F G G V M I P Q M P V N Y A Q N A Y A Y Q Y T P  
 253 CCTCCCTGGACAGCGGACAGGACACGGCTGTCAATCAGAGCTTTGTGGACTGTGGAGTCCAGACCATGCTGACTGTGCTG  
 85 P P W T A D Q R T R P V N Q S F V D C G V Q T M L T V L  
 337 TAGTCCACAGCTACTGAGAACCATGCCAGGCTCAGGGAGTCAGAATTTAGACAAGATTACACCTTGATTCTCCGGACGTCTGG  
 421 AGTAACCCAACCTTTCAGGCTGTTTTCCAAATGCCCTCGCCTCTCATTCCGTGCCTCAAA

**C**

1 ATGGTGAATTTCAAGGAGGTCGTGGTNNACGGGGTAGAGGAAGAGGAGGATTTAAAAAACTCATTCTTCTCAGGTGCTGAGGAC  
 1 M V N F K E V V V X G V E E E E D L K N S F F S G A E D  
 85 GGTGCAAACGATGGTGACGGCCAGAATAATACAGCAGAAAGGAGTAGCTTACGCCGAAGAGGAGGCCGTTGGGCGTGGCAGAGGA  
 29 G A N D G D G Q N N T A E R S S F S R R G G R G R G R G  
 169 TTTGGCAGAACGGATCACAGTGATTTTACGCCAATGAAGAGGATGGTGACAATAAAAAATGTGTCAAGAGGAAGAAGAGGAGGA  
 57 F G R T D H S D F D A N E E D G D N K N V S R G R R G G  
 253 AGCTATAGTCAAGGTGGTGTGAGCAGGGTGGCAGAGGTGGCTTTGGAGGAGGCTACCGTGGGAAAGATGAAGAGGTCTTTGCTCAA  
 85 S Y S Q G G E Q G G R G G F G G G Y R G K D E E V F A Q  
 337 GGGCACGGGGATACACCTGCAGAGAACGCAGATGCGAGTGATAGACCCAGGGTTACCTACGTCCCCCACCACCTCTGAAGAT  
 113 G H G D T P A E N A D A S D R P R V T Y V P P P P S E D  
 421 GAGGAGTCCATTTTTTCCCACTATGAGTCCGGTGTCAACTTTGACAAGTACGATGAGATCTTGGTGGATGTGAGTGAACCAAC  
 141 E E S I F S H Y E S G V N F D K Y D E I L V D V S G T N  
 505 CCACCACCAGCTATAATGACATTTGATGAAGCAGCGCTGTGCGAGTCCCTAAAGAGAAACGTCAGCAAGTCTGGTTATGTGAAG  
 169 P P P A I M T F D E A A L C E S L K R N V S K S G Y V K  
 589 CCCACCCCTGTGAGAAGCACGGCATCCCCATCATTTCTGCTGGCAGGGATCTCATGG  
 197 P T P V Q K H G I P I I S A G R D L M

**Figure 3. Nucleotide and amino acid sequences of tilapia (A) *boule* (B) *dazl* (C) *vasa*. Sequences underlined are primer sequences used for cDNA cloning and RT-PCR analysis which also flank the regions used for synthesis of RNA probes for *in situ* hybridization. Accession numbers *boule*: KF724902, *dazl*: KF724903, *vasa*: AB032467.1 (Bhat and Hong, 2014)**



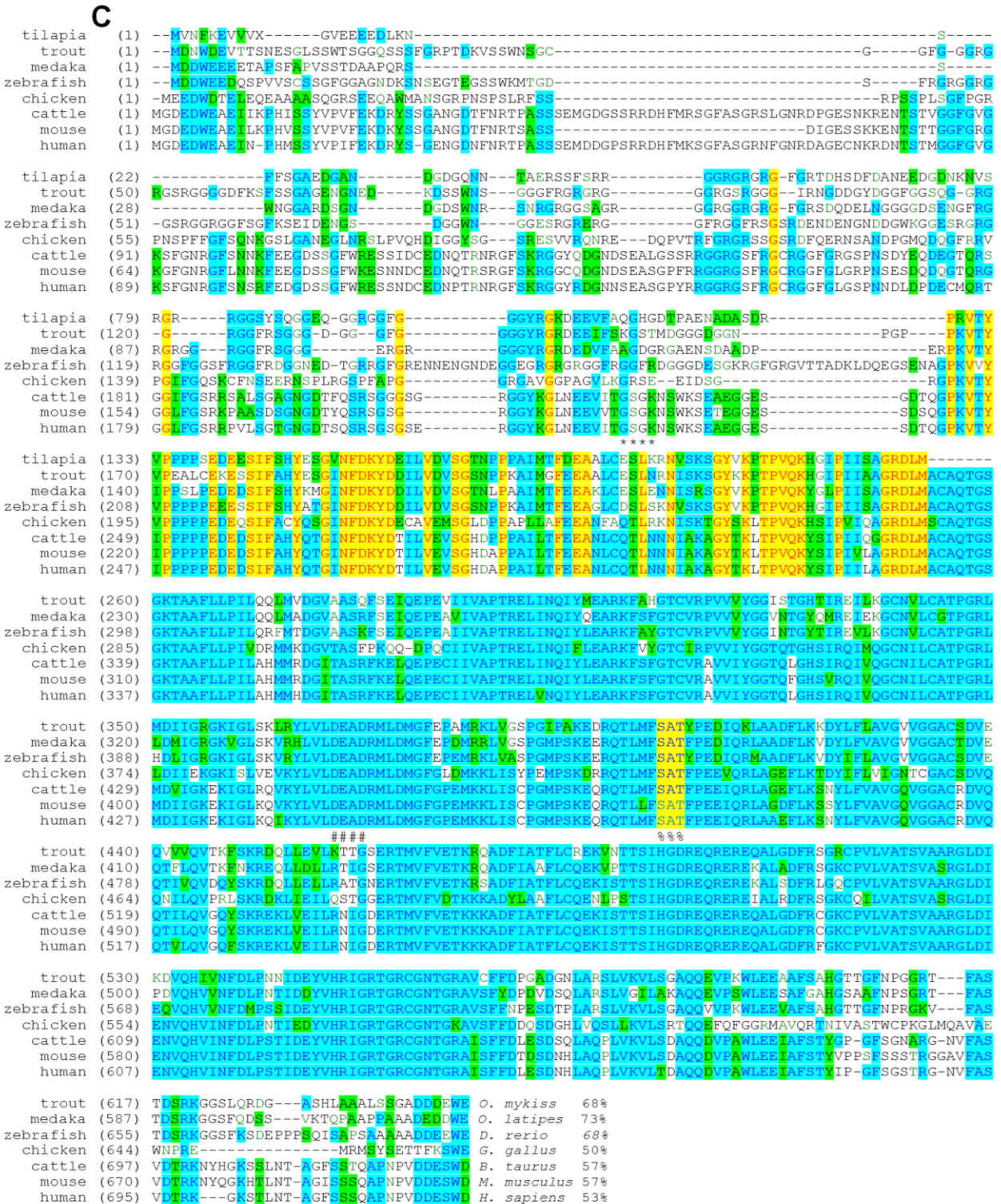


**Figure 5. Tilapia Vasa alignment with other organisms.** Cloned tilapia Vasa has many conserved domains. Different domains of DEAD box genes are labeled: Mg<sup>++</sup> binding domain (#), ATP binding domain (\*), Motif III (%).



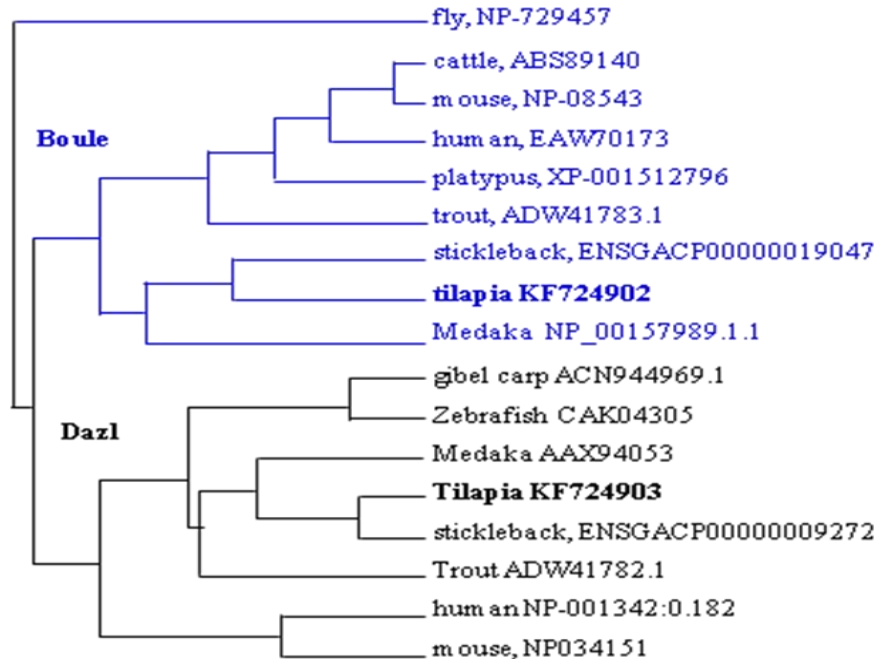


**Figure 6. Phylogenetic tree of Boule and Dazl proteins.** Boule and Dazl form separate clades. Branching between Boule and Dazl coincides with that between the fish and tetrapod lineages. Names of organisms and accession numbers are shown (Bhat and Hong, 2014).

### 1.3.3 Gonad-specific expression

The transcripts of *boule* and *dazl* were found in both male and female gonads (ovary and testis) by RT-PCR. Representative organs of ectodermal origin (brain and eye), mesodermal origin (heart and spleen) and endodermal origin (liver and gut) did not show the presence of both the genes (Figure 7). This demonstrates that both *boule* and *dazl* have bisexual gonad-specific expression in tilapia (Bhat and Hong, 2014). The slight difference in the intensity of the bands in the ovary and testis might be due to their level of expression in the tissues. Tilapia *vasa* was also cloned which is a standard germ cell marker (Kobayashi et al., 2000).  $\beta$ -actin was used as a control.



**Figure 7. RT-PCR of tilapia *boule*, *dazl* and *vasa*.** Transcripts of *boule*, *dazl* and *vasa* are present in ovary and testis similar to germ gene *vasa* but absent in somatic organs examined. *β-actin* was used as a control.

### 1.3.4 Expression of *vasa* in tilapia gonads

#### 1.3.4a Ovarian expression of *vasa* RNA

Adult ovary of tilapia has different sizes of oocytes which correspond to different stages of oogenesis (Figure 8A). Depending on the size and distribution of *vasa* RNA as described by (Kobayashi et al., 2000), oocytes were labeled from stage I-IV. There were significant differences in the expression pattern of *vasa* RNA among the stages of oogenesis as revealed by chemical ISH (Appendix 2). Strong *vasa* signals were evident in the cytoplasm of pre-vitellogenic oocytes of stage I and II. No *vasa* RNA was detected in the nuclei of germ cells. Although, the signals were seen throughout the cytoplasm, a few strong spots were observed (Appendix 2). Signals were much stronger as the vitellogenesis proceeded till stage III. The *vasa* signals decreased as vitellogenesis progressed to stage IV probably due to dispersion of RNA throughout the cytoplasm. This observation coincides with the findings of Kobayashi and group. RNA distribution was visualized in detail by FISH as it is a more sensitive staining technique to determine spatio-temporal distribution. RNA of *vasa* was uniformly distributed in post-vitellogenic oocytes whereas pre-vitellogenic oocytes had few clumps like structures in the cytoplasm which was clearly visualized by FISH

(Figure 8). The distribution pattern of *vasa* served as a platform in this study for germ cell visualization in more focused manner. As *vasa* is a well established germ cell marker, its distribution pattern analysis helped to channelize our observations.

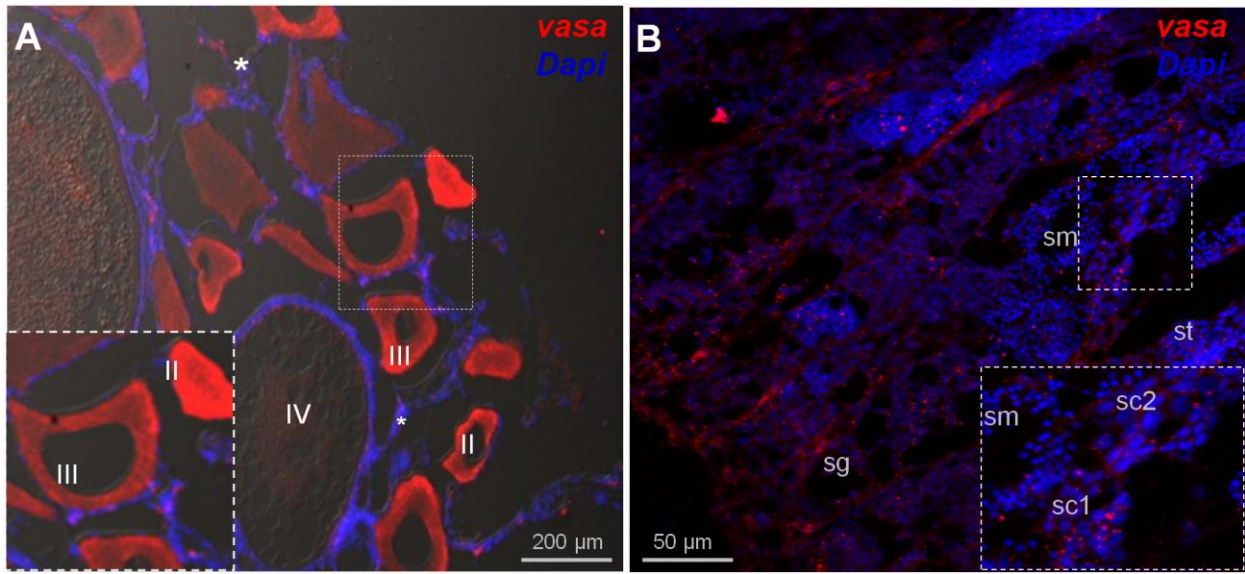


**Figure 8. Ovarian and testicular expression of *vasa* RNA.** (a) Schematic diagram to show the stages of oogenesis and spermatogenesis. Ovarian and testicular cryosections were subjected to hybridization with riboprobes against tilapia *vasa* and microscopically analyzed for the fluorescent signal (Red). (A) FISH on ovary sections. The *vasa* RNA is concentrated in pre-vitellogenic oocytes. Inset shows higher magnification of marked area to show *vasa* RNA in oocytes of stage II and III. Signals are absent in somatic cells (asterisks), which are visible by nuclear staining with Dapi (blue). (B) *vasa* RNA distribution in testis by FISH. Different stages of spermatogenesis are indicated: sg, spermatogonia; sc1, primary spermatocytes; sc2, secondary spermatocytes; st, spermatid; sm, sperm. sg, sc1 and sc2 have *vasa* RNA but spermatids have weaker and sm have no signal.

### 1.3.4b Testicular expression of *vasa* RNA

Testis section of tilapia reveals the ideal organization of spermatogenic components such as spermatogonia, primary and secondary spermatocytes, spermatids and spermatozoa or sperm. Male germ cells were positive for *vasa* RNA at stages from spermatogonia to early primary spermatocytes (Figure 8B). However, the signals were weaker in primary spermatocytes than spermatogonia and

were barely visible in secondary spermatocytes. The *vasa* RNA was hardly detectable in spermatids and sperm.

### **1.3.5 Germ cell-specific expression of *boule* in ovary**

CISH and FISH experiments were carried out to examine the ovarian expression pattern of *boule* RNA. ISH revealed that *boule* was expressed only in germ cells but not in surrounding somatic cells (Figure 9A). Interestingly, *boule* was prominent in stages I-III but barely detectable in stage IV oocytes. The *boule* RNA showed perinuclear distribution in stage I and uniform distribution in stage III and IV oocytes (Figure 9B). The signal was the strongest at stage III. Much detailed spatio-temporal signal distribution in oocytes was observed by FISH (Figure 10A and B). Granulated appearance of *boule* signal was seen in the cytoplasm of both pre and post-vitellogenic oocytes. Signal strength was at its peak in stage III as previously shown by CISH. Stage IV oocytes showed the weakest signal intensity and the distribution was granulated similar to earlier stages.

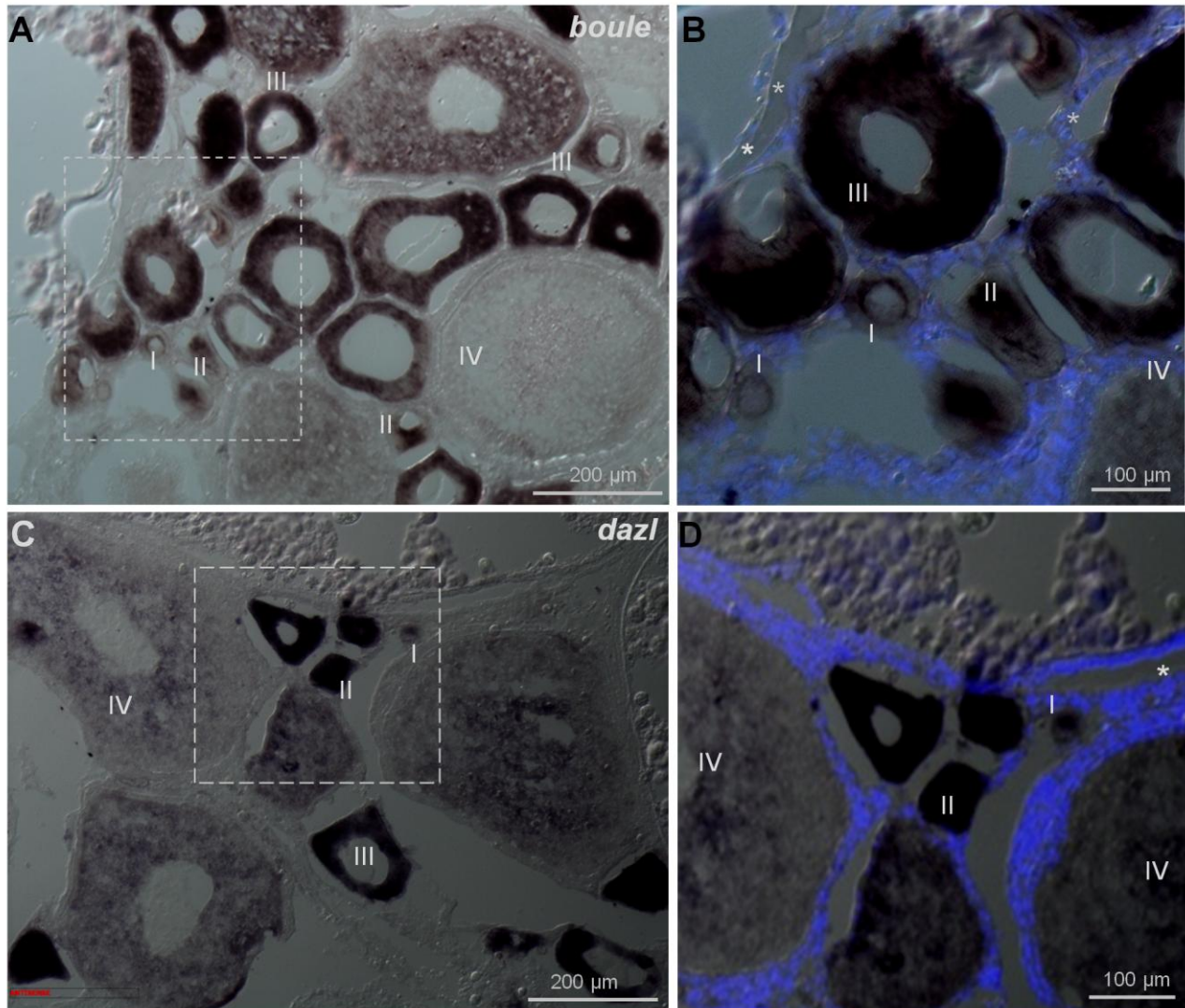


**Figure 9. Localization of *boule* and *dazl* RNA by CISH.** Ovarian cryosections were subjected to hybridization with riboprobes against tilapia *boule* or *dazl* and microscopically analyzed for the chromogenic signal (brown to black). (A) *boule* at low magnification and (B) high magnification of the framed area in (A) showing oocytes at four different stages (I-IV). The *boule* RNA is seen in the perinuclear region of stage I oocyte, concentrated at centre in stage II oocytes but dispersed in advanced oocytes. (C) *dazl* at low magnification (D) and high magnification of framed area in (C). The *dazl* signal is present in stage I- IV oocytes and has strong expression in early stages. Stage III showed weaker signal than stage II and stage IV was the weakest among all the four stages. Signals are absent in somatic cells (asterisks) which are visible by nuclear staining with Dapi (blue).

### 1.3.6 Germ cell-specific expression of *dazl* in ovary

CISH and FISH experiments with an antisense *dazl* riboprobe showed germ cell-specific expression (Figure 9C and D). Unlike *boule*, *dazl* expression was prominent in oocytes at stages I and II and

decreased gradually until it became hardly detectable in stage IV. Notably, the signal was the strongest in stage II oocytes. FISH analysis revealed that the distribution of *dazl* signal in the cytoplasm is uniform and non-granulated (Figure 10 C and D).

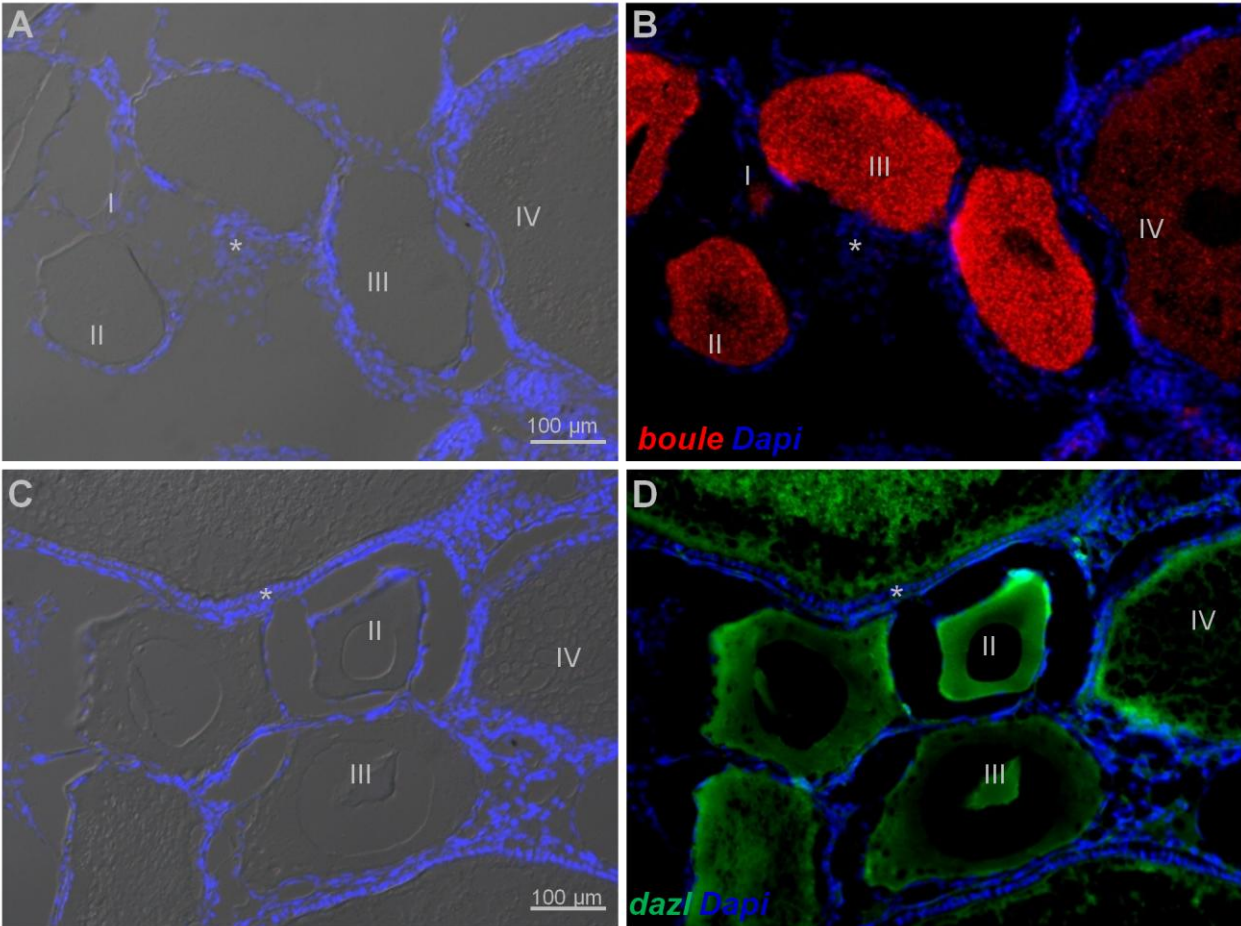


**Figure 10. Localization of *boule* and *dazl* RNA in ovary by FISH.** Ovarian cryosections were subjected to hybridization with riboprobes against tilapia *boule* or *dazl* and microscopically analyzed for the fluorescent signal (*boule*-Red, *dazl*-Green). (A) Bright field and Dapi (B) *boule* with Dapi. The *boule* RNA is dispersed in stage I-III oocytes. Stage IV has weak signal. (C) and (D) show ovarian sections with *dazl* distribution. (C) Bright field with Dapi, (D) *dazl* with Dapi. RNA of *dazl* is distributed in stage II-IV oocytes and has strong signal in stage II oocytes. Stage III has weaker signal than stage II and stage IV has the weakest. Signal of *dazl* is smooth in appearance. The *boule* and *dazl* signals are absent in somatic cells (asterisks) which are visible by nuclear staining with Dapi (blue).

### 1.3.7 Germ cell-specific expression of *boule* in adult testis

Testicular expression of *boule* RNA was analyzed by CISH and FISH. The expression of *boule* was restricted to male germ cells and absent in surrounding somatic cells (Figure 11A and B). The *boule* RNA was clearly detectable in spermatogonia, primary and secondary spermatocytes as well as in spermatids. Signal was barely detectable in sperm (Figure 12A and B).

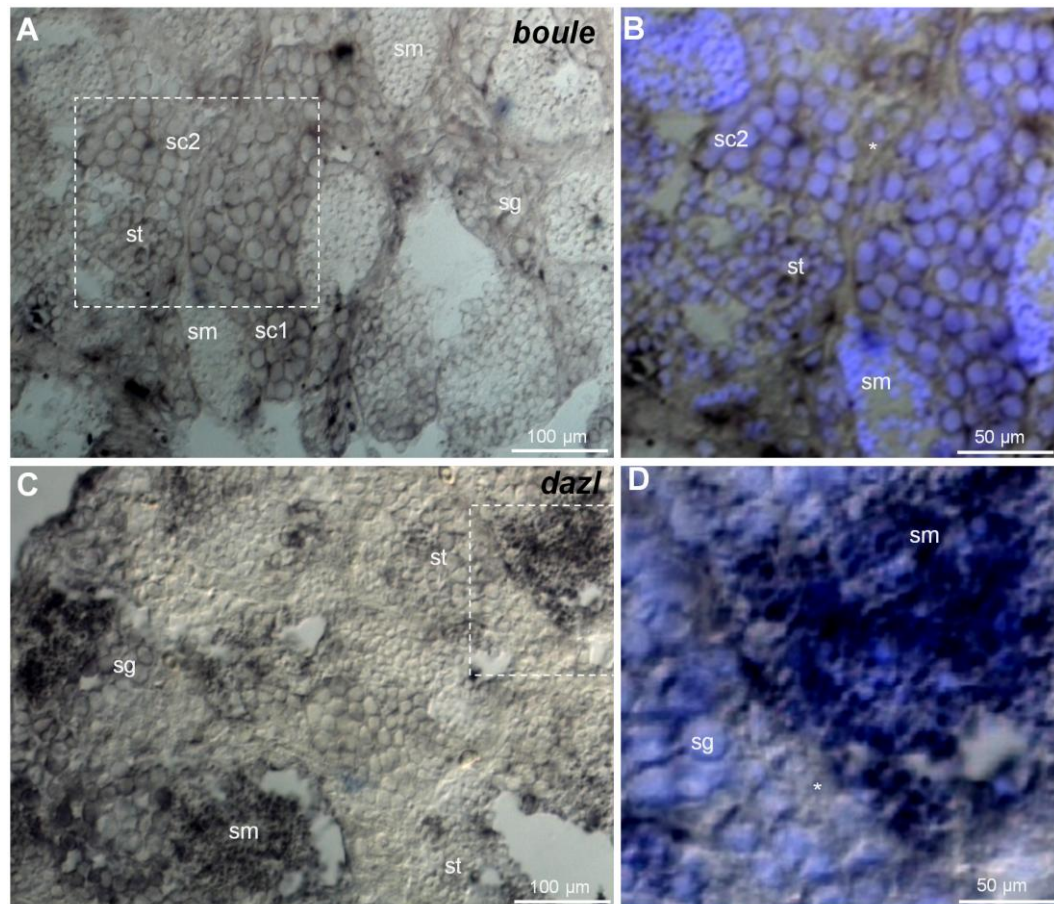


**Figure 11. Localization of *boule* and *dazl* RNA in testis by CISH.** Adult tilapia testicular cryosections were hybridized with antisense RNA probes and signals were visualized by Chromogenic staining. (A) Lower magnification of testis section showing the testicular architecture and position of different stages of gametes during spermatogenesis. Different stages of spermatogenesis are indicated: sg, spermatogonia; sc1, primary spermatocytes; sc2, secondary spermatocytes; st, spermatid; sm, sperm. The expression of *boule* is persistent in sg, sc1, sc2 and started declining in st and disappeared in sm. (B) Higher magnification of framed area in (A) showing residual distribution of *boule* RNA in st and absence in sm. (C) Lower magnification showing *dazl* distribution in different stages of spermatogenesis. (D) Higher magnification of framed area in (C) showing detailed distribution of *dazl* RNA. Signal increased from sg to sm as the meiosis progressed; sg shows low signal intensity which increased and peaked in sperm. Both *boule* and *dazl* signals are absent in somatic cells (asterisks).

### 1.3.8 Germ cell-specific expression of *dazl* in testis

The *dazl* signal was weak in spermatogonia and progressively increased as spermatogenesis progressed. Primary and secondary spermatocytes showed slightly stronger expression than spermatogonial cells (Figure 11C and D). The strongest expression of *dazl* was observed in spermatids and sperm by both CISH and FISH experiments (figure 12C and D).

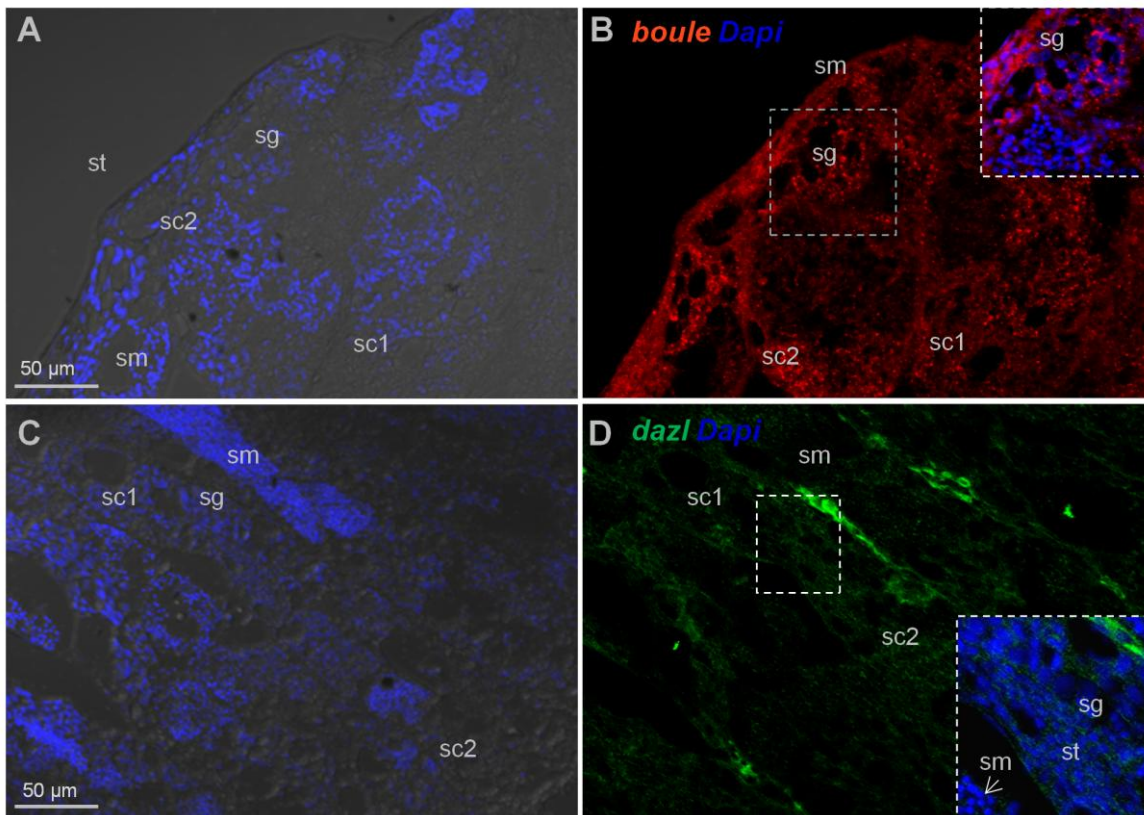


**Figure 12. Localization of *boule* and *dazl* RNA in testis by FISH.** Adult tilapia testicular cryosections were hybridized with antisense RNA probes and signals were visualized by fluorescent staining. (A) Bright field with Dapi. Different stages of spermatogenesis are indicated: sg, spermatogonia; sc1, primary spermatocytes; sc2, secondary spermatocytes; st, spermatid; sm, sperm. (B) *boule* (red) is visible in sg, sc1, sc2, declined in st and disappeared in sm. Inset with higher magnification of framed area in (B) showing presence of *boule* RNA in sg and absence in sm. (C) Bright field with Dapi. (D) Distribution of *dazl* RNA (green) from sg to sm. Expression increased as the spermatogenesis progressed.

Taken together, *boule* RNA expression increased as oogenesis proceeded from stage I-III with peak expression taking place at stage III. The *dazl* RNA was abundant throughout oogenesis but peaked at stage II. Therefore, *boule* and *dazl* in the ovary show a conserved germ cell-specific



expression and stage-specific peak expression. RNAs of *boule* and *dazl* exhibit conserved germ cell-specific expression also in the testis.

### **1.3.9 Localization of *vasa* with *boule* and *dazl***

#### **1.3.9a Expression of *vasa* and *boule* in ovary and testis**

Double color *in situ* hybridization (DISH) was performed for the visualization of two RNA probes on ovary and testis sections of tilapia. DISH allows the analysis of expression pattern of two genes simultaneously. RNAs of FITC labeled *vasa* and DIG labeled *boule* were localized in ovary. RNA of *vasa* was localized in early stages of oogenesis and gradually decreased as oocytes matured. RNA of *boule* was also present throughout oogenesis however, strong expression was observed in stage III. The expression was significantly reduced in stage IV (Figure 13A-F). In the testis, *vasa* and *boule* showed the differences in the signal intensities at different spermatogenic stages. RNA of *boule* was abundant throughout spermatogenesis except sperm. RNA of *vasa* was weaker in spermatocytes and spermatids. Signal of *vasa* decreased earlier than *boule* with the progression of spermatogenesis. Both RNAs showed overlapped expression till spermatogenesis progressed up to secondary spermatocytes after which they were hardly detectable (Figure14A-F).

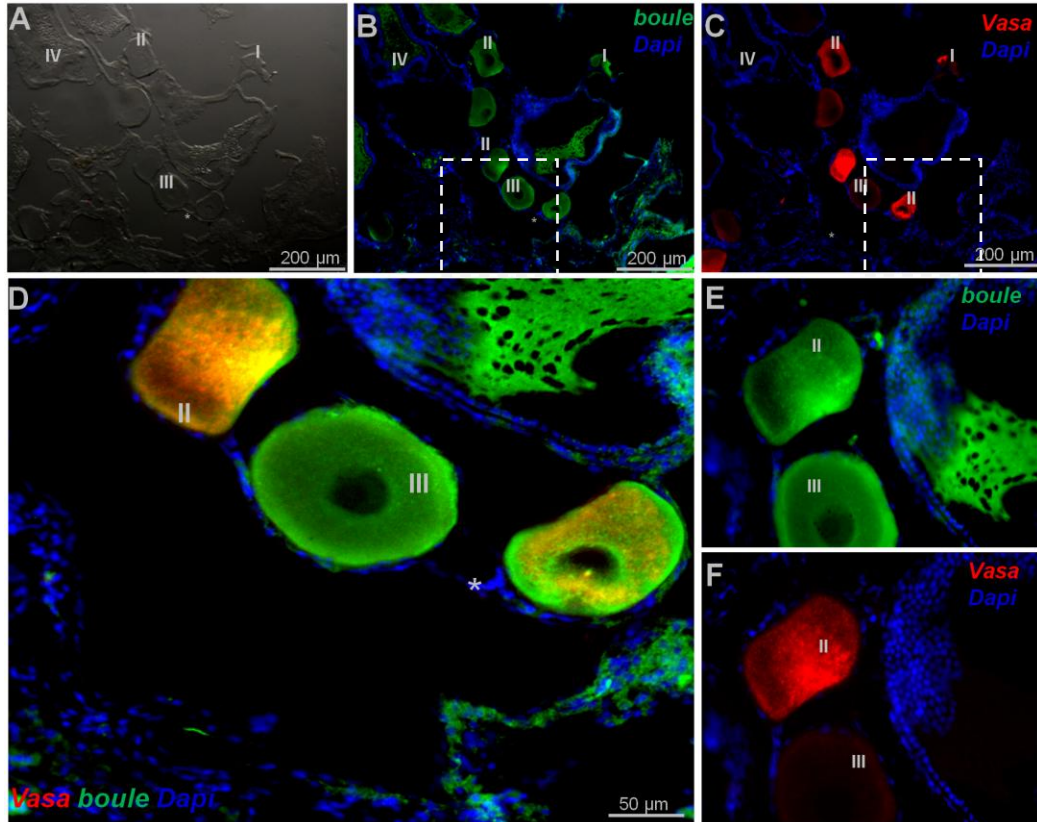


**Figure 13. Expression of *vasa* and *boule* in ovary.** Adult tilapia ovarian cryosections were hybridized with antisense RNA probes and signals were visualized by fluorescence. (A-F) *vasa* (red) and *boule* (green). Lower magnification of ovary sections, (A) bright field with Dapi (B) *boule* with Dapi (C) *vasa* with Dapi (D) merged image at higher magnification of the framed area in (B) and (C). RNA of *vasa* is present in early stages of oogenesis and gradually decreases as oocytes mature. RNA of *boule* shows uniform distribution but differs in intensity of expression among different stages of oogenesis. (E and F) Higher magnification of the area marked in (D).

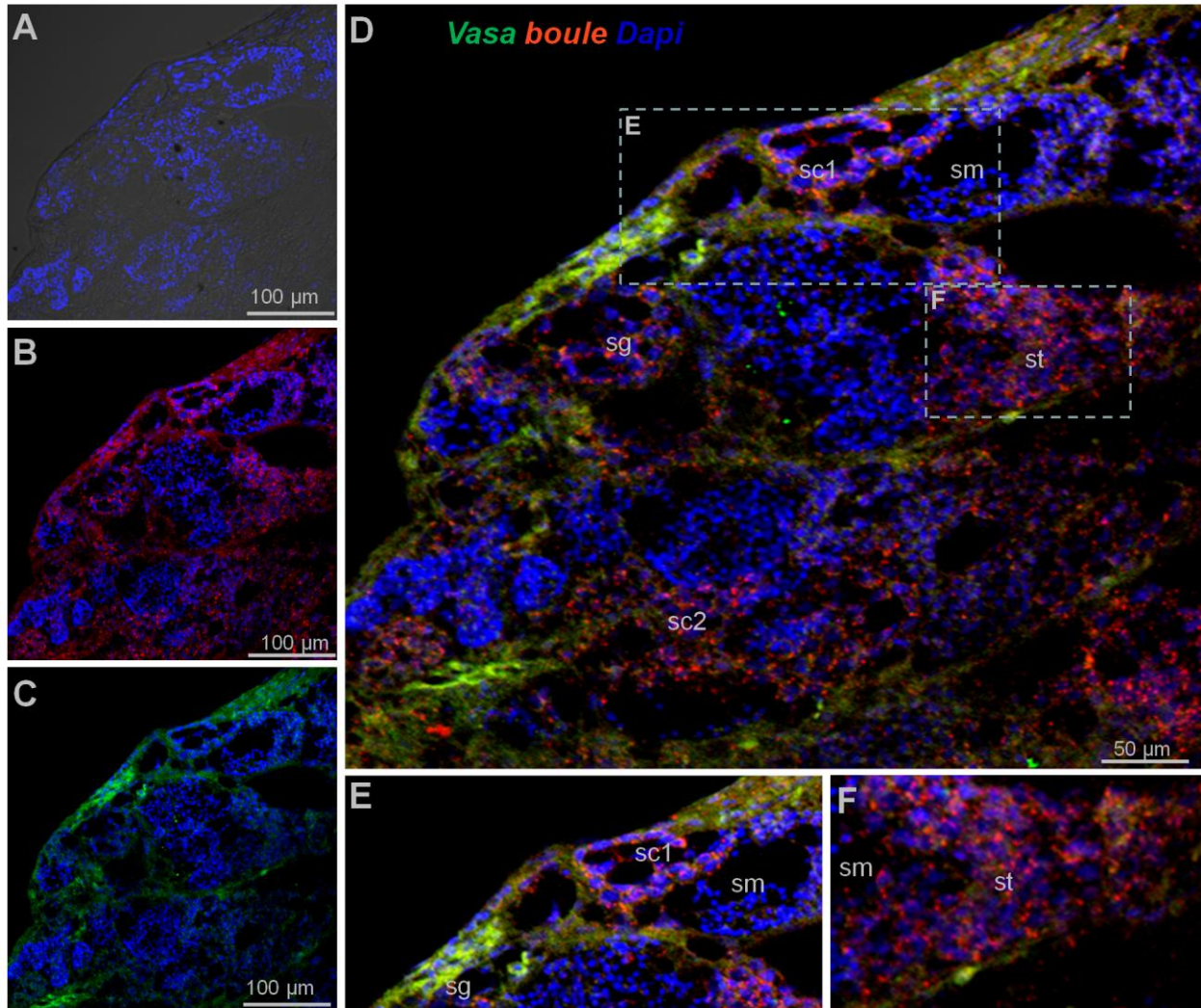


**Figure 14. Expression of *vasa* and *boule* in testis.** Adult tilapia testicular cryosections were hybridized with antisense RNA probes and signals were visualized by fluorescence. Lower magnification of testis sections (A) bright field with Dapi (B) *boule* with Dapi (C) *vasa* with Dapi (D) *boule*, *vasa* with Dapi. (E and F) Higher magnification of the areas marked in D). Different stages of spermatogenesis are indicated: sg, spermatogonia; sc1, primary spermatocytes; sc2, secondary spermatocytes; st, spermatid; sm, sperm. RNA of *boule* was abundant throughout spermatogenesis except sm despite signal strength. *boule* persisted till spermatogenesis reached final stage to form sm. Signals of *vasa* localized in sg but weaker in sc and st, which decreased with spermatogenic progression earlier than *boule*.

### 1.3.9b Expression of *vasa* and *dazl* in ovary and testis

Distribution of *vasa* and *dazl* were analyzed by DISH in ovary. By DISH, the expression of *vasa* was observed throughout oogenesis. Signal distribution was strong in pre-vitellogenic oocytes of stage I and II whereas slightly weaker in stage III and the weakest in stage IV (Figure 15A-D). Uniform

distribution with gradual reduction of expression of *vasa* was observed in the ovary as previously observed by chromogenic staining and single probe ISH. In addition to this, *dazl* was co-expressed with *vasa* in pre-vitellogenic oocytes however; the strongest expression was seen in stage II and declined gradually in advanced stages of oogenesis (Figure 15). Hence, both genes showed overlapped expression in early stages and reduced as the vitellogenesis progressed.

In the testis, *vasa* RNA was detectable in sg, sc1 and sc2 but was hard to be detected in st and was not detectable in sm (Figure 16 A-D). Similarly RNA of *dazl* was also present throughout spermatogenesis showing weak expression in sg and gradual increase as spermatogenesis progressed. The expression was the strongest in sm.

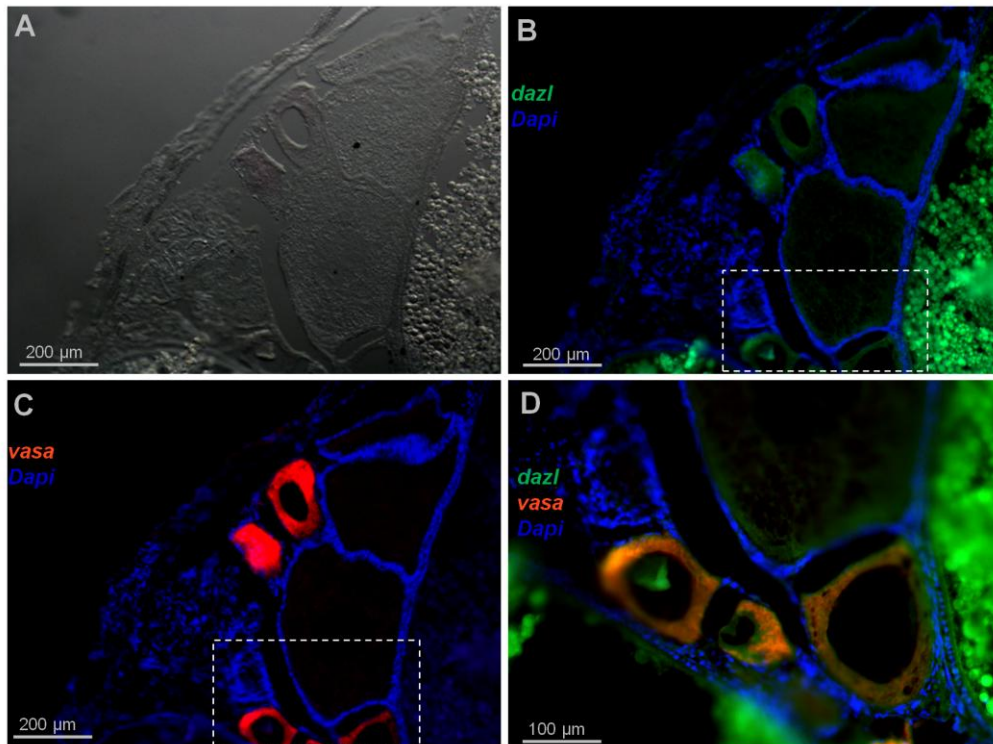


**Figure 15. Expression of *vasa* and *dazl* in ovary.** Adult tilapia ovarian cryosections were hybridized with antisense RNA probes and signals were visualized by fluorescence. (A) Bright field (B) *dazl* with Dapi (C) *vasa* with Dapi (D) Higher magnification of the framed areas in (B) and (C). (D) The *vasa* signal is present throughout oogenesis but stronger in pre-vitellogenic oocytes of stage I-III. Stage IV has the least signal intensity. The *dazl* is present in pre-vitellogenic oocytes. Both the expressions gradually diminished as vitellogenesis progressed.

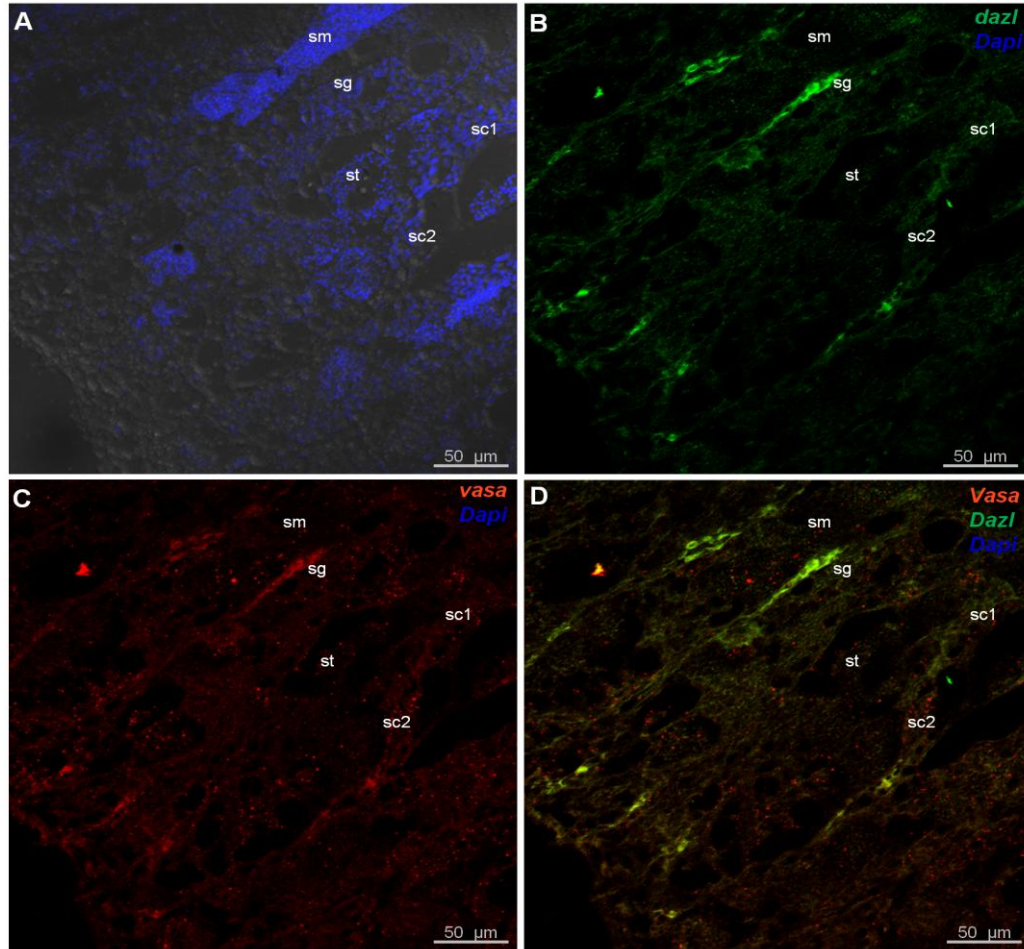


**Figure 16. Expression of *vasa* and *dazl* in testis.** Adult tilapia testicular cryosections were hybridized with antisense RNA probes and signals were visualized by fluorescence. (A) Bright field with Dapi (B and C) Distribution of *vasa* (red) and *dazl* (green). *vasa* is expressed in sg, sc1 and sc2, decreased in st and diminished in sm. Signal of *dazl* was present from sg to sm as the spermatogenesis progressed; sg shows low signal intensity which increased and peaked in sm (B). Signal in sm is less visible because of less cytoplasmic content in them. (D) Merged image to show *vasa* is co-expressed with *dazl* but differs in intensity of signal during early spermatogenesis.

### 1.3.10 Localization of *boule* and *dazl* RNAs in ovary

Previously as shown by chromogenic staining, *boule* was distributed in stage I-IV oocytes though the signal intensity differed among the stages. Signal was persistent throughout oogenesis including oogonia, but higher intensity was observed in stage III oocytes which matched with the previous observation. Expression of *dazl* RNA also was present in stage I-III oocytes but barely detectable in stage IV. Unlike *boule*, *dazl* showed the strongest expression in stage II oocytes

which significantly reduced as vitellogenesis progressed. Oogonial cells which were very few in the adult ovary sections showed both the signals (Figure 17A-F). However, DISH revealed that *boule* signal intensity was slightly weaker than *dazl* even though the concentration of probes was equal.

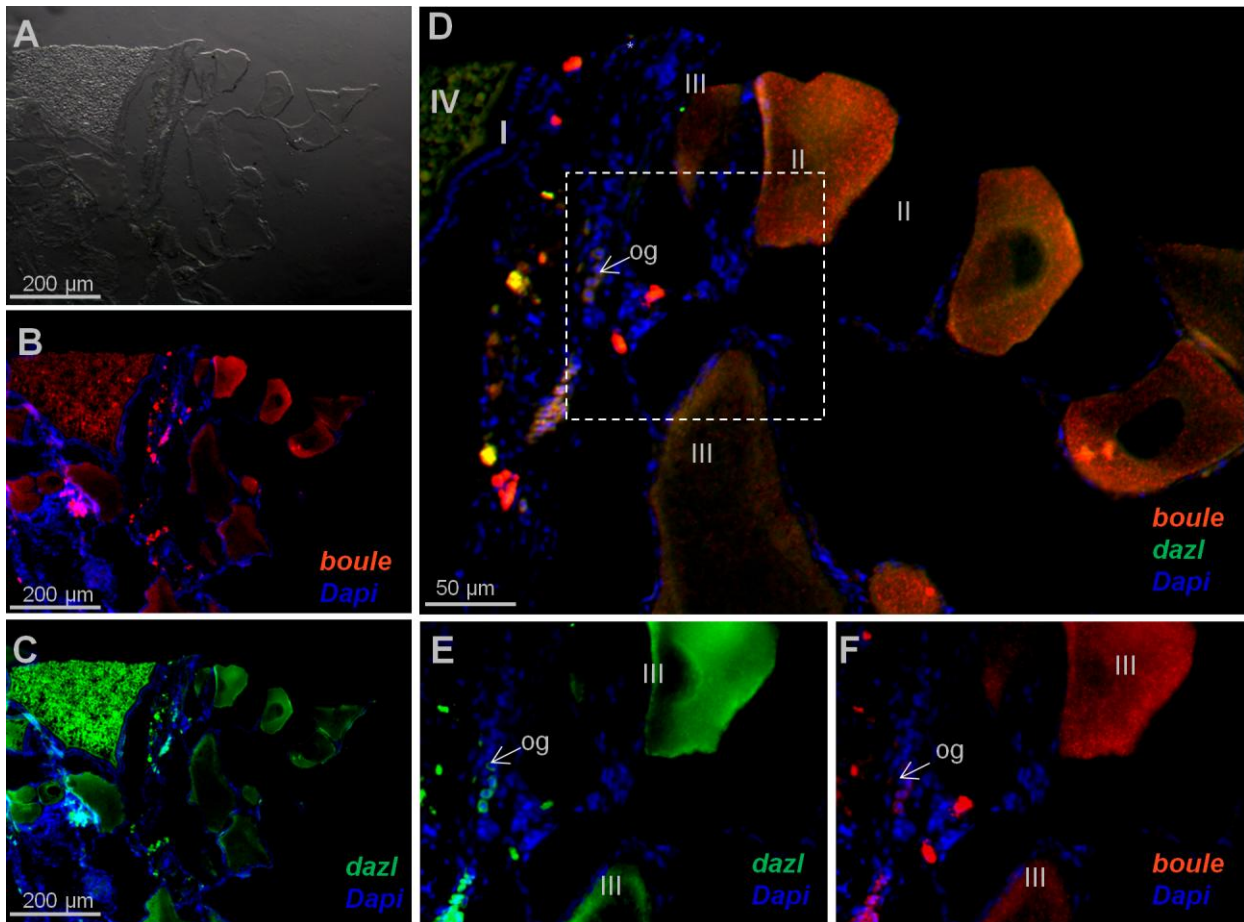


**Figure 17. Localization of *boule* and *dazl* in ovary.** Adult tilapia ovarian cryosections were hybridized with antisense RNA probes and signals were visualized by fluorescence staining. (A) Bright field (B) *boule* with Dapi (C) *dazl* with Dapi (D) *boule*, *dazl* with Dapi. (E and F) Higher magnification of the area marked in (D). The *boule* RNA is expressed in oogonia and in stage I-III oocytes. The *dazl* is also expressed in oogonia and stage I-III oocytes.

### 1.3.11 Localization of *boule* and *dazl* RNAs in testis

DISH revealed that both *boule* and *dazl* were present throughout spermatogenesis. However signal intensity varied as shown previously in chemical ISH. FISH is much sensitive to detect the signals

hence appropriate in RNA localization. Both *boule* and *dazl* were localized in spermatogenic components (Figure 18A-G). Expression of *boule* was persistent in sg, sc1, sc2 and was declined in st which ultimately disappeared in sm. Higher magnification showed residual distribution of *boule* RNA in st, and absence in sm (Figure 18G). Distribution of *dazl* RNA was also observed from sg to sm as the spermatogenesis progressed where sg showed lower signal intensity which increased and peaked in sperms.

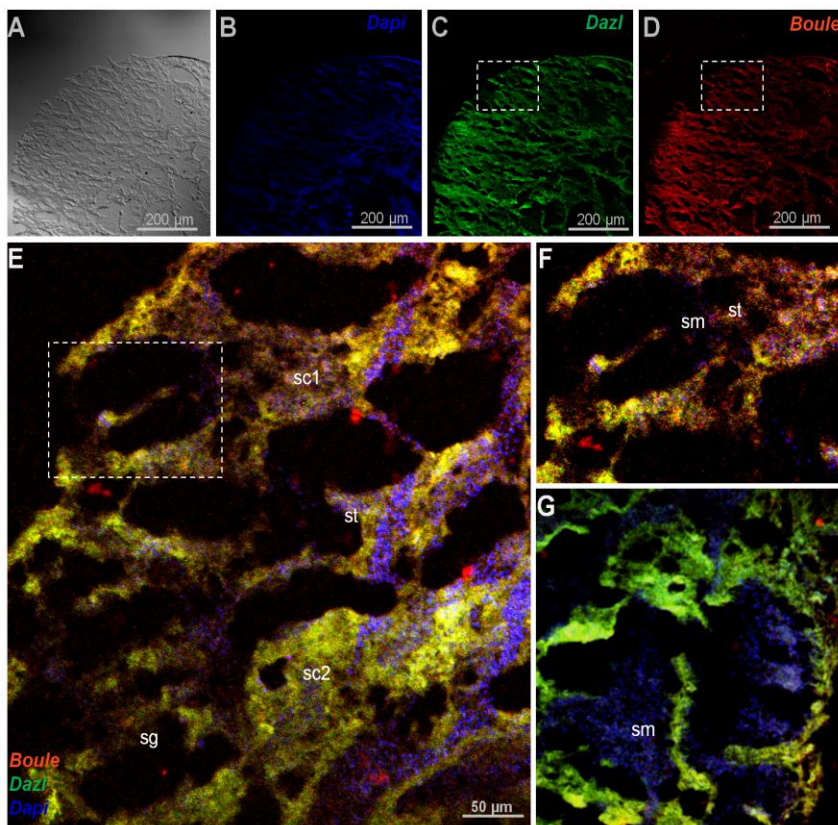


**Figure 18. Localization *boule* and *dazl* in testis.** Adult tilapia testicular cryosections were hybridized with antisense RNA probes and signals were visualized by fluorescence staining. Lower magnification of testis sections (A) bright field (B) Dapi (C) *dazl* (D) *boule*. Different stages of spermatogenesis are indicated: sg, spermatogonia; sc1, primary spermatocytes; sc2, secondary spermatocytes; st, spermatid; sm, sperm. The expression of *boule* is persistent in sg, sc1, sc2 and was declined in st which disappeared in sm. (E) Higher magnification of framed area in (C and D) showing presence of *boule* RNA in sg-st and absence in sm. *dazl* RNA expression increased from sg to sm as the spermatogenesis progressed; sg showed lower signal intensity which increased and peaked in sperms. (F and G)

higher magnification of the area marked in (E) to show the absence of *boule* in sm and presence of *dazl* in them.

Taken together, both *boule* and *dazl* RNAs showed germ cell-specific and overlapped expression during gametogenesis of both the sex in the Nile tilapia.

## **Part 2: Improvement of medaka stem cell culture and Primordial Germ cell cultures.**

### **2.1. Introduction**

#### **2.1.1. Embryonic stem cells**

Embryonic stem (ES) cells are produced from the inner cell mass (ICM) of the blastocyst. A stem cell can divide to produce many daughter cells that are identical to each other and to parent stem cell. A stem cell is also capable of producing specialized cells. The ability of self-renewal and differentiation are the defining properties which make stem cells distinguishable from other cells. Since the establishment of first ES cell line in mice, stem cells are the focus of active research because of their enormous potential for basic research, medicine and animal biotechnology. Criteria for characterizing putative stem cell lines include cell morphology, surface markers and gene expression profile (Hong et al., 2010). ES cells represent a convenient model to investigate fundamental aspects of cell stemness and early embryo development. ES cells are the only stem cell types that are able to show indefinite self-renewal and differentiation into cellular derivatives of ectodermal, mesodermal and endodermal lineages. Recent studies have revealed that ES cells maintain self-renewal and pluripotency with a self-organizing network of transcription factors and intracellular pathways activated by extracellular signaling that together prevent their differentiation and promote their proliferation (De Felici et al., 2009).

ES cells have an indefinite proliferative life span and generate long-living subclones obtained by single-cell expansion (Martello and Smith, 2014). ES cells of mouse originate from the ICM cells which tend to differentiate spontaneously. Spontaneous differentiation is a major challenge for ES cell derivation. Inhibition of spontaneous differentiation in mice is achieved by using a layer of feeder cells (Evans and Kaufman, 1981) or conditioned medium (Martin, 1981). Since the establishment of mouse ES cells, many such attempts were made towards ES cell derivation in many



different mammalian species. Such partially successful short-term ES cell cultures raised a question whether the ability to achieve ES cells was limited to mouse or the conditions to inhibit spontaneous differentiation were inappropriate in other mammalian species (Hong et al., 2011).

Work towards fish ES cells dates back to 20 years by adopting the feeder layer technique in zebrafish (Collodi et al., 1992) and medaka (Wakamatsu et al., 1994). The small laboratory fish medaka (*Oryzias latipes*) is an excellent model system for analyzing vertebrate development (Wittbrodt et al., 2002) and stem cell biology in lower vertebrates (Hong, 2011). Independently a feeder-free culture condition for fish ES cell derivation from medaka was developed leading to the establishment of three ES cell lines MES1 to MES3 in 1996 (Hong et al., 1996). Since mouse is one of the most advanced vertebrates and medaka is among the most primitive vertebrates, the success in medaka ES cells provided direct evidence for the possibility to derive ES cells in diverse vertebrate species. Subsequently human ES cells were obtained from the ICM of the blastocyst of an early-staged embryo (Thomson et al., 1998).

In feeder-free culture system of medaka ES cells, an essential component of ES cell medium is the embryo extract from medaka which together with basic fibroblast growth factor and fish serum is capable of supporting self-renewal of disassociated midblastula embryo (MBE) cells on a gelatin-coated culture plate (Hong et al., 1996). In this organism, a male germ stem cell line from adult spermatogonia was also developed (Hong et al., 2004). It was found that one of the diploid ES cell lines from medaka was capable of directed differentiation into melanocytes by ectopic expression of the microphthalmia-associated transcription factor (Bejar et al., 2003). These studies prove the potential of ES cells from medaka as a lower vertebrate which can be utilized to analyze several biological problems.

### **2.1.2 Medaka haploid ES (hES) cells**

Haploid embryonic stem cells combine the properties of haploidy and pluripotency, enable direct genetic analysis of recessive phenotypes in vertebrates (Yi et al., 2009). Haploidy is the presence of single set of chromosomes like yeast, a powerful platform to analyze molecular events. In 2009, it was a major step achieved in vertebrate stem cell biology where hES cell lines from medaka were successfully generated (Yi et al., 2009; Yi et al., 2010). The condition for medaka hES cell derivation was similar to that for diploid MES1 but haploid blastula embryos were used for cell culture initiation instead of fertilized diploid blastulae (Figure 19). Briefly, sperm of *i3* strain of medaka were treated with an elaborate dose of ultra-violet light irradiation to destroy their nuclei and to trigger egg activation. These genetically inactivated sperm were mixed with mature oocytes of *i1* strain resulting in eggs only with a haploid female nucleus. Such embryos undergo gynogenesis where all the resulting embryos will be females. At midblastula stage, the gynogenetic haploid embryos were dissociated into single cells and seeded for feeder-free culture on gelatin-coated substrata. Haploid ES cell derivation is more demanding and additionally requires media conditioned by MES1 and MO1, a medaka ovary-derived cell line. However, once established, hES cells are not different from diploid ES cells in conditions for maintenance. Haploid ES cells show all characteristics of MES1, including stable and competitive growth, genetic stability and pluripotency *in vitro* and *in vivo* (Yi et al., 2009; Yi et al., 2010).

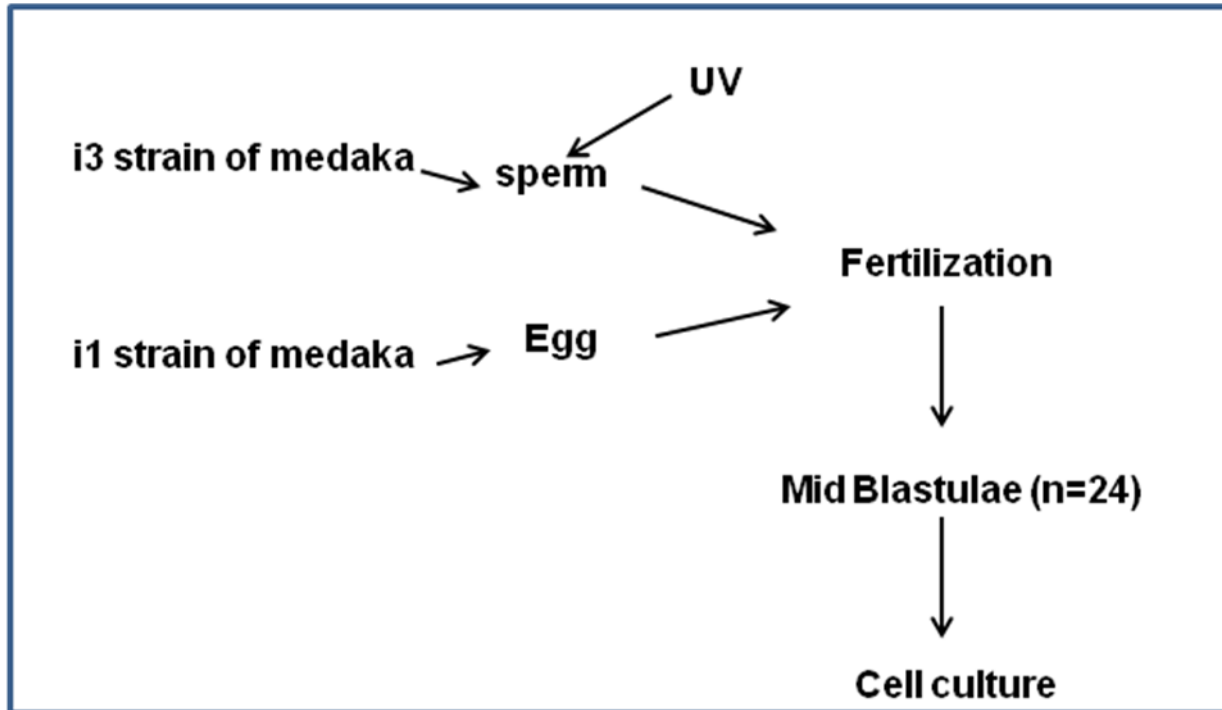


**Figure 19. Procedure for medaka hES cell derivation.** UV-irradiation destroys the nucleus of sperm without compromising their ability to trigger egg activation for haploid gynogenesis. Resulting haploid embryos are then dissociated at the midblastula stage into single cells for cell culture initiation (Yi et al., 2009).

Haploidy, is a strong system for genetic analyses of molecular events because any recessive mutations of essential genes will show a clear phenotype due to the absence of a second gene copy. ES cells are pluripotent and thus are able to differentiate into almost all cell types, providing an excellent system for experimental analyses of cellular and developmental events *in vitro* (Wobus and Boheler, 2005). However, repetitive subculture, cryopreservation and thawing lead to higher rate of cell death. Rapid diploidization was also observed in mouse hES cells (Leeb and Wutz, 2011). High rate of apoptosis upon recovery after long-term freezing in medium containing DMSO is a major concern in most ES cell systems.

#### **2.1.4 Primordial Germ cells**

All sexually reproducing organisms arise from gametes which are highly specialized and contain genetic information for the production of whole organism. All gametes arise from primordial germ cells (PGCs), a small population of cells set aside from other cell lineages very early in embryonic life in most animal species (Wylie, 1999). Soon after fertilization of male and female gametes, the resulting embryo divides and produces multiple cells (blastomeres) which acquire their specificity after several divisions. Cells in the early developmental stage are able to become any cell type upon stimulus. As the early development with division of blastomeres progresses, specificity to become particular cell type also increases. When PGCs first appear in the embryo, they have the potential to become gametes of either sex. These cells are pluripotent cells having the capacity to produce whole new organism rather than just organs. Hence PGCs are the real stem cells of the organism where other cells do not have the ability to give whole new organism. They are the means of evolution and also carriers of hereditary diseases. PGCs with their unique ability to retain true developmental totipotency, are considered as the mother of all stem cells. Despite several similarities with ES cells, they display only transient self-renewal capability and distinct lineage-specific characteristics. In fact, in normal condition PGCs are believed to differentiate into germ cells only, oogonia/oocytes in the female, and prospermatogonia in the male which ultimately produce eggs and sperm respectively (De Felici et al., 2009).

#### **2.1.5 Germ cell identity**

Germ cells can often be distinguished from somatic cells during early development using histological and molecular characteristics. In laboratory organisms, descriptive techniques can be combined with experimental methods to identify PGCs. Although experimental data are not available for most non-model organisms, often a combination of histological and molecular data can

indicate the site and developmental timing of PGC formation. Most cell types were identified by their histological characteristics until the advent of molecular techniques. Germ cells were recognized by their characteristic large round nucleus, single large nucleolus, cytoplasm relatively clear of organelles and granular cytoplasmic material. Transmission electron microscopy (TEM) revealed that electron-dense masses exist in the cytoplasm of germ cells of all phyla studied to date. These dense bodies are known as nuage or germ granules and can be used to identify PGCs at early developmental stages. Germ cell-specific organelles such as the mitochondrial cloud and Balbiani body contain dense bodies.

Other than morphology, enzyme markers such as alkaline phosphatases can be used to identify PGCs. However, because these markers are not always expressed by PGCs at all stages of development, they are usually only suitable for identifying germ cells at certain times of development. Modern studies often identify PGCs by identifying the products of germ cell-specific genes. Products of the *vasa* gene family are the most widely used molecular PGC markers. *vasa* encodes a DEAD-box RNA helicase that is usually expressed specifically in the germline. The high conservation of motifs in these genes made them easy to clone from many phyla. Similar to many other organisms, zebrafish *vasa* mRNA is maternally supplied and it is detected in the PGCs during all stages of germ line development.

The findings obtained in zebrafish were extended generally to fish that PGCs are specified by determinants found in the germ plasm and that the position of the germ plasm could be inferred from the position of RNA molecules such as *vasa* and *nanos* which mark the early germ plasm. Surprisingly, the cloning of the *vasa* and *nanos* genes from another teleost, medaka (*Oryzias latipes*) and analysis of their mRNA expression patterns did not provide direct support for the notion that germ plasm is responsible for PGC specification in all fish species (Herpin et al., 2007). Hence, the

prediction of the earliest time point at which germline specification happens in medaka remains as an unsolved puzzle. Such debatable questions can be answered by the attempts to culture PGCs in order to analyze them in detail.

### **2.1.6 Transcriptional and translational regulation**

When first specified, PGCs often remain transcriptionally quiescent, while the surrounding soma is transcriptionally active. Germ cell transcriptional repressors can be gene-specific (e.g. *germ cell-less* in *Drosophila*) or global (e.g. *pie-1* in *C. elegans*). Translational repression in the germline has also been documented in *Drosophila* and *C. elegans*, but it is not clear how widely the mechanisms are shared (Extavour and Akam, 2003). It would be interesting to know the mechanism behind PGC formation provided that they are able to be cultured for sufficient duration to carry out any studies.

### **2.1.7 Importance of Primordial germ cell culture**

Germ cells play an important role in carrying genetic information to the next generation thereby help in species continuation. In many species, germ cells start with a small population of cells with tremendous potential to become gametes. They represent the earliest cell lineage to be determined. The following sections deal with the approach and advances in PGC culture from the various organisms in the past few years. Identification, isolation and requirements for PGC culture from various other organisms as well as medaka are described in consequent sections.

The isolation and culture of PGCs allow both the analysis of gene expression in these cells as well as studies of their behavior and growth requirements. Following their specification, PGCs have unique control over their basic cell functions, such as transcription, translation, stabilizing of RNAs and proteins and responses to differentiation cues. Considering these properties of PGCs, it is useful to culture them *in vitro* (De Miguel and Donovan, 2000). Several studies show the importance of

germ cell cultures in studying signaling pathways, for example those on LIF receptor disruption (Yoshida et al., 1996).

### **2.1.8 Challenges in PGC culture**

Embryonic germ (EG) cell-mediated gene transfer has been successful in the mouse for more than a decade. However this approach is limited in other species due to the difficulty of isolating the small numbers of progenitors of germ cell lineage (PGCs) from early-stage embryos and the lack of information on the *in vitro* culture requirements of the cells (Fan et al., 2008). Feeder dependent culture of PGCs from mouse up to 7 days was achieved previously (Resnick et al., 1992). In 2008, zebrafish PGCs were cultured by Fan and group and they showed in optimal growth conditions, PGCs continued to proliferate for at least 4 months in culture. Mid blastula embryos are capable of generating ES-like cells in culture was reported by our group (Li et al., 2011c). Recently, PGC formation and cultivation *in vitro* from blastomeres dissociated from midblastula embryos (MBEs) of medaka has also been reported (Li et al., 2014).

A major problem in understanding of germline in model organisms is inability to culture PGCs for significant period of time. Failure of PGCs to proliferate *in vitro* as they do *in vivo* suggests the requirement of factors other than LIF, fish serum, and bFGF, hEGF as used in several studies (Resnick et al., 1992; Fan et al., 2008). This study utilizes several small molecules to reduce cell death thereby improving PGC culture conditions. Next section deals with the details of such apoptosis inhibitors.

### **2.1.9 Apoptosis inhibitors**

In an effort to circumvent the problem of apoptosis in hES cell culture (as explained in section 2.1.2) effects of several caspase inhibitors, growth factors, trophic factors and kinase inhibitors were tested by several research groups. Among the compounds tested, Y-27632, a selective inhibitor of p160-

Rho associated coiled-coil kinase (ROCK) was the most potent inhibitor of apoptosis (Watanabe et al., 2007; Zhang et al., 2011). It is been reported that disruption of actin-myosin contraction in human ESC improves cell survival and cloning efficiency. Recently, inhibition of ROCK was shown to regulate cloning efficiency and epithelial structure of human ESCs. Actin-myosin contraction is a downstream target of ROCK regulation in cloning and survival (Chen et al., 2010).

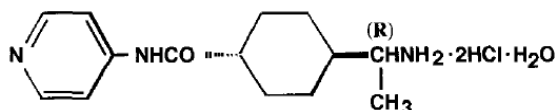


**Figure 20. Structure of Y-27632, ROCK inhibitor.** (R)-(+)-trans-4-(1-aminoethyl)-N-(4-pyridyl)cyclohexanecarboxamidedihydrochloride monohydrate (C<sub>14</sub>H<sub>21</sub>N<sub>3</sub>O<sub>2</sub>·2HCl·H<sub>2</sub>O, molecular weight 338.3)

Kinetic analysis revealed that Y-27632 inhibits ROCK by competing with ATP for binding to the catalytic site. However, in contrast to general ATP competitive inhibitors where kinase inhibition can be reversed by the millimolar physiological concentrations of ATP seen in the cell, Y-27632 can potently inhibit ROCK-mediated cellular responses at micromolar concentrations. The improvement in the cloning efficiency conferred by Y-27632 is advantageous for isolating relatively rare clones and also for recloning hES cells to obtain a uniform cell quality. So far obvious adverse effects of continuous Y-27632 treatment on pluripotency or chromosomal stability were not observed in culture even after a substantial number of passages. ROCK inhibitors such as Y-27632 and Fasudil are already used clinically in cardiovascular therapies suggesting that they are safe for use with hES cells (Hu and Lee, 2005). The mechanism of Y-27632's action in blocking apoptosis is an intriguing question that awaits future investigation. The upstream activation mechanism of ROCK is complex and involves both Rho-independent and dependent pathways (e.g., ROCK is also activated by Caspase-3 cleavage). Future studies of the mode of action of Y-27632 may shed new light on why hES cells, unlike mES cells, are so prone to die upon dissociation.



Various inhibitors in stem cell cultures were utilized to maintain their pluripotency and to reduce apoptosis induced cell death. Among them few of the inhibitors were tested in addition to Y-27632, in this study to see their effects on PGC culture. Endogenous differentiation-inducing signaling and the suppression of proliferation are additional reasons for cell death. Hence, several compounds known to inhibit such processes are utilized individually or in combination with Y-27632 in this study. One of them is PD184352 (Sigma) which is a highly selective non-competitive inhibitor of MEK (MKK1; MAPK kinase, mitogen activated protein kinase) and the closely related MKK2. It has an anti-cancer activity, suppresses the ERK (Extracellular signal-regulated kinase) pathway, and has been used along with other classes of inhibitors to establish embryonic stem cell lines (Versieren et al., 2012). SU5402 which is also a synthetic small molecule and is a FGFR antagonist and angiogenesis inhibitor (Ying et al., 2008). Another inhibitor tested is 1-Azakenpaullone (AZ) is a glycogen synthase kinase 3 (GSK3) inhibitor (Ying et al., 2008).

Cell Permeable Caspase Inhibitor (Casi) is the most used compound in various *in vitro* assays. Ac-AAVALLPAVLLALLAPVAD-al is a cell permeable peptide that contains the VAD-CHO motif making it useful for inhibition of multiple caspases inside cells (Assefa et al., 1999). Similarly, Cyclopamine hydrate (CHi) is a Hedgehog signaling pathway inhibitor; inhibits the growth of medulloblastoma cells (Seifert et al., 2009).

In addition to apoptosis pathway inhibitors, several growth factors were also tested for their effect on PGC culture in this study. One of them is SDF-1 $\beta$  from mouse Stromal cell-derived factor-1 $\beta$  which is a stromal derived CXC chemokine. It signals through CXCR4 receptor. Recombinant mouse SDF-1 $\beta$  is an 8.5 kDa protein containing 72 amino acid residues (D'Apuzzo et al., 1997). Bone Morphogenetic Protein 4 (BMP4) which is known to stimulate angiogenesis by inducing the production of VEGF-A by osteoblasts. Cellular responses to BMP-4 are mediated by the formation

of hetero-oligomeric complexes of type I and type II serine/threonine kinase receptors (Kawabata et al., 1998; ten Dijke et al., 2003).

Adrenocorticotrophic hormone (ACTH) was also utilized to derive mouse embryonic stem cell lines from single blastomeres. It was hypothesized that ACTH signaling for mESC survival and proliferation might be via inhibition of adenyl cyclase activity. A simple and efficient establishment method of mESC lines from a single blastomere of 2–8-cell embryos with medium containing ACTH fragments (Wakayama et al., 2007). Hence ACTH was also tested on PGC culture in this study.

There are multiple factors involved in successful establishment of ES lines or PGC cultures. Above mentioned chemical compounds and growth factors contribute in various ways either by inhibition of apoptosis inducing molecules or downstream effectors or by enhancing the cell proliferation and inhibiting differentiation. Hence, their individual and combined effects are examined in PGC culture in order to see if the PGC culture would be improved.

### **2.1.9 Y-27632 and stem cell culture**

It was shown that a ROCK inhibitor, Y-27632, supported the survival of dissociated human embryonic stem cells (Watanabe et al., 2007). Disruption of actin-myosin contraction by Y-27632 in individual human embryonic stem cells dramatically improved cell survival and cloning efficiency (Chen et al., 2010). Y-27632 has also proved that it increases thaw-survival rates and preserves stemness and differentiation potential of human Wharton's jelly stem cells after cryopreservation (Gauthaman et al., 2010). All these studies suggest that ES cells can be treated with ROCK inhibitor for the better survival, maintenance and derivation of cell lines. In this study, Y-27632 is used in the cryopreservation of freshly isolated blastomeres from mid blastula embryos as well as in PGC culture. Since blastomeres do not have scope for immediate freezing because of their fragile nature

and large size which leads to cell death either by mechanical damage, necrosis or apoptosis. PGC culture from medaka is also tried with the presence of Y-27632 in this thesis, where long term maintenance was a major concern.

#### **2.1.10 Significance**

Cryopreservation is indispensable for the preservation of the cell lines for future utilization and to store genetic resource. Rapid freezing and thawing in the presence of DMSO is the most common procedure used to preserve cells. However the procedure has a disadvantage of less survival rate upon recovery. This study addressed the problem of apoptosis upon recovery of cryopreserved cells and freshly isolated blastomeres. Improved survival rate of medaka hES cells in the presence of Y-27632 is shown in this study. Better recovery of cryopreserved blastomeres which can be utilized to generate ES cells is also shown. Another significant step achieved from this project is to culture PGCs from single blastula cultures for the duration of 18 days in the presence of Y-27632.

#### **2.1.11 Limitations**

This study utilized Y-27632 and other inhibitors as well as growth factors of appropriate concentrations stated in previous studies. The same concentrations of inhibitors which work in mouse and human cell lines were used in medaka. PGC culture in the presence of apoptosis inhibitors showed impressive number of GFP positive cells during 6-9 days. Pooled culture and isolation of PGC population at this time point could be a promising step towards generating a germ cell line. However, prolonged survival and their proliferation were not observed after 18 days.

### **2.2 Materials and methods**

#### **2.2.1 Fish strains and maintenance**

Work with fish was followed in strict accordance with the recommendations in the Guide for the Care and Use of Laboratory Animals of the National Advisory Committee for Laboratory Animal Research in Singapore and approved by this committee (Permit Number: 067/12). The fish strains

used for this experiment are wild type medaka, hdRr and transgenic strain with *vasa*GFP expression. Medaka strains were maintained under an artificial photoperiod of 14 h light to 10 h darkness at 26 °C (Hong et al., 1996; Hong et al., 2010). Embryogenesis was staged as described (Iwamatsu, 2004). Transgenic medaka, Vg contains the *olvas-gfp* transgene and expresses green fluorescent protein (GFP) under the control of medaka *vasa* promoter (Li et al., 2009). Heterozygous Vg embryos were produced by crossing homozygous Vg males to non-transgenic females and were used for cell culture.

### **2.2.2 Medaka haploid stem cell line**

Haploid embryonic stem (hES) cells have the combination of haploidy and pluripotency, enabling direct genetic analyses of recessive phenotypes in vertebrate cells (Yi et al., 2009; Hong, 2010; Yi et al., 2010). Haploid medaka ES cells can stably maintain normal growth, pluripotency, and genomic integrity. Haploid cells when generated showed 70% haploidy but the efficiency of haploidy maintenance is decreased due to many passages and rapid thawing and freezing. They tend to become diploid cells over time during proliferation. So to prevent this, one way is to recover and pick the colonies; another way is to find some reagent which can reduce this freezing shock and post thawing differentiation, apoptosis and death. Hence these cells were used to test the effect of apoptosis inhibitor, (ROCK inhibitor Y-27632) as haploid cells are prone to undergo spontaneous apoptosis and diploidy.

### **2.2.3 Media components**

#### **2.2.3a Preparation of medaka embryo extract**

Embryos were collected, separated by rolling with two needles and incubated in a 10cm petri dish containing 1X ERM (NaCl 1.00 g, KCl 0.03 g, CaCl<sub>2</sub> ·2H<sub>2</sub>O 0.04 g, MgSO<sub>4</sub>·7H<sub>2</sub>O 0.16 g, Methylene blue 0.0001g in 1L of water) at 28 °C with medium replacement every day. Dead

embryos stained with blue color were removed to prevent subsequent mould contamination if any. On the 7th day, embryos were collected, drained and stored at -20 °C. When embryos were up to 10,000, they were homogenized on ice. The homogenates were diluted with PBS to a final concentration of 400 embryo/ml, fast frozen in liquid nitrogen, thawed at 37 °C with three cycles and spun at 18,000 rpm at 4 °C for 30 min. The upper lipid layer was removed and the homogenates were re-centrifuged until lipid layer was invisible. Then the clear supernatant was transferred to EP tubes in 1ml aliquot and stored at -20 °C.

### **2.2.3b Preparation of fish serum**

Fish serum has mitogenic roles in culturing medaka ES cells. Fish serum from rainbow trout (*Oncorhynchus mykiss*), common carp (*Cyprinus carpio*) and seabass (*Lates calcarifer*) has been used successfully in our lab. Fish blood was collected from tail vein by a 10-ml syringe with trace of anti-coagulation (heparin or EDTA) and spun at 4 °C for 30 min at 4,000 rpm. Then the upper clear supernatant was stored at -20 °C in 1 ml aliquot until used.

### **2.2.3c Preparation of cell culture plate**

Culture dish or plates for medaka ES cells should be pre-coated with gelatin (Sigma). Briefly, 0.1% gelatin solution was autoclaved, filtered through 0.22 um filter, added into the dishes or plates and incubated at room temperature for 1 h. Then the gelatin solution was aspirated followed by air-drying for at least 2 h.

### **2.2.3d Composition of embryonic stem cell media**

The standard culture medium for medaka ES cells is ESM4 which consists of DMEM 13.4 g/l (Gibco), 20 mM Hepes (sigma), 15% FBS (Gibco), 1X penicillin and streptomycin (Invitrogen), 2 nM L- glutamine (Invitrogen), 1X Non-essential amino acids (Invitrogen), 1X Na pyruvate (Invitrogen), 100 µM 2-mercaptoethanol (Sigma), 2 nM Na selenite (Sigma), 0.2% seabass serum, 10

ng/ml bFGF, 0.4 embryo/ml medaka embryo extract (MEE), final pH 7.5. For ESM2 which is used for PGC culture, 2 X times extra MEE and 5 X times of bFGF were added (Hong Yunhan, 1996; Hong and Scharl, 2006).

#### 2.2.4 Cryopreservation of hES cells

ES cells were cultured in four groups; Group I: control, Group II: Pretreated with Y-27632 (Calbiochem) for 24h, group III: Y-27632 in freezing medium, Group IV: Y-27632 in post thawing medium. ES cells were trypsinized, resuspended in ESM4 and mixed with equal volume of pre-chilled 2 X freezing medium (35%FBS, 20% DMSO, 45% DMEM). The cells were made into 1ml aliquot in 2-ml cryotubes, kept on ice for 30 min and frozen gradually to -80 °C with a freezing box containing isopropanol. On the second day, these frozen cells were transferred to -150 °C cell bank freezer for long term storage.

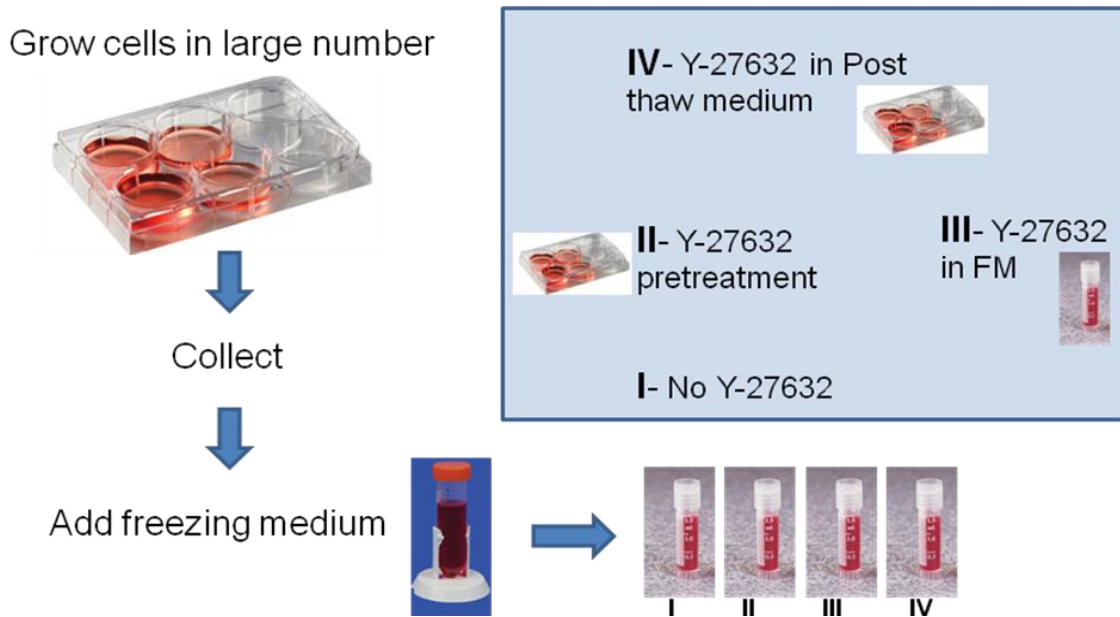


**Figure 21: Cryopreservation procedure.** Cells were grown in large numbers and collected by trypsinization. Freezing medium was added to the collected cells in cryovials. Cells were frozen in four different batches with Y-27632 added at different steps.

### **2.2.5 Cell recovery by rapid thawing**

Recovery of hES was carried out with a quick procedure known as rapid thawing. Cells in cryovials were thawed in 37 °C water bath for less than 1 min till the ice was molten in the tube with occasional mixing and spun briefly at 300 g. The freezing medium was removed and fresh ESM4 was added to the cryotubes. After being resuspended, the cells were transferred to 6-well plate and incubated at 28 °C.

### **2.2.6 Cell count - trypan blue vital staining**

Trypan Blue is a vital dye. The reactivity of trypan blue is based on the fact that the chromophore is negatively charged and does not interact with cells unless the cell membrane is damaged. Therefore, all the cells which exclude the dye are viable. Aliquot of cells were taken in separate tubes for trypan blue staining. Cell suspension was centrifuged and washed with PBS once. Cells were then resuspended in 400 µl of DMEM and 100 µl of 0.4% trypan blue solution (Life technologies) was added. Cells were then incubated at room temperature for 30 min. 10 µl of cell suspension was loaded to the counting chamber (Sigma). Cell counting was done according to the standard method.

### **2.2.7 Live – dead staining and Annexin V- FITC assay**

Upon recovery, hES cells were washed with cold 1 X PBS. Cells were then centrifuged at 5000 rpm and resuspended in 1 ml of fresh cold 1 X PBS. 100 µg/ml of Hoechst 33342 (Sigma) and 100µg/ml of PI (Sigma) was added to the suspended cells. Cells were incubated for 5-15 min at room temperature and then washed with 1 X annexin-binding buffer and imaged after they settled on the bottom of the culture plates.

For FACS analysis, recovered hES were grown in desired sized plates according to the experimental requirements. Media was removed by vacuum and 1ml of 1 X PBS was added. Plates were slightly tilted to get all the unattached dead cells to come into solution. PBS was then removed and 0.05% EDTA-Trypsin (ET) was added. Cells were incubated at room temperature for about 1

min under observation. ET was carefully removed and cells were resuspended by gentle pipetting. Cells were then collected in 1.5 ml tubes and washed twice in cold 1 X PBS. Cells were then centrifuged at 5000 rpm and resuspended in 100 µl of 1 X annexin-binding buffer (BD Biosciences). It was prepared by adding 100 µl of 10 X annexin-binding buffer stock solution to 900 µl of sterile water. 5 µl of annexin V conjugate and 2 µl of 100 µg/ml of PI was added to the cell suspension and incubated for 30 min. Cells were then analyzed in fluorescent assorted cell sorting (FACS).

### **2.2.8 Cell attachment upon recovery and proliferation efficiency assay**

Cells were seeded in appropriate sized gelatin coated wells with 1.5 ml of ESM4. Plates were then incubated at 28 °C in CO<sub>2</sub> incubator. After 3-4 h, the floating cells were collected from each group of cells and counted. Attached cells were also trypsinized and collected and counted. Both the numbers were recorded and used for finding percentage (%) of floating cells in each group. Proliferation efficiency was assessed by counting attached cells every 4 days till 16<sup>th</sup> day of recovery. The graph was then plotted using the cell numbers in each group at every time point.

### **2.2.9 Clonal expansion assay**

Cryopreserved and recovered cells of four test groups after 48 h of culture were seeded in low density in 10 cm dishes. Cells were allowed to form colonies from single cells up to a week. Cells were then imaged at the interval of 4-5 days.

### **2.2.10 Embryo staging and preparation for primary culture**

Medaka male and female fish were separated on the previous evening of the experiment. Fish were mixed on the next morning in a fresh tank with appropriate amount of sea weed. After few minutes, the released embryos were collected (Figure 22). They were staged according to the staging details (Iwamatsu, 2004). Embryos were separated using sticks with needles and washed thoroughly with clean water and treated in 1mg/ml proteinase K (Sigma) at 28°C for 60-90 min.





**Figure 22. Medaka maintenance in continuous water flow system** (A) System, (B) adult male and female medaka, (C) Mid blastula embryo.

### 2.2.11 Cryopreservation of blastomeres with Y-27632

Biological safety cabinet was sterilized under UV for 30 min. Mid blastula embryos treated with proteinase K were then washed 5 times with 1 X PBS and treated in 0.1% bleach for 40 sec. Again 5 times washes were performed and embryos were taken on the lid of a clean culture dish. Embryos were carefully dissected and blastomeres were resuspended in small amount of ESM2 (Li et al., 2011c). Cells were made into 3 groups, Group I (Control), Group II: Y-27632 in freezing medium, Group III: Y-27632 in post thawing medium (Table 1). The cell suspension was equally distributed to different test groups and equal amount of pre-chilled 2 X freezing medium was gently added. They were labeled accordingly and 10  $\mu$ M Y-27632 was directly added in the cell suspension to Group II. The cells were aliquoted into 2-ml cryotubes and frozen gradually to -80 °C with a freezing box containing isopropanol. On the second day, frozen cells were transferred to -150 °C cell bank for long-term storage.

Group	Media	+/- Y-27632
Group I	ESM2+ FM	-
Group II	ESM2+FM	+
Group III	ESM2 +FM	+( in post thawing media)

**Table 1. Blastomere cryopreservation with/without Y-27632.**

### 2.2.12 Media formulation for PGC culture

Culture medium ESM2 was prepared as described (Hong Yunhan, 1996; Hong and Scharl, 2006). ESM2 contains several protein supplements including 15% fetal bovine serum (FBS), fish serum (FS) from the rainbow trout (1%), basic fibroblast growth factor (bFGF; 10 ng/ml), and medaka embryo extract (MEE; 1 embryo/ml) (Hong et al., 1996; Hong, 2010). To test the effects of various small molecules in PGC culture, many apoptosis inhibitors and growth factors were added to medium individually or in combination table 1 and 2).

Group name	ESM2+Inhibitor	Final concentration
Control	-	-
Y-27632	ROCK inhibitor (Calbiochem)	10 $\mu$ M/ml
SU5402	FGFR inhibitor (Calbiochem)	2 $\mu$ M/ml
PD184352	MAPK inhibitor (Sigma)	0.8 $\mu$ M/ml
AZ	GSK3 inhibitor (1-Azakenpaullone) (Sigma)	3 $\mu$ M/ml
BMP4	Bone Morphogenetic Protein 4 human (Sigma)	10 ng/ml
Sdf1 $\beta$	Stromal cell-derived factor-1 beta (Sigma)	20 ng/ml
Casi	Cell-permeable caspase inhibitor (Sigma)	1 $\mu$ M/ml
CHi	Cyclopamine Hedgehog inhibitor (Cyclopamine hydrate) (Sigma)	1 $\mu$ M/ml
ACTH	AdrenoCorticoTropic Hormone (Sigma)	10 $\mu$ M/ml

**Table 2. Inhibitors and growth factors used in PGC culture.**

Y-27632 with other apoptosis pathway inhibitors was added in combination to culture media ESM2 to test the combined effect on PGC survival. Growth factors were also included in the combinations.

Group	ESM2+inhibitor combinations
Control	-
1	Y-27632+AZ
2	Y-27632+SU5402+PD184352
3	Y-27632+PD184352+AZ
4	Y-27632+Casi
5	Y-27632+CHi
6	Y-27632+ACTH
7	Y-27632+BMP4
8	Y-27632+BMP4+Sdf1 $\beta$

**Table 3. Blastomere culture in different test groups and media composition**

**2.2.13 primordial germ cell culture**

All cell culture plates were coated with 0.1% gelatin and air dried (Hong et al., 1996; Hong Yunhan, 1996; Hong, 2010). MBE cells were dissociated from pooled embryos and were seeded in 96-well plate so that each well has cells equivalent to one embryo (Figure 23). Cells were incubated at 28 °C. 10 batches of single inhibitor treatment and 12 batches of combinations were performed. Observations for cell attachment, and PGC formation were carried out for the period of 18 days. PGCs were visualized every 3 days under green fluorescence filter and identified by their typical morphology and green fluorescence. Partial medium change was performed as and when needed (Li et al., 2011c).

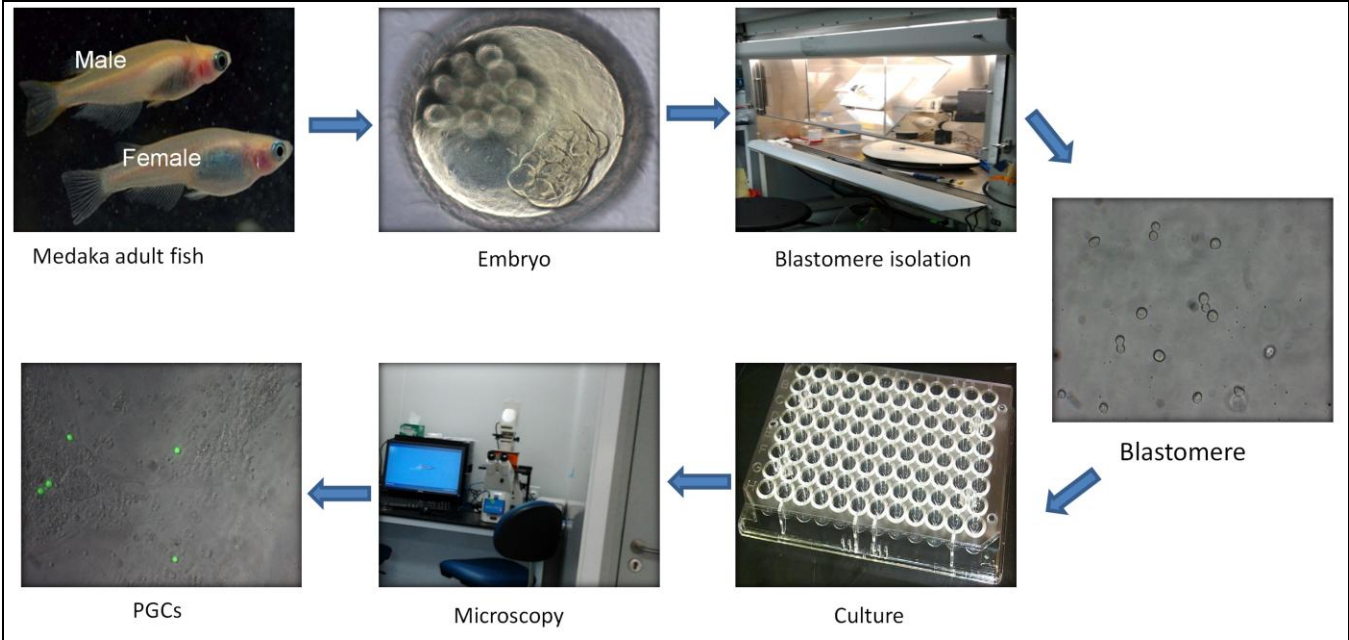


**Figure 23. Flow chart illustration of PGC culture.** Images are in order: separation of fertile adults, 16-cell embryo and operation inside biological safety cabinet under sterile conditions, dissociated midblastula cells, 96-well plate and fluorescence enabled Zeiss Axiovert2 inverted microscope, GFP positive PGCs.

#### **2.2.14 Observation and imaging**

Microscopy was performed as described (Xu et al., 2009; Yi et al., 2009; Hong et al., 2012). Briefly, live embryos were visualized by using a Leica MZFLIII stereo microscope equipped with a Fluo III UV-light system and a GFP2 filter and photographed by using a Nikon E4500 digital camera. For documentation at higher magnification, live embryos were observed and photographed on Zeiss Axiovert2 inverted microscope equipped with Zeiss AxioCam MRc digital camera. Images were processed using either AxioVision 4 or ImageJ (NIH) softwares AxioVision 4 software.

#### **2.2.15 Statistical analysis**

All the result analyses were carried out using 3 biological replicates. Results were analyzed by a two- way Analysis of variance (ANOVA) to calculate the significance among test groups. P value <0.05 is taken as significant.

### **2. 3: Results**

#### **2.3.1 Y-27632 enhances thawing efficiency of hES cells**

Frozen hES cells from Y-27632 treated groups showed higher thaw-survival rate than untreated group as shown by conventional trypan blue staining (Figure 24). Percentages of group II, III and IV were slightly higher compared to control or untreated group.

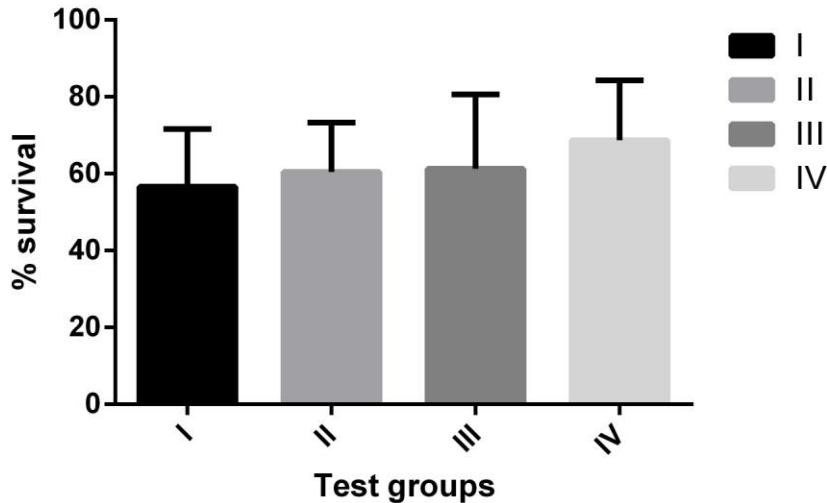
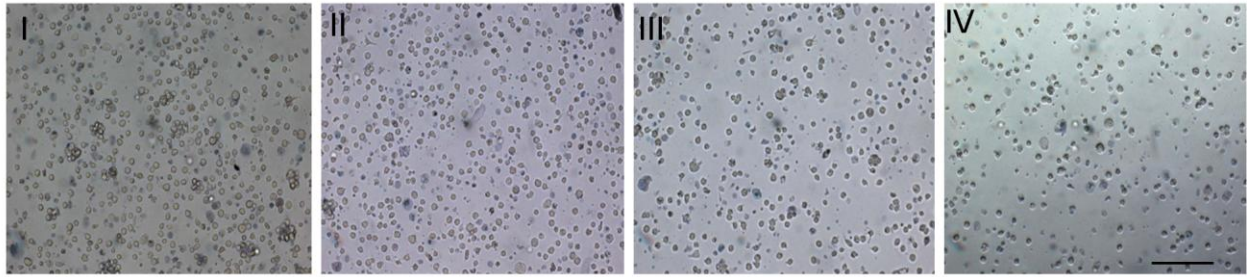


**Figure 24. Effect of Y-27632 on survival of cryopreserved medaka hES cells.** Graph showing % survival of hES cells upon recovery in 4 test groups assessed by trypan blue vital staining. Group I is (untreated) control, group II is Y-27632 (10  $\mu$ M) in pretreatment for 24h before freezing, group III is Y-27632 (10  $\mu$ M) in freezing medium and Y-27632 (10  $\mu$ M) in post thawing medium. Error bars are expressed as mean $\pm$ SEM from 3 biological replicates. Though the difference between the survival rates of test groups compared to control is obvious in the graph, it is not significant when calculated by Analysis of variance (ANOVA).

### 2.3.2 Y-27632 reduces floating cells

Floating cells in each test group were collected and counted after 5 h of recovery. The number of floating cells was high in control group than Y-27632 treated groups. It is evident that control group has higher percentage of floating cells than Y-27632 treated groups (Figure 25).

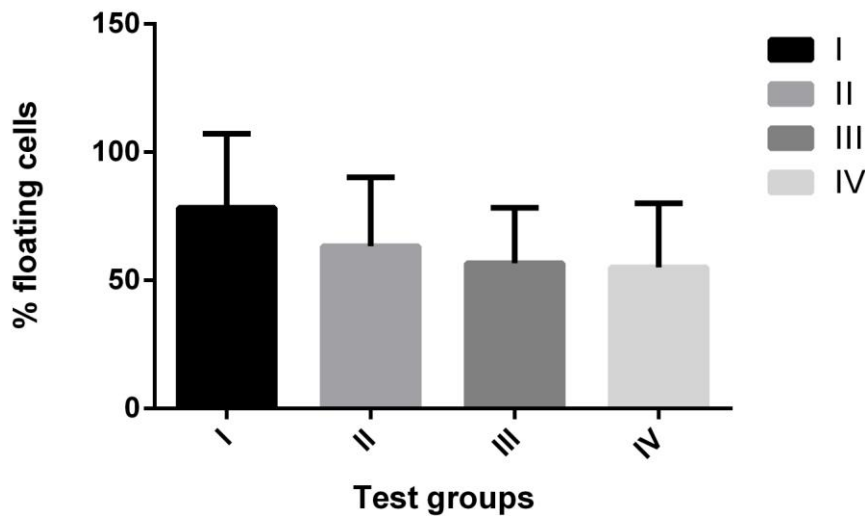


**Figure 25. Floating cell count at 5 h post recovery.** Graph shows % floating cells in control and test groups. Group I is (untreated) control, group II is Y-27632 (10  $\mu$ M) in pretreatment for 24h before freezing, Y-27632 (10  $\mu$ M) in freezing medium is group III and Y-27632 (10  $\mu$ M) in post thawing medium is group IV. All values are expressed as mean  $\pm$ SEM from 3 replicates. Though the difference in the % of floating cells of test groups compared to control is observed in the graph, it is not significant when calculated by Analysis of variance (ANOVA).

### 2.3.3 Y-27632 retains normal cell morphology of hES cells upon recovery

Frozen hES cells showed similar morphology upon recovery both in control and treated groups. However more cells were found dead and floating in control group than treated groups. This influenced further reduction in the number of attached and proliferated cells in control group in subsequent experiments.

### 2.3.4 Y-27632 enhances post recovery cell survival

Recovered cells were stained for annexin V-FITC and PI to visualize cells undergoing apoptosis. Annexin V stained cells were found to be more in control group whereas Y-27632 treated groups showed fewer annexin V positive cells (Figure 26). Recovered hES cells after 24 h of culture at 28°C were analyzed for apoptosis. Fluorescence-activated cell sorting (FACS) analysis by Annexin V-FITC staining revealed that the group pretreated for 24 h with Y-27632 showed fewer apoptotic cells than the rest of the groups. Cells were analyzed for annexin V-FITC positive after 72 h of culture to

see if there is persistent effect of Y-27632 (Figure 26). Similar trend was observed as previously seen where there were high number of apoptotic cells in untreated group and fewer apoptotic cells in treated groups. This revealed that apoptotic cells became fewer upon Y-27632 treatment. The % of annexin V +ve cells is represented in a bar graph (Figure 26).

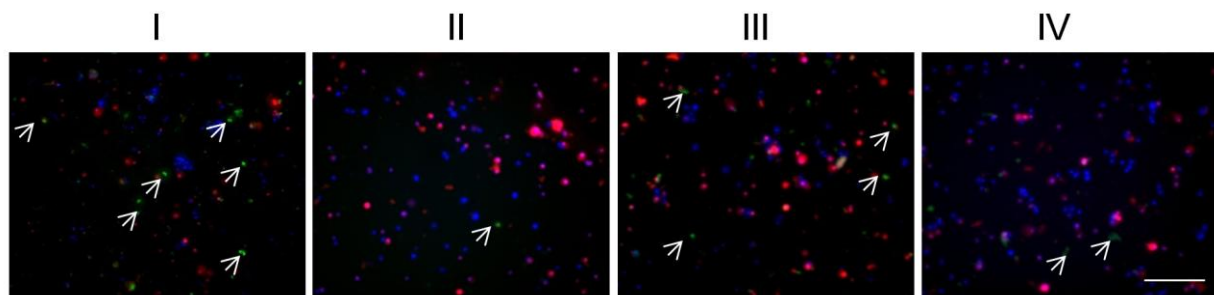


**Figure 26. Annexin V-FITC assay.** (Above) Phase contrast images of medaka hES cells stained with Annexin V-FITC+PI+Hoechst after 30 min post recovery. Group I is (untreated) control, group II is Y-27632 (10  $\mu$ M) in pretreatment for 24 h before freezing, group III is Y-27632 (10  $\mu$ M) in freezing medium and Y-27632 (10  $\mu$ M) in post thawing medium is group IV. Annexin V-FITC labeled cells are more in control group than treated groups (arrows). Also, PI stained cells are more in control group than treated groups. Scale bars 100  $\mu$ m.

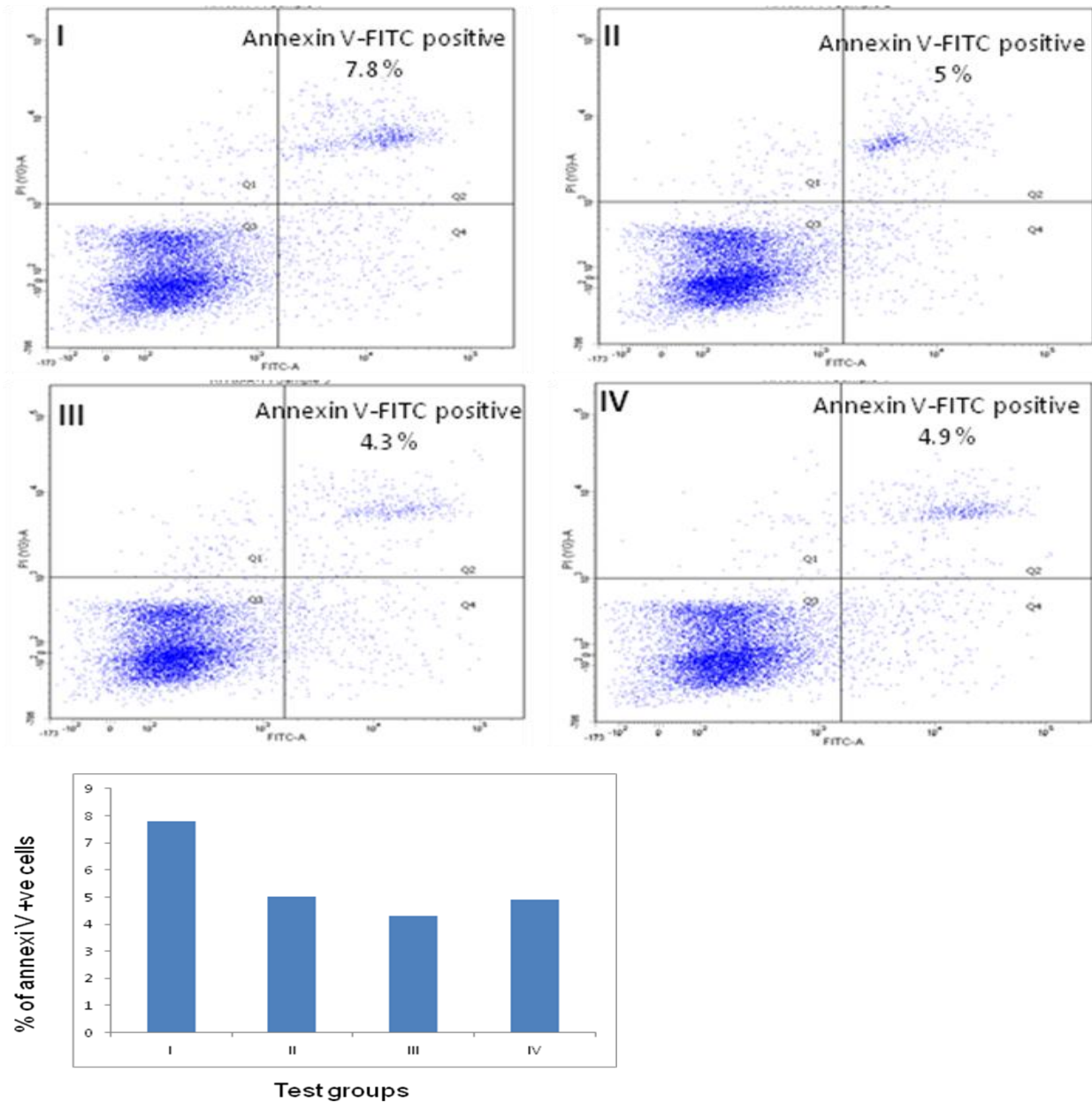


**Figure 27. Annexin V-FITC assay at 72 h post recovery.** Group I is (untreated) control, group II is Y-27632 (10 μM) in pretreatment for 24 h before freezing, group III is Y-27632 (10 μM) in freezing medium and group IV is Y-27632 (10 μM) in post thawing medium. Q2 population (Late apoptotic cells which are stained for both annexin and PI) has more number of cells whereas treated groups have less. Group II and III cells showed fewer apoptotic cells than group I and IV. Bar chart shows the % of Annexin +ve cells in each test groups.



### **2.3.5 Y-27632 enhances cell attachment and proliferation**

The control group showed slower proliferation rate than treated groups when recovered cells were seeded into multiwell plates and observed at different time points. A few attached cells were observed in control group whereas a monolayer was formed in the treated groups after 24 h. A similar trend was observed in prolonged culture. Trypsinization and subculture revealed significant differences in the number of attached cells between control and treated groups (Figure S3).

Proliferation efficiency was assessed by harvesting and counting the cells from treated and untreated groups at the interval of 4 days. Equal number of cells was seeded into new wells at every harvest for further proliferation. Y-27632 treated groups showed more cells than control group in every harvest. The proliferation efficiency in treated groups was higher compared to control. Among treated groups, group III showed the highest proliferation efficiency indicated by higher number of cells (Figure 28). However, the cell number did not increase significantly among the treated groups at 4<sup>th</sup> and 8<sup>th</sup> day of culture after recovery. Treated groups had more cells than control group at 12<sup>th</sup> and 16<sup>th</sup> day of culture indicating that their proliferation efficiency increased rapidly after 8 days of recovery.

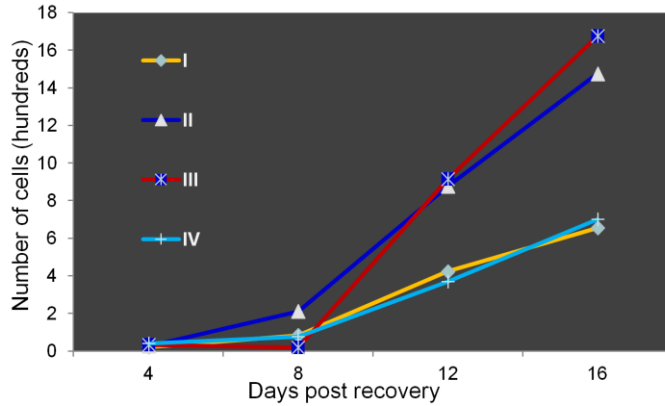


**Figure 28. Proliferation efficiency of medaka hES cells upon recovery.** Group I is (untreated) control and group II is Y-27632 (10  $\mu$ M) in pretreatment for 24 h before freezing, group III is Y-27632 (10  $\mu$ M) in freezing medium and group IV is Y-27632 (10  $\mu$ M) in post thawing medium. Graph represents cell number in each group upon recovery at the interval of 4 days. Treated groups show higher proliferation rate indicated with higher number of cells than control group. However, the difference between control and test groups was not significantly increased.

### 2.3.6 Y-27632 increases clonal expansion

All the four groups of hES cells were seeded in 10 cm culture dish in low density for colony formation. After the incubation at 28 °C for a week, there was visible difference in the colony size among four groups of hES cells. Colonies formed in the control group were smaller compared to treated groups. They were slow in growth and consisted fewer cells in the colony. Among three treated groups, group III showed rapid expansion of colonies. The colony size was also larger than group II and IV. Colony expansion was much quicker in the treated groups compared to control and Group III showed the fastest expansion efficiency among all (Appendix S4).

### 2.3.7 Y-27632 enhances thaw-survival efficiency of medaka blastomeres

MBE cells were dissociated and cryopreserved in 3 test groups depending on the presence or absence of Y-27632 in the freezing medium and recovery medium. Untreated or control in which there was no Y-27632, group II where Y-27632 was added to the freezing medium and group III in which Y-27632 was added to recovery medium. Blastomeres of untreated group upon cryopreservation and rapid thawing showed no attachment. Treated groups II and III showed

attachment after 24 h. The damage during pipetting and transfer was predicted to be much higher as blastomeres are bigger in size than ES cells. Group II and III showed attachment at the periphery of culture wells after rapid thawing. However, more than 50% of the cells in all the groups showed dead and floating blastomeres (Figure 29).

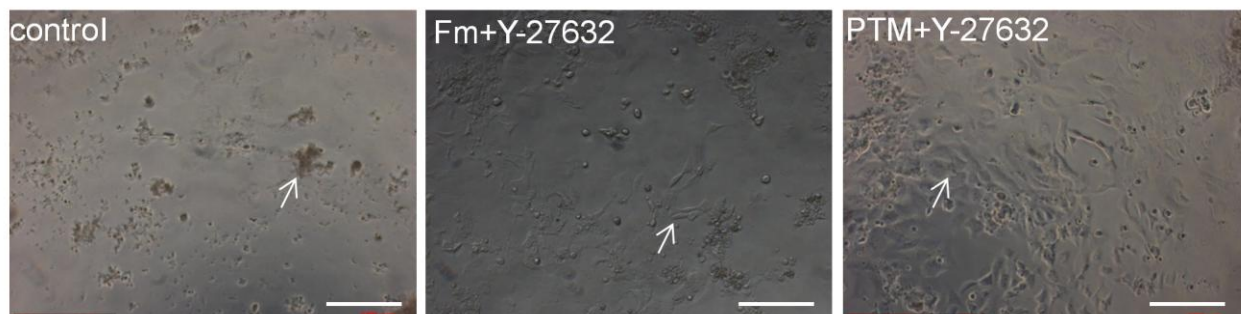


**Figure 29. Effect of Y-27632 on medaka blastomere cryopreservation.** Phase contrast images of blastomeres upon rapid thawing showed the attachment in the cell culture plates. Treated groups (Fm+Y-27632 and PTM+Y-27632) either in Freezing medium or post thawing medium showed attachment whereas control group showed little or no attachment (shown by arrows). Scale bar 100  $\mu$ m.

### 2.3.8 ESM2 maintains PGC culture

Embryonic stem cell media (ESM2) used for PGC culture has the following components which are specifically chosen for fish cell culture in the lab. Although the basic ingredients are similar for mammalian cell culture, few ingredients like fish serum and embryo extracts were specific to ESM2. Basic medium contains 13.37 g/L of DMEM powder and 20 mM of HEPES. DMEM (Dulbecco's Modified Eagle's Medium) is an essential medium that contains a four-fold higher concentration of amino acids and vitamins, as well as additional supplementary components like glutamine and sodium bicarbonate. HEPES (*4-(2-hydroxyethyl)-1-piperazineethanesulfonic acid*) is widely used in cell culture, largely because it is better at maintaining physiological pH despite changes in carbon dioxide concentration produced by cellular respiration when compared to bicarbonate buffers. The following additional components are also added in ESM2: L-glutamine - as a cellular energy source, next to glucose; Non essential amino acids - When these amino acid concentrations are low, cells

need to consume more glucose and glutamine in the media and produce excess by-products which might affect cell growth. Adding NEAA into the cell culture medium could mitigate the potential side effects caused by self-production of these non-essential amino acids; Sodium pyruvate - as an additional source of energy; sodium selenite - as a source of an essential trace element, selenium;  $\beta$ -mercapto ethanol - a potent reducing agent used in cell culture medium to prevent toxic levels of oxygen radicals; penicillin-streptomycin - antibiotics; Fetal bovine serum - serum-supplement; Human recombinant bFGF-support the maintenance of undifferentiated embryonic stem cells. In addition, fish serum (from seabass or trout) and medaka embryonic extract (explained in section 2.3.1) were also added. All these ingredients were previously tested and the media was formulated to establish ES line from medaka blastula cells, hence ESM2 meets the need for blastomere culture.

### **2.3.9 Midblastula cells are capable of survival and PGC formation**

Medaka wild type females crossed with *vasa*-GFP transgenic male fish produced the embryos with only germ cells expressing GFP. Rest of the cells which were not destined to become PGC lacks the GFP expression. Naturally, PGCs appear on the second day *in vivo*, however the time doesn't differ significantly when embryos were *in vitro*. Although the germ cells with GFP are detectable at 48 h, strong signal can be seen only after 72 h in embryos. This study successfully showed the possibility of culturing midblastula cells from germ cell transgenic embryos up to 3 weeks. It also showed the variation in their number when cultured in the presence of different small molecules. The small molecules are the apoptotic inhibitors which act on different apoptosis inducing pathways thereby reducing the death of PGCs.

### **2.3.10 Early attachment of blastomeres in culture**

Midblastula cells cultured in the presence of small molecules: SU5402, PD184352, Y-27632 and growth factors: Sdf1 $\beta$ , BMP4, ACTH showed significant improvement in the early attachment than

untreated cultures (Abbreviations and concentrations are given in table 3 and 4). All the blastomeres were attached when they were imaged after 12 h of culture. Normal duration of attachment after the dissociation and distribution of blastomeres into culture wells is 3-5 h. Cell attachment was nearly 100% in Y-27632, BMP4 and Sdf1 $\beta$  treated groups. PD184352 and AZ treated cells were clumped together into small islands of cells but appeared to be attached. SU5402, CHi and Casi treated groups didn't show attachment (Figure 30).

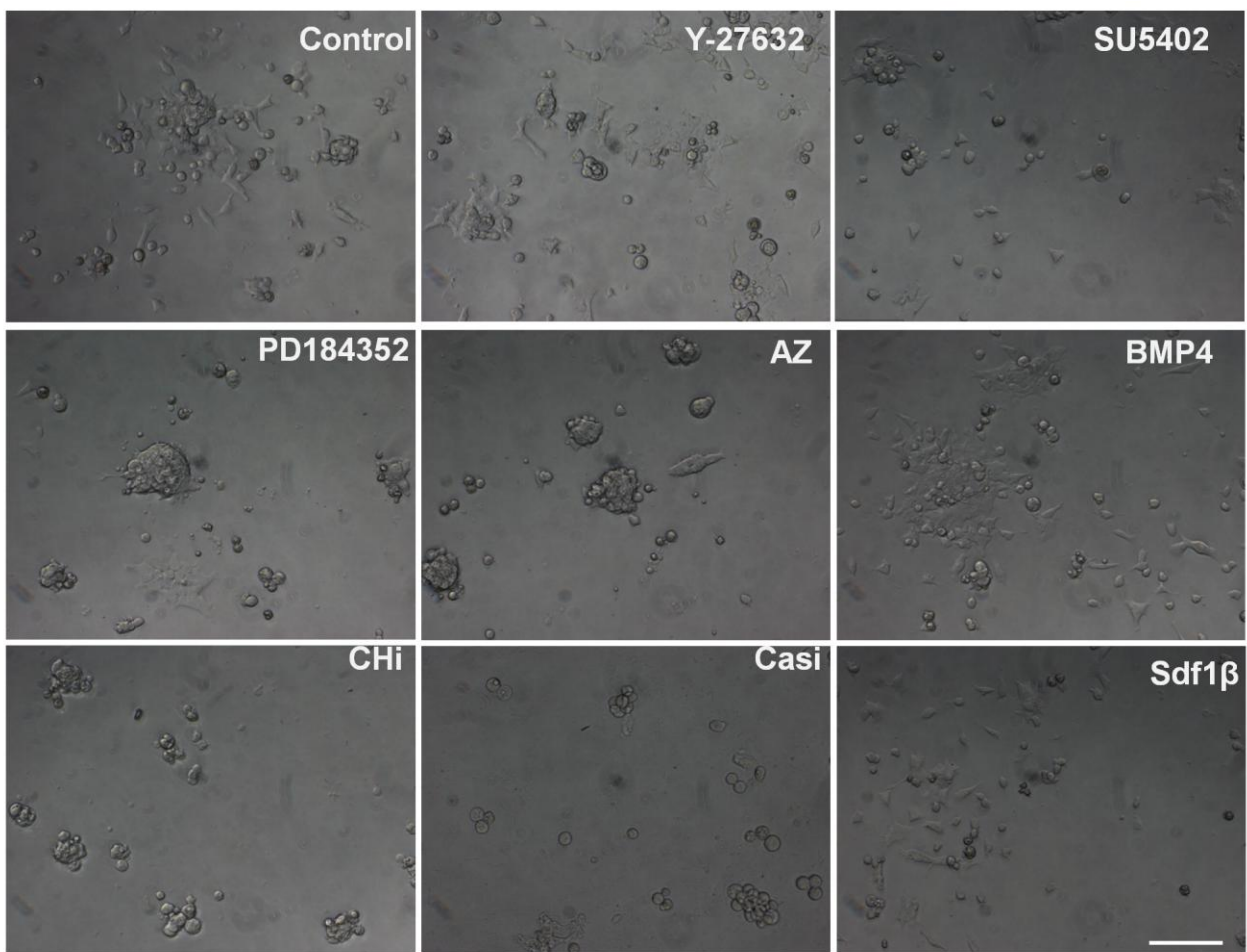


**Figure 30. Blastomere attachment at 12 hpc.** Phase contrast images of blastula cells treated with Y-27632 (ROCK inhibitor), SU5402 (FGFR inhibitor), PD184352 (MAPK inhibitor), AZ (GSK3 inhibitor), CHi (Cyclopamine-Hedgehog inhibitor) and Casi (Caspase inhibitor), BMP4 (Bone morphogenetic protein 4), Sdf1 $\beta$  (Stromal derived growth factor 1 $\beta$ ), ACTH (Adrenocorticotrophic hormone). CHi, Casi, AZ, PD184352 and SU5402 showed poor attachment of blastomeres compared to control, y-27632, BMP4 and Sdf1 $\beta$ . Scale bar 100  $\mu$ m.

### **2.3.11 Apoptosis inhibitors increase PGC number in culture**

The numbers of PGCs those appeared and survived significantly differed among treated and untreated groups at different time points. PGC count was performed when the GFP signal was strong on 3<sup>rd</sup> day of culture. PGCs were identified by their round shape and larger size. GFP expression was uniformly distributed and expression was strong without any background from somatic cell layer to which germ cells were adhered. PGCs were counted by their GFP expression with the help of fluorescent microscope at 20X optical zoom and recorded at every three days interval till 18 days. Treated groups Y-27632 and ACTH as well as control group showed higher number of PGCs till 9<sup>th</sup> day when compared to rest of the test groups (Figure 31-34). However, this trend did not continue after 9<sup>th</sup> day as PGCs number started declining and there were no PGC in control group by 15<sup>th</sup> day. Groups Y-27632, Sdf1 $\beta$  and SU5402 retained at least 1 PGC till 18<sup>th</sup> day of culture. Overall, the maximum number of PGC appearance in all the groups including control was on 6<sup>th</sup> day. The number of PGCs reduced drastically after 6<sup>th</sup> day. The maximum number of PGCs in control group was 17 on 6<sup>th</sup> day and the minimum was 3 on 12<sup>th</sup> day. But in Y-27632, maximum was more than 20 on 3<sup>rd</sup> day and minimum was 1 which survived till 18<sup>th</sup> day. This signifies the potential of Y-27632 to prevent apoptosis in PGCs for the period of 3 weeks. Notably, BMP4, Csi and CHI were also able to retain at least 1 PGC till 15<sup>th</sup> day whereas ACTH and AZ retained PGC only till 12<sup>th</sup> day. There was significant improvement in survival of PGCs observed at 9dpc by SU5402 and AZ. Only Y-27632 was able to retain the PGC till 18<sup>th</sup> day of observation. Though there were differences in the number of PGCs observed in test groups, they were not significantly high.

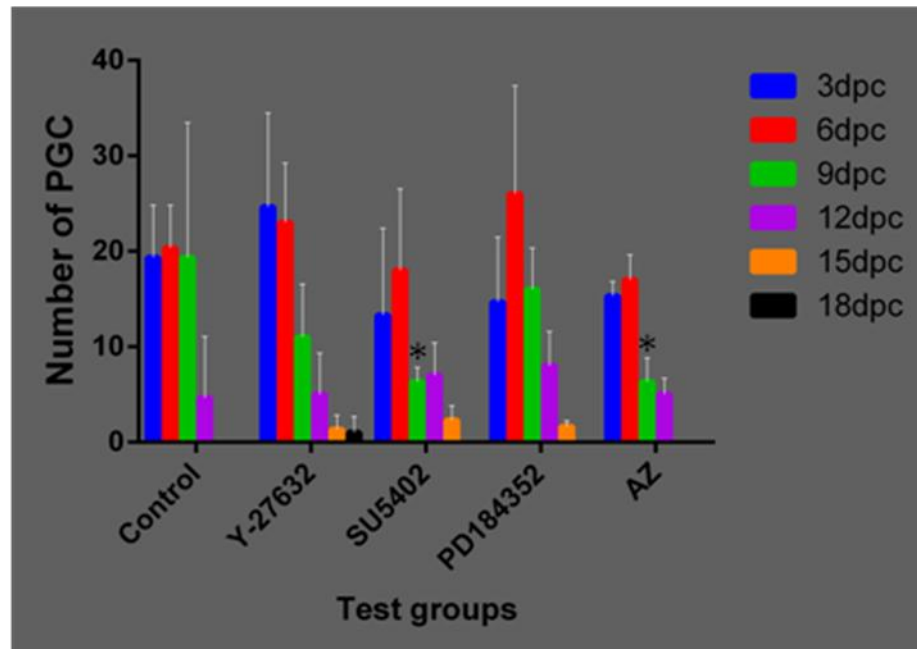


**Figure 31. Effect of Y-27632, proliferation enhancers, differentiation inhibitors on PGC culture.** Line graph showing number of PGCs at different time points in inhibitor treatments. Y-27632 (ROCK inhibitor), SU5402 (FGFR inhibitor), PD184352 (MAPK inhibitor), AZ (GSK3 inhibitor), CHi (Cyclopamine-Hedgehog inhibitor) and Casi (Caspase inhibitor), BMP4 (Bone morphogenetic protein 4), Sdf1 $\beta$  (Stromal derived growth factor 1 $\beta$ ), ACTH (Adrenocorticotrophic hormone). Y-27632 showed persistent effect on PGC survival till 18<sup>th</sup> dpc whereas control group has no PGC survived. SU5402, Sdf1 $\beta$ , AZ, PD184352 also showed significant effect on PGC survival for prolonged duration. Errors bars represent are expressed as mean $\pm$ SEM from 3 independent experiments. Although there was difference in the number of PGCs observed in test groups compared to control, the difference was insignificant except SU5402 and AZ at 9dpc (\*=  $p < 0.05$ ) calculated by Analysis of variance (ANOVA).

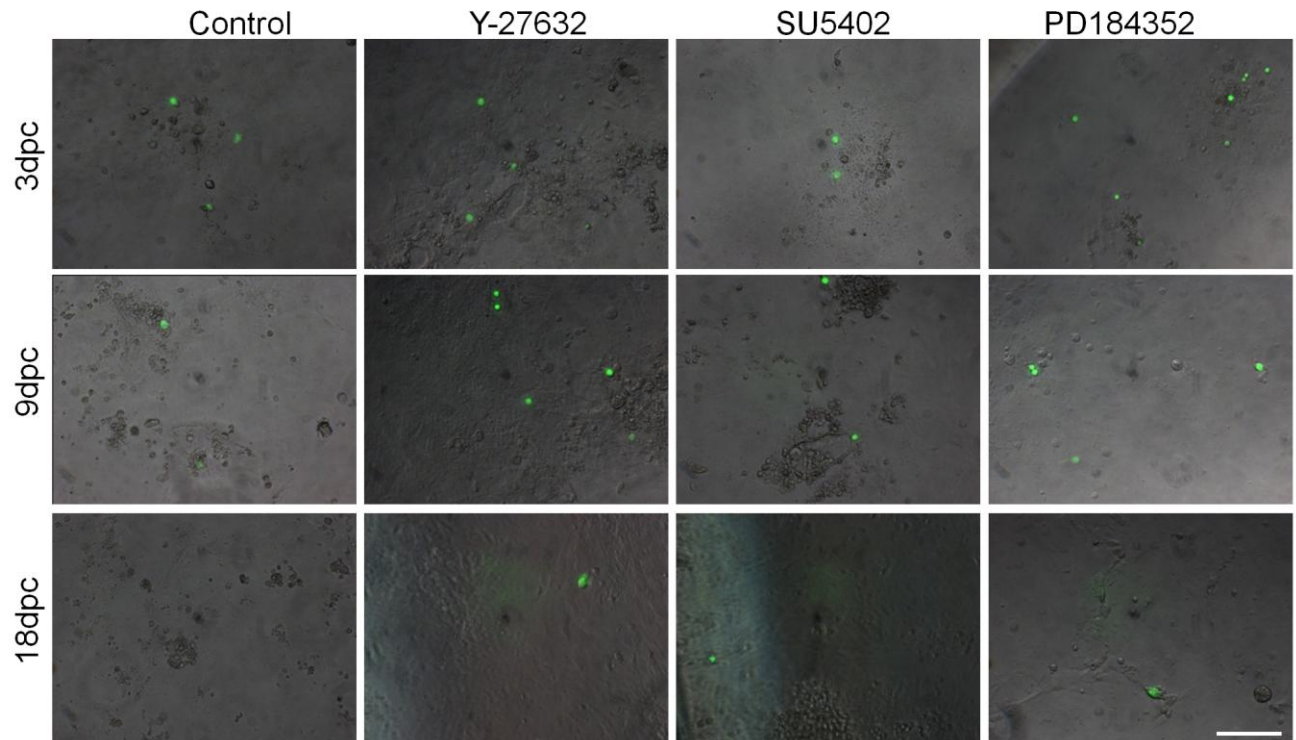


**Figure 32. Phase contrast images of PGCs.** Y-27632 (ROCK inhibitor), SU5402 (FGFR inhibitor) and PD184352 (MEK inhibitor) and control. PGCs are identified by their GFP (green fluorescent protein) expression, round and larger size than somatic non-fluorescent cells. PGCs are attached to somatic cells. There was increase in the number of PGCs in inhibitor treated blastula embryonic cell cultures compared to control. The difference is obvious during initial 9 days (Only selected time points are shown). Scale bar 100  $\mu$ m.



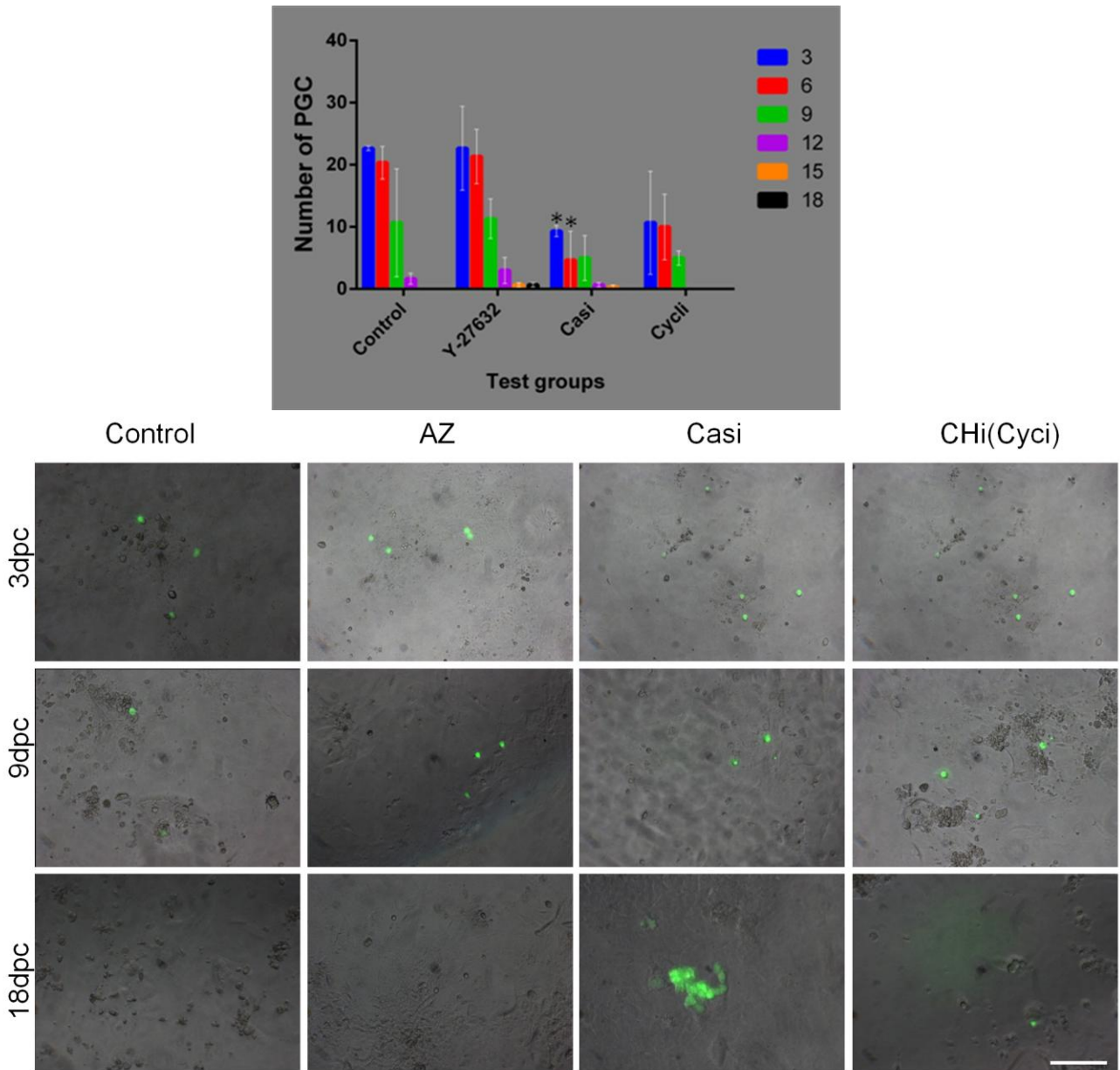


**Figure 33. Above, Effect of Y-27632 and other inhibitors on PGC culture.** Bar graph shows number of PGCs at different time points in inhibitor treatments. Y-27632 (ROCK inhibitor), (Cyclopamine-Hedgehog inhibitor) and Casi (Caspase inhibitor). Y-27632 showed persistent effect on PGC survival till 18<sup>th</sup> dpc whereas control group has no PGC survived. All values are expressed as mean±SEM from 3 independent experiments. Although there was difference in the number of PGCs observed in test groups compared to control except Casi at 3 and 6dpc, the difference was insignificant (\*p<0.05) as calculated by Analysis of variance (ANOVA). Below: **Phase contrast images of PGCs.** AZ (GSK3 inhibitor), Casi (Caspase inhibitor) and Chi (Cyclopamine Hedgehog inhibitor) and control. PGCs are identified by their GFP expression, round and bigger than non-fluorescent somatic cells. PGCs are attached to somatic cells. There was increase in the number of PGCs in inhibitor treated blastula cell cultures when compared to control. The difference is obvious during initial 9 days (Only selected time points are shown). Scale bar 100 µm.

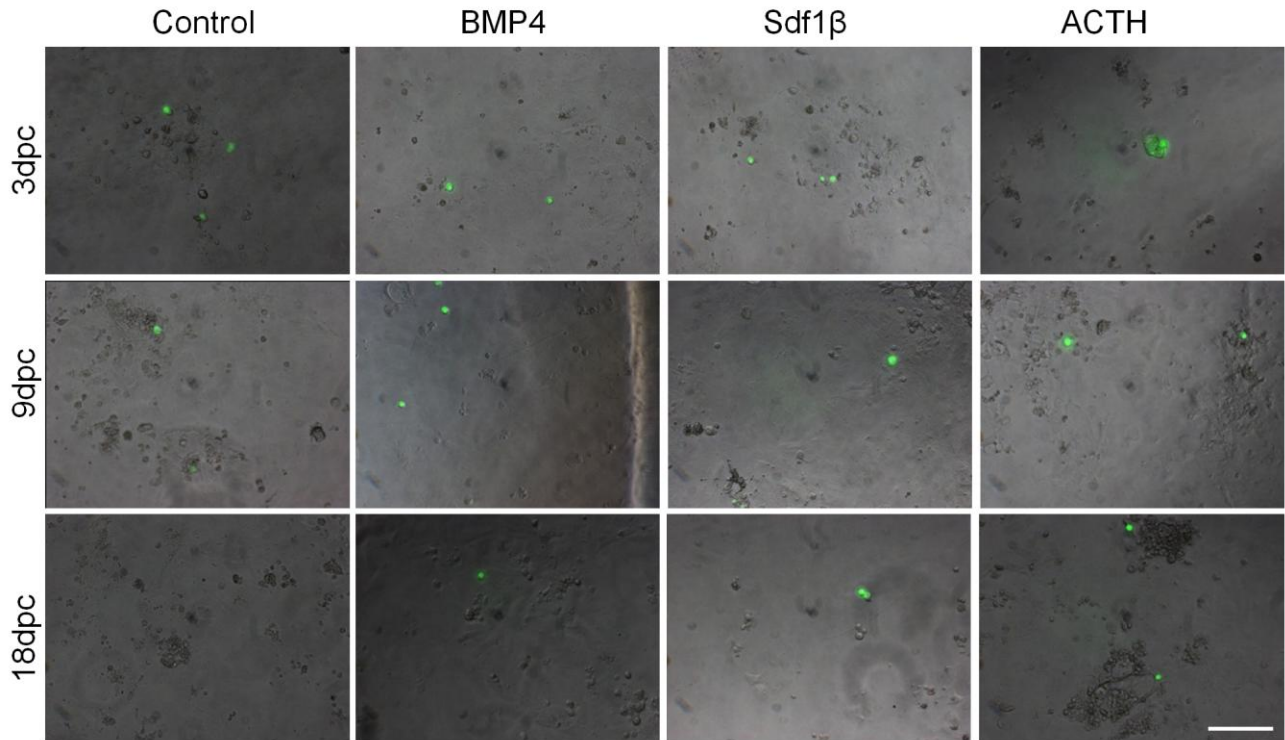
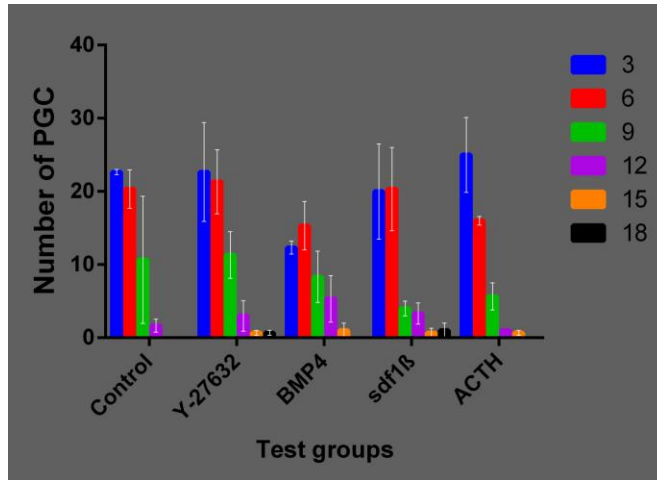


**Figure 34.** Above: **Effect of Y-27632 and growth factors on PGC culture.** Bar graph showing number of PGCs at different time points in inhibitor treatments. Y-27632 (ROCK inhibitor), BMP4 (Bone morphogenetic protein 4), Sdf1 $\beta$  (Stromal derived growth factor 1 $\beta$ ), ACTH (Adrenocorticotrophic hormone). Y-27632 and Sdf1 $\beta$  showed persistent effect on PGC survival till 18<sup>th</sup> dpc whereas control group has no PGC survived. All values are expressed as mean $\pm$ SEM from 3 independent experiments. Although there was difference in the number of PGCs observed in test groups compared to control, the difference was insignificant as calculated by Analysis of variance (ANOVA) Below: **Phase contrast images of PGCs.** BMP4 (Bone Morphogenetic Protein 4), Sdf1 $\beta$  (Stromal derived factor 1  $\beta$ ), ACTH (Adrenocorticotrophic hormone) and control. PGCs are identified by their GFP expression, round and bigger than somatic non-fluorescent cells. PGCs are attached to somatic cells. There was increase in the number of PGCs in treated blastula cultures than in control. The difference is obvious during initial 9 days (Only selected time points are shown). Scale bar 100  $\mu$ m.

### **2.3.12 Y-27632 is the most potent enhancer of PCG number**

Y-27632 treated group showed the most promising results by retaining PGCs till the end of third week when compared to rest of the test groups and control. Few groups like AZ were not considerable as they were less significant than control (Figure 31). Groups treated with BMP4, PD184352, SU5402 and Sdf1 $\beta$  showed higher number of PGCs at day 12 than control (Figure 32 and 34). PGCs in the control group disappeared by 12<sup>th</sup> day and only Y-27632, Sdf1 $\beta$  and SU5402 were able to retain PGCs up to 18<sup>th</sup> day (Figure 32). After 18<sup>th</sup> day, Y-27632 was capable of maintaining the remaining PGCs for two more extended days but they diminished after 20<sup>th</sup> day. This showed the effect of Y-27632 in delaying or inhibiting the apoptotic pathways in PGCs.

### **2.3.13 Effect of apoptosis inhibitors and growth factors in PGC culture**

Y-27632 (ROCK inhibitor) in combination with other inhibitors like GSk3 inhibitor (AZ), ERK inhibitor (SU5402), MAPK inhibitor (PD184352), Cyclopamine Hedgehog inhibitor (CHi), Caspase inhibitor (Casi) and growth factors BMP4, Sdf1 $\beta$  as well as AdrenoCorticoTropic Hormone (ACTH) were tested in PGC under culture. Combinations are: Y-27632+AZ, Y-27632+SU5402+PD184352, Y-27632+PD184352+AZ, Y-27632+Casi, Y-27632+CHi and Y-27632+ACTH, BMP4+Y-27632, Y-27632+BMP4+Sdf1 $\beta$ , ACTH+Y-27632+BMP4. Among combinations, Casi with Y-27632 (Y-27632+CHi) showed the highest impact on PGC number till 18 days (Figure 35). Control had only 1 PGC survived at 15<sup>th</sup> day whereas Y-27632+Casi had 3 PGCs. Another effective combination was Y-27632+Chi which had 17 PGC on 3<sup>rd</sup> day and 1 PGC survived till 18<sup>th</sup> day. One more effective combination was Y-27632+ACTH in which PGCs survived till 18<sup>th</sup> day (Figure 35 and appendix 5 and 6). There was no PGC survival till 18<sup>th</sup> day in combinations Y-27632+AZ, Y-27632+SU5402+PD184352, Y-27632+AZ+PD184352.

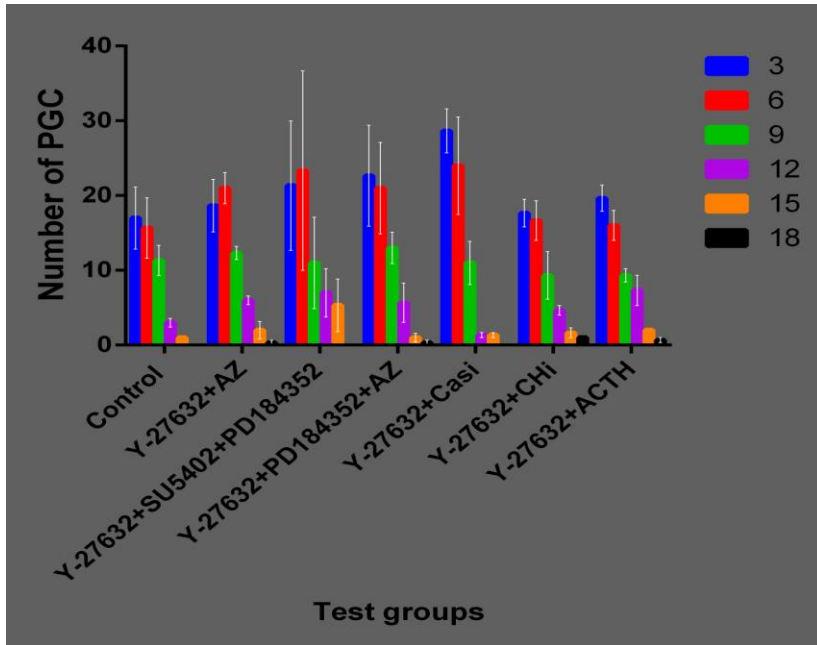


**Figure 35. Effect of Y-27632 with other inhibitors on PGC culture.** Graph showing number of PGCs at different time points under the treatment of Y-27632 with other apoptotic inhibitors. Combinations of inhibitors and growth factors are Y-27632+AZ, Y-27632+SU5402+PD184352, Y-27632+PD184352+AZ, Y-27632+Casi, Y-27632+CHi, Y-27632+ACTH. Y-27632+Casi showed maximum effect till 9 days. Y-27632+ACTH showed consistent effect till 18<sup>th</sup> day of observation. Also Y-27632+CHi and Y-27632+PD184352+AZ showed similar effects whereas control group had no PGC survived after 15<sup>th</sup> day. All values are expressed as mean±SEM from 3 independent experiments. Though the difference in the number of PGCs is observed, they were not significantly high as calculated by analysis of variance (ANOVA).

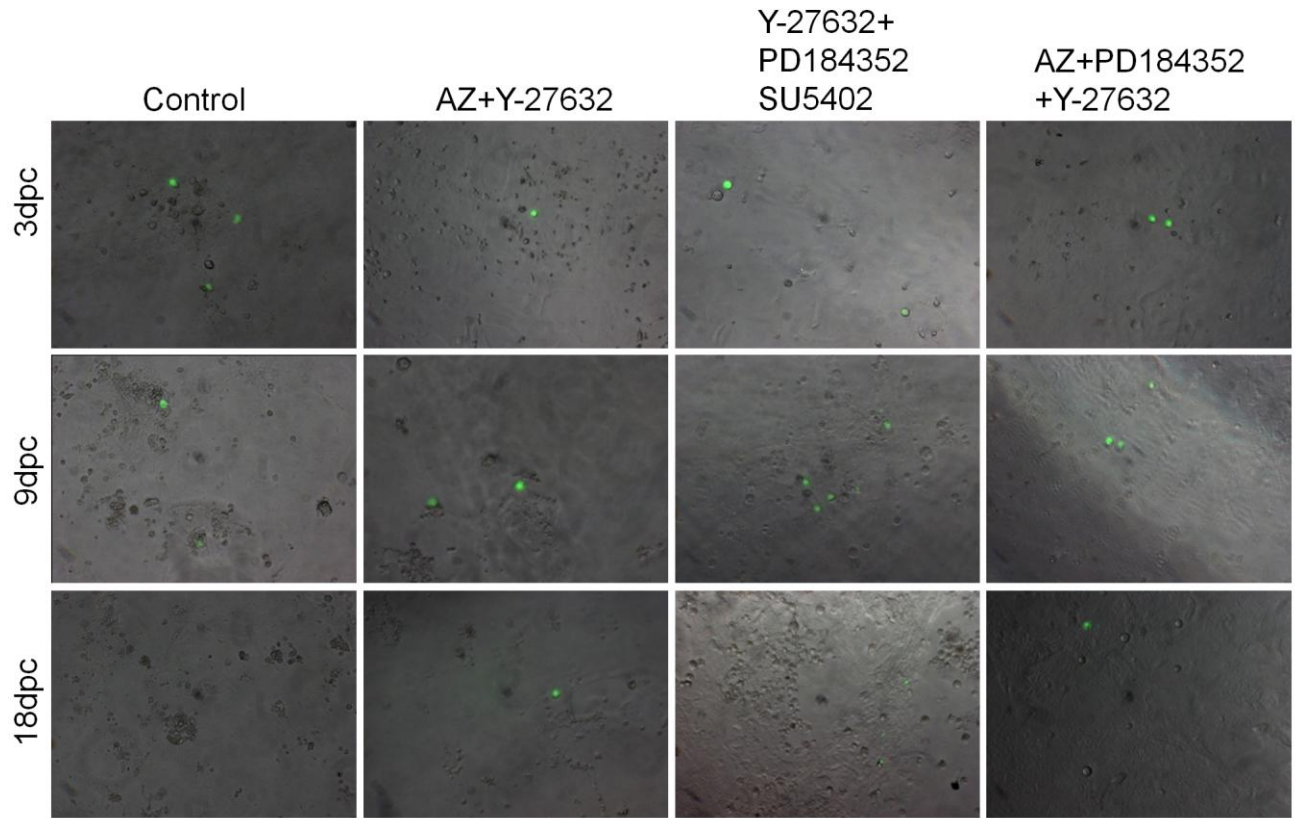


**Figure 36. Phase contrast images of PGCs.** Effect of Y-27632 with other inhibitors on PGC culture are shown at different time points. Combinations of the inhibitors used are AZ+Y-27632, Y-27632+SU5402+PD184352, Y-27632+PD184352+AZ. PGCs are identified by their GFP expression, round and bigger size than somatic non-fluorescent cells. PGCs are attached to somatic cells. There was an increase in the number of PGCs in inhibitor treated blastula embryonic cells than in control. The difference is obvious during initial 9 days (Only selected time points are shown). Scale bar 100  $\mu$ m.

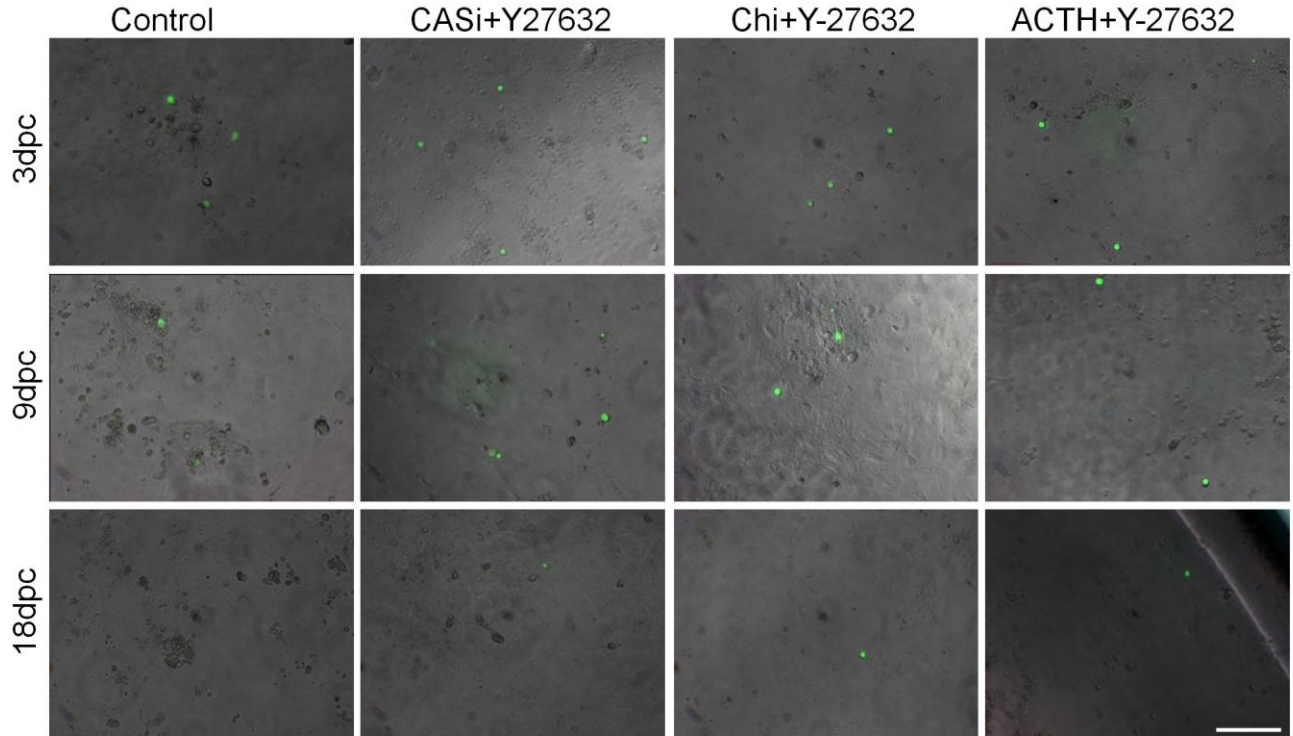


**Figure 37. Phase contrast images of PGCs.** Effects of ROCK inhibitor other inhibitors on PGC culture are shown at different time points. Combinations are; Casi+Y-27632, CHi+Y-27632, ACTH+Y-27632. PGCs are identified by their GFP expression, round and bigger size than somatic non-fluorescent cells. PGCs are attached to somatic cells. There was increase in the number of PGCs in inhibitor treated blastula embryonic cells than in control. The difference is obvious during initial 9 days. Scale bar 100  $\mu$ m.

Y-27632 in combination with growth factors also showed the enhancement in promoting PGC survival in long term culture. Y-27632+BMP4+ACTH showed significant improvement in PGC number from 3<sup>rd</sup> day to 18<sup>th</sup> day than control and Y-27632+BMP4. Y-27632+BMP4+Sdf1 $\beta$  showed significant increase in the number of PGCs on 3<sup>rd</sup> day. On 18<sup>th</sup> day control had no PGC survived whereas Y-27632+BMP4+ACTH and had 1 PGC. Y-27632+BMP4+Sdf1 $\beta$  also improved the survival of PGCs compared to control (Figure 38 and 39). However, Y-27632+BMP4+Sdf1 $\beta$  had only 2 PGC survived till 18<sup>th</sup> day though it had the maximum number of PGCs at the beginning (Figure 39).

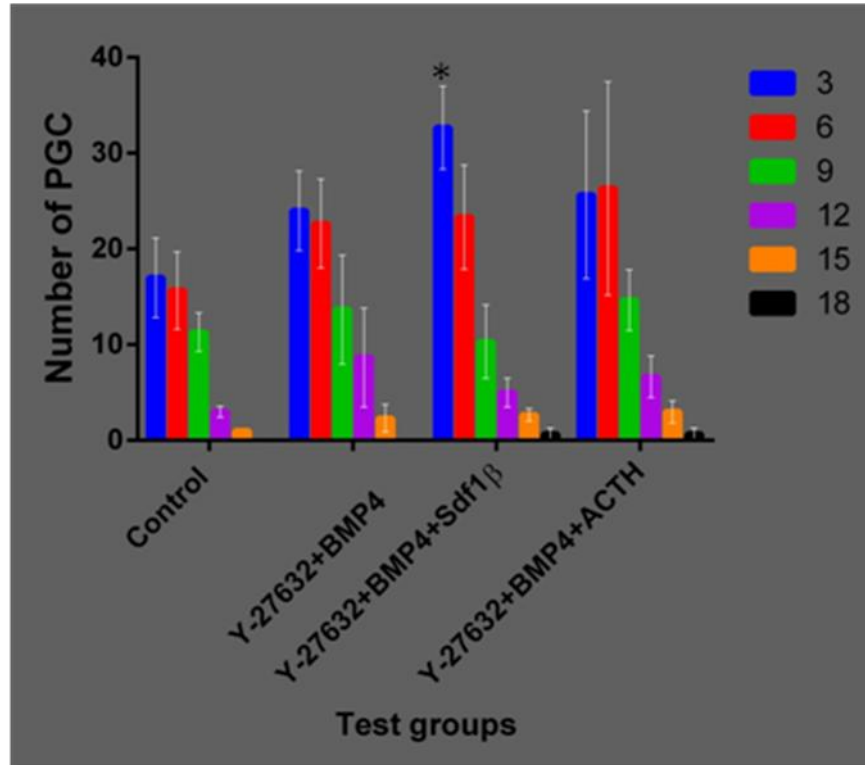


**Figure 38. Effect of Y-27632 with growth factors on PGC culture.** Graph showing number of PGCs at different time points with the treatment of Y-27632 in addition with other apoptotic inhibitors. Combinations are; Y-27632+BMP4, Y-27632+BMP4+Sdf1 $\beta$ , ACTH+Y-27632+BMP4. The combination Y-27632+ACTH+BMP4 showed maximum and persistent effect on PGC survival. Also Sdf1 $\beta$  with Y-27632 and BMP4 showed prolonged effect. All values are expressed as mean $\pm$ SEM from 3 independent experiments. The differences among the control and test groups were not significant except Y-27632+BMP4+Sdf1 $\beta$  at 3<sup>rd</sup> day as as calculated by analysis of variance (ANOVA) (\*p<0.05).

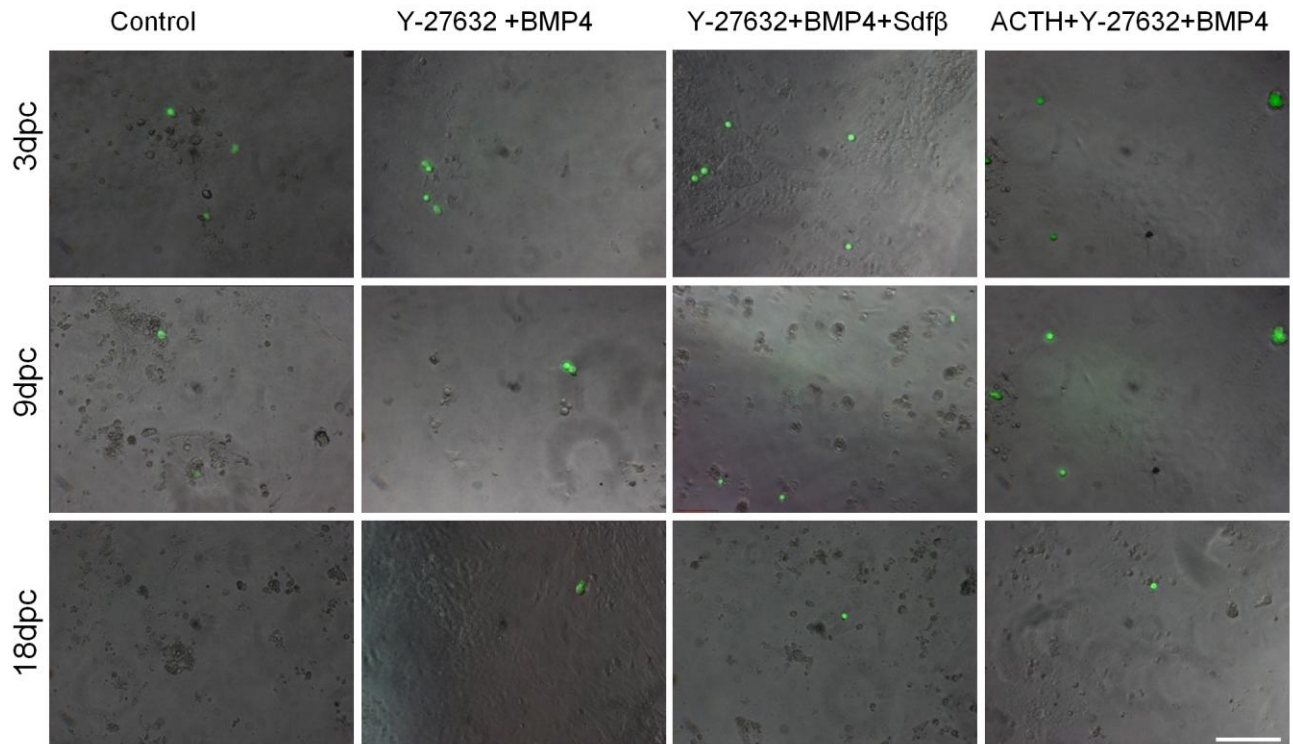


**Figure 39. Phase contrast images of PGCs.** Effect of Y-27632 with growth factors on PGC culture. Combinations are Y-27632+BMP4, Y-27632+BMP4+Sdf1 $\beta$ , ACTH+Y-27632+BMP4. PGCs are identified by their GFP expression, round and larger size than somatic non-fluorescent cells. PGCs are attached to somatic cells. There was increase in the number of PGCs in inhibitor treated cell culture than in control. The difference is obvious during initial 9 days (Only selected time points are shown). Scale bar 100  $\mu$ m.

### Chapter 3: Discussion

Germline stem cells with the ability to self-renew and generate gametes are unique stem cells. They are solely dedicated to transmit genetic information from generation to generation. The germ cells have a special place in the life cycle because they are able to retain the ability of recreation of the organism, a property known as totipotency. Recent advances in cellular therapies have led to the emergence of a multidisciplinary scientific approach to develop therapeutics for a wide variety of diseases and genetic disorders. Although most cell-based therapies currently consist of heterogeneous cell populations, it is anticipated that the standard of care needs well-characterized stem cell. Several lines of evidence have suggested extensive proliferation activity and pluripotency



of germline stem cells. This study demonstrates an effort towards an ambitious goal of generating germ stem cell line from an excellent model organism medaka. In addition to that, identification of the most potential stage of germ cell is also a challenge for the conservation of genetic pool from any species. Hence, this study also covers the expressions of genes which show germ cell specific expressions in a teleost fish. By identifying germ cell markers, it is easier to take a leap towards germ cell conservation (Mardanpour et al., 2008).

However, gametogenesis process is one of the most debated issues in biology from past many decades. Many efforts have been made by several research groups to answer the question whether the process of gametogenesis evolved independently in different organisms or it has a common ancestral prototype. Among many such efforts, studying DAZ family genes in diverse organisms is the most discussed approach. Because they are highly conserved family of genes with ancestral *Boule* present in sea anemones through humans, conserved *dazl* among vertebrates and *DAZ* present only in higher primates (Vangompel and Xu, 2011). This study focused on the expression pattern analysis of genes *boule* and *dazl* in the Nile tilapia. Purpose of this study was to investigate if DAZ family genes follow bisexual germ cell-specific expression in the Nile tilapia as seen in other teleost species and to check their presence in stage specific manner. These findings along with the expression analysis of a widely studied germ gene *vasa* helped to see their expression during gametogenesis of the Nile tilapia. Putative sequences of *boule* and *dazl* of tilapia were obtained by BLAST search using medaka sequences against the testis cDNA library of tilapia available at NCBI when its genome sequence data was not yet available. Thus, the genes *boule* and *dazl* were identified and partially cloned for the first time in this fish. RT-PCR using the primers designed based on putative sequences of *boule* and *dazl* showed their exclusive expression in the ovary and testis in female and male respectively indicating their bisexual gonad-specific expression.

Multiple sequence alignment of cloned tilapia Boule with other organisms showed the conserved positions reside within the RRM whereas tilapia Dazl contained downstream sequence to RRM motif but was in alignment with further downstream sequence. Hence, length of cloned products was sufficient for the synthesis of RNA probes to analyze their expression pattern. Also, this demonstrates a successful application of homology approach to identify most conserved genes of interest across species.

Phylogenetic tree showed that Boule and Dazl proteins from closely related vertebrates clustered into two separate clades. Tilapia Boule groups with stickleback but is separated from medaka Boule suggesting that stickleback and tilapia evolved in parallel. Similarly, tilapia Dazl also groups with stickleback and is separated from medaka (Figure 6). The branching in Boule and Dazl proteins coincides with the separation of fish and tetrapod lineages. Fly remains as outgroup suggesting its place in the evolution is primitive from which all the vertebrate modifications of Boule and Dazl were evolved.

Purpose of this thesis was to study the expression pattern *boule* and *dazl*, the most conserved germ genes which can be potential germ cell markers in tilapia. So far *vasa* is the only gene identified which can specifically identify germ cells in tilapia (Kobayashi et al., 2000). Following the findings from Kobayashi and group, tilapia *vasa* (DDBJ Accession number: AB032467) was cloned up to 646 nt containing the most conserved domains. The expression pattern of *vasa* RNA in this study aligns with the findings of Kobayashi and group (Kobayashi et al., 2000) with insignificant differences in sub-cellular distribution. Hence, in this study, *vasa* served as a positive reference for stages of gametogenesis in the adult tilapia.

Among all reproduction-associated genes known to date, the DAZ gene family is a group of fertility factors that attracted more interest. Expression pattern of *boule* and *dazl* have been described

in various vertebrate species including several fish species. Because of their ancestral history and differential role during gametogenesis, DAZ family has attracted several researchers to understand the mechanistic role of these genes in vertebrates. There is sufficient evidence for the requirement of the DAZ family in germ cell development. *Drosophila* male *boule* mutants are sterile and their spermatocytes are arrested at the G2/M transition stage indicating the requirement of BOULE for male meiosis (Yen, 2004). On the contrary, the *C. elegans daz-1* gene is only required for the female reproduction system and hermaphrodites deficient in *daz-1* are sterile because of blocked oogenesis (Karashima et al., 2000). In the vertebrates, deletion of *Xdazl* mRNA in *Xenopus* oocytes results in tadpoles with no primordial germ cells, indicating the involvement of DAZL in germ development (Houston et al., 1998). Mice homozygous for a *Dazl* null mutation are sterile in both sexes lacking any spermatozoa or oocytes (Ruggiu et al., 1997). The testes of a 9-day old null mutant mouse contain few germ cells which are actively proliferating (Schrans-Stassen et al., 2001). Hence, based on the expression patterns and the phenotypes of null mutants of the various DAZ genes, it is concluded that DAZL and DAZ function both in the development of primordial germ cells and in germ cell differentiation and maturation, whereas the role of BOULE is restricted to meiosis. The success of human BOULE and *Xenopus Xdazl* to rescue the spermatogenic defect of *Drosophila boule* mutants and the abilities of human DAZ and DAZL transgenes to partially rescue the mouse *Dazl* null phenotype indicate that the structures and functions of the DAZ proteins are highly conserved across animal kingdom (Houston et al., 1998).

In teleosts like trout, *boule* exhibits both mitotic and meiotic expression in males but only meiotic expression in females, whereas *dazl* is expressed in mitosis and meiosis of both sexes (Li et al., 2011a; Li et al., 2011b). In the Asian seabass, the expression of *boule* is predominant at the late stages of both oogenesis and spermatogenesis except in the sperm and the expression of *dazl* is

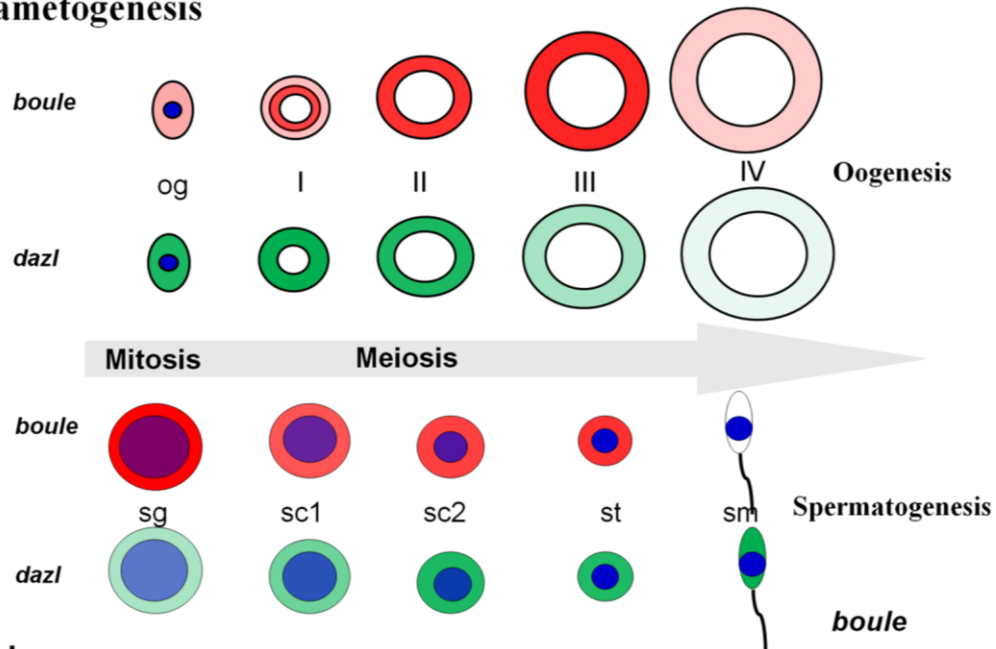
prominent in late spermatogenesis, also throughout the cytoplasm during late oogenesis (Dwarakanath et al., 2014). In gibel carp, *dazl* transcripts were localized in germ plasm organelle during oogenesis (Peng et al., 2009). In early vitellogenic oocytes of zebrafish, *dazl* mRNA was detected at or near the cortex, which extends over one-quarter of the oocytes (Maegawa et al., 1999). The *dazl* RNA was observed adjacent to the germinal vesicle at stage I and localized to the vegetal cortex of stage II oocytes of zebrafish ovary (Kosaka et al., 2007). In medaka *boule* is expressed in adult germ cells at pre-meiotic and meiotic stages of spermatogenesis and oogenesis in the testis, the *dazl* RNA is low at premeiotic stages, abundant at meiotic stages, but absent in postmeiotic stages. In the ovary, the *dazl* RNA persists throughout oogenesis and also show differential expression at premeiotic, meiotic and postmeiotic stages (Xu et al., 2007; Xu et al., 2009).

*Tilapia boule* RNA was localized in the cytoplasm of oocytes while being absent in gonadal somatic cells. Expression was strong in stage I-III oocytes but was the strongest in stage III which gradually disappeared in stage IV. Chromogenic staining showed perinuclear distribution in stage I but uniform distribution in advanced stages. RNA of *boule* expression was granular, uniformly distributed and was maintained throughout oogenesis. Gradual increase in the expression indicated their requirement as the oogenesis progressed. Also it seems like the expression was started in oogonia and gradually increased from perinuclear to whole cytoplasmic expression in advanced oocytes (figure 43). In the testis, *boule* RNA was expressed throughout spermatogenesis but with barely detectable signal in sperm. Despite their weak or strong expression, all the spermatogenic stages expressed *boule* RNA except sperm. Expression of *boule* RNA was gradually decreased as meiosis progressed and ceased in meiotic products. Hence in testis, *boule* RNA may be required for the meiosis to get started and gradually decreases in intensity as meiosis progresses. This

observation denotes that *boule* has bisexual germ cell-specific and stage-specific expression in tilapia like in previously examined teleost fish species.

RNA of *dazl* persisted in the ovary throughout oogenesis with strong expression in stage II oocytes. The expression decreased as oogenesis proceeded from pre-vitellogenesis to post-vitellogenesis. Cytoplasm of stage IV oocytes had the weakest expression. This also might be because of the yolk accumulation in stage IV oocytes. However, difference in the expression of *dazl* RNA among stages of oogenesis was clearly visible in adult tilapia ovary. Unlike *boule*, *dazl* RNA distribution was not granular instead it was a smooth and uniform distribution in the cytoplasm. Hence, *dazl* RNA expression was not gradual increase in oogenesis as in the case of *boule*, but a curve of detectable expression before and after a peak expression in stage II oocytes. This interesting and unique observation in ovary speculates the role of *dazl* during different stages of oogenesis. In testis, *dazl* was expressed throughout spermatogenesis being strong in sperm. The expression seemed to increase gradually and peaked in sperm showing it might be required for the completion of meiosis.

## A Gametogenesis



## B Phylogeny

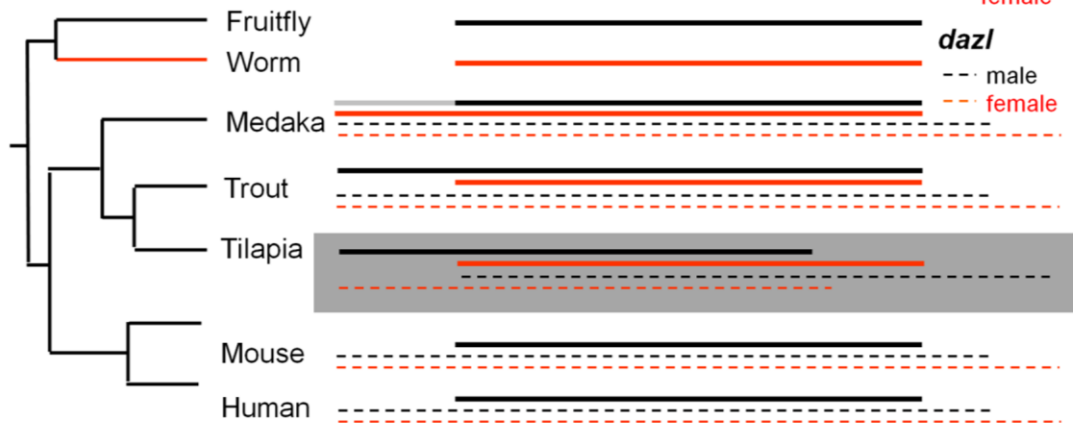


**Figure 40. Symbolic illustration of the expression of *boule* and *dazl* during oogenesis and spermatogenesis in tilapia.** (A) The *boule* and *dazl* RNA distribution in different stages of oogenesis in tilapia ovary. Major stages of gametogenesis are drawn as timeline for *boule* and *dazl* expression. The expression is indicated in color. (brown-*boule* and *dazl*; blue-Dapi; color intensity-relative expression level). (B) Left, phylogeny. Sex specificity of expression is indicated in different colors (male, black; female, red). Right, gametogenic expression. Expression pattern is indicated by extent of horizontal lines. Genes *boule* and *dazl* show bisexual expression in fish species examined. *boule* expression in the ovary is obvious during meiosis, similar to rainbow trout. In male tilapia, *boule* showed both mitotic and weaker meiotic expression. The *dazl* also showed meiotic expression during oogenesis. In males, *dazl* showed its increasing expression as meiosis progressed.

The observations in tilapia support the diversity in the expression pattern of DAZ family genes throughout the vertebrate lineage. A schematic representation gives the simplified explanation of the findings in the Nile tilapia gonads (Figure 40A). The genes *boule* and *dazl* were expressed throughout gametogenesis in both the sex but with stage-specificity. Phylogeny with the expression of DAZ family genes show that the expression in the Nile tilapia is similar to other fish species examined (Figure 40B). Observations of this study speculate that there might be a gradient of *boule* and *dazl* needed for the gametogenesis which can be supported by their overlapped expression in the ovary. As gametogenesis involves several complicated gene expression cascades, *boule* and *dazl* may contribute for the whole event by their presence and level of expression. It will be interesting to know how DAZ family genes correlate with their conserved specific expression at different stages of germline development from embryogenesis to adult in tilapia. Expression pattern of these genes throughout the lifespan of fish may reveal additional evolutionary details of DAZ family genes in fish lineage. In this regard, this study contributes significantly to the evolutionary interests of DAZ family in vertebrates. Also, together with *vasa*, *boule* and *dazl* may serve as potential germ cell markers in the Nile tilapia. Further investigation on the functional aspects of DAZ family genes in this fish is awaited to study the mechanistic role of them during gametogenesis.

Another aspect addressed in this thesis was to improve culture conditions of medaka ES cells. Haploid ES cells from medaka offer immense opportunity for genetic analysis in this fish and is an important genetic asset for the stem cell community. Cryopreservation followed by rapid thawing leads to high apoptosis resulting in loss of large number of cells is a major problem faced by stem cell field. Y-27632 is a selective inhibitor of p160-Rhoassociated coiled-coil kinase (ROCK) and is known as the most potent inhibitor of apoptosis tested (Ishizaki et al., 2000; Watanabe et al., 2007). In this study, Y-27632 was used to see if cryopreservation induced apoptosis can be reduced

in medaka hES cells and blastomeres. Combining haploidy and pluripotency, medaka hES cell lines provide an unique system for direct analysis of recessive and disease phenotypes in various cell lineages of a vertebrate *in vitro* (Yi et al., 2009; Yi et al., 2010). However, upon continuous subculture and cryopreservation process, cells are prone to undergo rapid apoptosis and reduction in the number of haploid percentage. This study showed treatment with Y-27632 significantly increases the survival rate of medaka hES cells after rapid thawing procedure confirmed by trypan blue vital staining. 24 h pretreatment before freezing, addition of Y-27632 in freezing medium and recovery medium containing Y-27632 showed higher survival rates than untreated cells. This effect was proved also by less number of floating cells in treated groups. Further, annexin V-FITC assay showed reduced apoptosis in treated groups. Among the treated groups, presence of Y-27632 in freezing medium has shown the maximum effect than pre and post-freezing treatment. It suggests that there might be an improved uptake of the Y-27632 molecule during rapid freezing. In support to this, proliferation assay for extended days showed that the treated cells have better efficiency in proliferation. Y-27632 in freezing and recovery media showed an improved efficiency in proliferation than pretreated cells and untreated cells which showed the least proliferation for extended days (Appendix, Figure S3). This finding suggests that the effect of Y-27632 was for prolonged time after recovery in group III and IV where it was added in freezing and recovery media respectively.

After treatment with Y-27632 at different times of cryopreservation and complete dissociation, hES cells were grown on a gelatin coated culture dishes at low density (1500 cells/10 cm dish). By day 8, untreated dissociated hES cells generated very few colonies (Figure S4). In contrast, Y-27632-treated dissociated hES cells produced many large colonies. Though better survival, colony formation and proliferation were observed by Y-27632 treatment in medaka hES



cells, experiments are needed to verify whether the treatment retained the pluripotency and transplantation efficiency as observed in human ES cells. The mechanism of Y-27632's action in blocking apoptosis is an intriguing question that awaits future investigation. ROCK is a reasonable candidate target of the antiapoptotic activity of Y-27632. The upstream activation mechanism of ROCK is complex and involves both Rho-independent and dependent pathways (e.g., ROCK is also activated by Caspase-3 cleavage). Future studies on the mode of action of Y-27632 may shed light on why hES cells, unlike mES cells, are so prone to die upon dissociation.

Additional step towards improvement of medaka ES cell culture was taken where Y-27632 was used in the cryopreservation of medaka blastomeres from which the ES cell lines can be established. But, upon dissociation of midblastula embryos into single cells followed by immediate cryopreservation reduces the survival rate of blastomeres upon recovery. This study showed that cells treated with Y-27632 had better survival rate and attachment upon recovery whereas untreated group failed to attach. Blastomeres with Y-27632 in freezing media and recovery media showed improved survival and attachment may be due to the prolonged presence of the compound in them. Previously we have shown that dissociation of early embryos (128 cell stage) is possible and they form ES-like cells in culture (Li et al., 2011c). Utilization of Y-27632 for culture of early stage embryos and their cryopreservation might help us to get successful ES cell lines from medaka which also can be cryopreserved.

In addition to understand the process of gametogenesis on which our previous study was focused, it is also necessary to preserve germ cell pools from economically/genetically/evolutionarily important species. Germ cells are the propagators of the genetic content from generation to generation thereby contributing to species continuation. Also the germ cells play their role in speciation during evolutionary process by carrying adaptive changes

introduced into their genome. Hence, preservation of genetic pool of any species can be achieved by the preservation of its germ cells. There have been several attempts in the past decade to conserve germ cells from endangered species and economically important species. Oocytes vitrification from endangered species like Mexican gray wolves (Boutelle et al., 2011), sperm storage from genetically important fruit flies (Bertin et al., 2010; Perez-Staples et al., 2010), oocytes preservation from economically important breed of sheep (Bhat et al., 2014), Horse oocytes (Curcio Bda et al., 2014), canine sperms (Mota Filho et al., 2014; Yu, 2014). Attempts have been done for the preservation of oocytes of humans to treat probable fertility issues in future (Rodriguez-Wallberg and Oktay, 2012; Oktay and Bedoschi, 2014).

Also several successful attempts have been made to isolate and culture PGCs from various organisms. In fish, germ cell culture has been derived from the testis of medaka (Hong et al., 2004), trout (Sawatari et al., 2007), carp (Panda et al., 2011), and zebrafish (Kawasaki et al., 2012), from the ovary of zebrafish (Wong et al., 2013), from zebrafish embryos at the 26-somite stage (Rao et al., 2011), and from medaka gastrula embryos (Li et al., 2009; Li et al., 2012; Li et al., 2014). Our finding in this study, where isolated medaka blastomeres can form serially cultivable PGCs, provides the basis for PGC derivation which ultimately can be utilized for cryopreservation, transplantation for the production of whole animals and genetic manipulation as has been reported in zebrafish (Kawakami et al., 2010). In zebrafish, attempts have been made to maintain PGCs for few passages with different media formulations. However, the PGCs were isolated from late stage embryos where somatogenesis was already complete and also the feeder layer was used (Fan et al., 2008). We have recently showed the possibility to culture PGCs, which makes medaka an excellent lower vertebrate model for the cell-mediated production of whole animals with defined genetic alterations (Li et al., 2014). This study explored the possibility of early identification and *in vitro* culture of medaka

PGCs. This study also showed the effects Y-27632 and PGC inducers *in vitro*. Midblastula cell culture from *vasa*-transgenic medaka revealed the formation of PGCs in 48 h post-culture *in vitro* resembling the situation *in vivo*. Followed by the formation on 2<sup>nd</sup> day, PGCs also showed increase in their number till 9 dpc. Naturally, the number of PGCs numbers will be the highest during 6-9 day and then decline in prolonged culture, ultimately perish by 15 dpc in the absence of additional growth factors and inducers. Y-27632 and BMP4 showed positive effects on PGC number and survival than rest of the inhibitors examined (Figure 34-37). The obvious increase in the number of PGCs during 3-9 days in Y-27632 and BMP4 treated, either individually or combined may be because they reduced the disappearance of PGCs by inhibiting apoptosis and promoting cell survival. Extended survival of few PGCs up to 18 days is also observed whereas untreated group had no PGC survived. Extended survival was reduced in untreated groups as PGCs undergo apoptosis or instant differentiation under culture conditions due to the absence of embryonic environment. This was partially overcome by Y-27632 treatment also in combination with BMP4 and Sdf1 $\beta$ . PGC survival was prolonged in the cultures with the inhibitors of apoptosis pathway, both ROCK kinases and downstream molecules, in addition to the growth factors to promote the survival. Though there were obvious increase in the number of PGCs appeared in Y-27632 treated cultures and non treated cultures, it was not significantly different at all time points. Few inhibitors even had negative effect on PGC number. However, there was significant increase in the culture treated with Y-27632, BMP4 and Sdf1 $\beta$ . This combined effect may have improved both their initial number and survival for long duration. Although, attempt to culture PGCs for a prolonged time with their enhanced number was successful with apoptosis inhibiting factor, it seems a cocktail of such factors are required for better results. Utilization of such a cocktail would help in large scale culture of germ cells. Germ stem cells

offer immense opportunity for genetic analysis and manipulation as well as their preservation thereby contribute for the conservation of genetic pool.

#### 4. Conclusions

- Genes *boule* and *dazl* are cloned by homology approach and are shown to exhibit bisexual germ cell-specific expression in the Nile tilapia.
- The gene *boule* shows gradual increase in the expression as oogenesis progresses and shows stage specific peak expression. In testis, *boule* exhibits mitotic and meiotic expression but absence in sperm.
- The gene *dazl* expression is stronger in early oogenesis than *boule*, but maintained throughout oogenesis exhibiting stage specific peak expression. In testis, *dazl* shows meiotic expression with a strong expression in sperm.
- Diversity in stage-specific peak expression of *boule* and *dazl* is observed in the gonads of both sexes which prove that the Nile tilapia also exhibits differential expression pattern of DAZ family genes as observed in many other teleosts.
- Improved survival rate of cryopreserved medaka hES cells upon recovery is achieved using Y-27632.
- Improved proliferation and clonal expansion is also shown in the presence of Y-27632.
- Freshly isolated midblastula cells are also able to be cryopreserved and recovered for ES cell establishment in the presence of Y-27632.
- Y-27632 and growth factors like BMP4 improved the survival of PGCs thereby improved PGC culture for prolonged time.
- PGC culture for more than 2 weeks is possible in the presence of Y-27632 and if isolated, there is immense hope to generate germ stem cell line.

## References

- Aeckerle, N., Drummer, C., Debowski, K., Viebahn, C. and Behr, R., 2014. Primordial germ cell development in the marmoset monkey as revealed by pluripotency factor expression: suggestion of a novel model of embryonic germ cell translocation. *Mol Hum Reprod*.
- Assefa, Z., Vantieghem, A., Declercq, W., Vandenabeele, P., Vandenheede, J.R., Merlevede, W., de Witte, P. and Agostinis, P., 1999. The activation of the c-Jun N-terminal kinase and p38 mitogen-activated protein kinase signaling pathways protects HeLa cells from apoptosis following photodynamic therapy with hypericin. *J Biol Chem* 274, 8788-96.
- Bejar, J., Hong, Y. and Scharl, M., 2003. Mitf expression is sufficient to direct differentiation of medaka blastula derived stem cells to melanocytes. *Development* 130, 6545-53.
- Bertin, S., Scolari, F., Guglielmino, C.R., Bonizzoni, M., Bonomi, A., Marchini, D., Gomulski, L.M., Gasperi, G., Malacrida, A.R. and Matessi, C., 2010. Sperm storage and use in polyandrous females of the globally invasive fruitfly, *Ceratitis capitata*. *J Insect Physiol* 56, 1542-51.
- Bhat, M.H., Sharma, V., Khan, F.A., Naykoo, N.A., Yaqoob, S.H., Ruby, Khan, H.M., Fazili, M.R., Ganai, N.A. and Shah, R.A., 2014. Comparison of slow freezing and vitrification on ovine immature oocytes. *Cryo Letters* 35, 77-82.
- Bhat, N. and Hong, Y., 2014. Cloning and expression of boule and dazl in the Nile tilapia (*Oreochromis niloticus*). *Gene* 540, 140-5.
- Boutelle, S., Lenahan, K., Krisher, R., Bauman, K.L., Asa, C.S. and Silber, S., 2011. Vitrification of oocytes from endangered Mexican gray wolves (*Canis lupus baileyi*). *Theriogenology* 75, 647-54.
- Chen, G., Hou, Z., Gulbranson, D.R. and Thomson, J.A., 2010. Actin-myosin contractility is responsible for the reduced viability of dissociated human embryonic stem cells. *Cell Stem Cell* 7, 240-8.
- Cheng, M.H., Maines, J.Z. and Wasserman, S.A., 1998. Biphasic subcellular localization of the DAZL-related protein boule in *Drosophila* spermatogenesis. *Dev Biol* 204, 567-76.
- Collodi, P., Kamei, Y., Ernst, T., Miranda, C., Buhler, D.R. and Barnes, D.W., 1992. Culture of cells from zebrafish (*Brachydanio rerio*) embryo and adult tissues. *Cell Biol Toxicol* 8, 43-61.
- Cooke, H.J., Lee, M., Kerr, S. and Ruggiu, M., 1996. A murine homologue of the human DAZ gene is autosomal and expressed only in male and female gonads. *Hum Mol Genet* 5, 513-6.
- Curcio Bda, R., Pereira, G.R., Antunes, L.I., Boff, A.N., dos Santos, F.C., Lucas, T., Jr., Nogueira, C.E., Corcini, C.D., Liu, I. and Deschamps, J.C., 2014. Vitrification of equine oocytes with a polyvinyl alcohol after in vitro maturation with equine growth hormone and insulin-like growth factor-I. *Cryo Letters* 35, 90-4.
- D'Apuzzo, M., Rolink, A., Loetscher, M., Hoxie, J.A., Clark-Lewis, I., Melchers, F., Baggiolini, M. and Moser, B., 1997. The chemokine SDF-1, stromal cell-derived factor 1, attracts early stage B cell precursors via the chemokine receptor CXCR4. *Eur J Immunol* 27, 1788-93.
- De Felici, M., Farini, D. and Dolci, S., 2009. In or out stemness: comparing growth factor signalling in mouse embryonic stem cells and primordial germ cells. *Curr Stem Cell Res Ther* 4, 87-97.
- De Miguel, M.P. and Donovan, P.J., 2000. Isolation and culture of mouse germ cells. *Methods Mol Biol* 137, 403-8.
- de Moor, C.H. and Richter, J.D., 2001. Translational control in vertebrate development. *Int Rev Cytol* 203, 567-608.
- Dwarakanath, M., Lim, M., Xu, H. and Hong, Y., 2014. Differential expression of boule and dazl in adult germ cells of the Asian seabass. *Gene* 549, 237-42.
- Eirin-Lopez, J.M. and Ausio, J., 2011. Boule and the Evolutionary Origin of Metazoan Gametogenesis: A Grandpa's Tale. *Int J Evol Biol* 2011, 972457.
- Elis, S., Batellier, F., Couty, I., Balzergue, S., Martin-Magniette, M.L., Monget, P., Blesbois, E. and Govoroun, M.S., 2008. Search for the genes involved in oocyte maturation and early embryo development in the hen. *BMC Genomics* 9, 110.
- Evans, M.J. and Kaufman, M.H., 1981. Establishment in culture of pluripotential cells from mouse embryos. *Nature* 292, 154-6.

- Extavour, C.G. and Akam, M., 2003. Mechanisms of germ cell specification across the metazoans: epigenesis and preformation. *Development* 130, 5869-84.
- Fan, L., Moon, J., Wong, T.T., Crodian, J. and Collodi, P., 2008. Zebrafish primordial germ cell cultures derived from vasa::RFP transgenic embryos. *Stem Cells Dev* 17, 585-97.
- Gauthaman, K., Fong, C.Y., Subramanian, A., Biswas, A. and Bongso, A., 2010. ROCK inhibitor Y-27632 increases thaw-survival rates and preserves stemness and differentiation potential of human Wharton's jelly stem cells after cryopreservation. *Stem Cell Rev* 6, 665-76.
- Gevers, P., Dulos, J., Schipper, H. and Timmermans, L.P., 1992. Origin of primordial germ cells, as characterized by the presence of nuage, in embryos of the teleost fish *Barbus conchoniuis*. *Eur J Morphol* 30, 195-204.
- Hamaguchi, S., 1982. A light- and electron-microscopic study on the migration of primordial germ cells in the teleost, *Oryzias latipes*. *Cell Tissue Res* 227, 139-51.
- Hay, B., Ackerman, L., Barbel, S., Jan, L.Y. and Jan, Y.N., 1988a. Identification of a component of *Drosophila* polar granules. *Development* 103, 625-40.
- Hay, B., Jan, L.Y. and Jan, Y.N., 1988b. A protein component of *Drosophila* polar granules is encoded by vasa and has extensive sequence similarity to ATP-dependent helicases. *Cell* 55, 577-87.
- Herpin, A., Rohr, S., Riedel, D., Kluever, N., Raz, E. and Schartl, M., 2007. Specification of primordial germ cells in medaka (*Oryzias latipes*). *BMC Dev Biol* 7, 3.
- Hong, N., Chen, S., Ge, R., Song, J., Yi, M. and Hong, Y., 2012. Interordinal chimera formation between medaka and zebrafish for analyzing stem cell differentiation. *Stem Cells Dev* 21, 2333-41.
- Hong, N., Li, M., Zeng, Z., Yi, M., Deng, J., Gui, J., Winkler, C., Schartl, M. and Hong, Y., 2010. Accessibility of host cell lineages to medaka stem cells depends on genetic background and irradiation of recipient embryos. *Cell Mol Life Sci* 67, 1189-1202.
- Hong, N., Li, Z. and Hong, Y., 2011. Fish stem cell cultures. *Int J Biol Sci* 7, 392-402.
- Hong, Y., 2010. Medaka haploid embryonic stem cells. *Methods Cell Biol* 100, 55-69.
- Hong, Y., 2011. Fishing fish stem cells and nuclear transplants. *Int J Biol Sci* 7, 390-1.
- Hong, Y., Liu, T., Zhao, H., Xu, H., Wang, W., Liu, R., Chen, T., Deng, J. and Gui, J., 2004. Establishment of a normal medakafish spermatogonial cell line capable of sperm production in vitro. *Proc Natl Acad Sci U S A* 101, 8011-6.
- Hong, Y. and Schartl, M., 2006. Isolation and differentiation of medaka embryonic stem cells. *Methods Mol Biol* 329, 3-16.
- Hong, Y., Winkler, C. and Schartl, M., 1996. Pluripotency and differentiation of embryonic stem cell lines from the medakafish (*Oryzias latipes*). *Mech Dev* 60, 33-44.
- Hong Yunhan, S.M., 1996. Establishment and growth responses of early medaka (*Oryzias latipes*) embryonic cells in feeder layer-free culture. *Mol Mar Biol Biotechnol* 5, 93-104.
- Houston, D.W., Zhang, J., Maines, J.Z., Wasserman, S.A. and King, M.L., 1998. A *Xenopus* DAZ-like gene encodes an RNA component of germ plasm and is a functional homologue of *Drosophila* boule. *Development* 125, 171-80.
- Hu, E. and Lee, D., 2005. Rho kinase as potential therapeutic target for cardiovascular diseases: opportunities and challenges. *Expert Opin Ther Targets* 9, 715-36.
- Irie, N., Tang, W.W. and Azim Surani, M., 2014. Germ cell specification and pluripotency in mammals: a perspective from early embryogenesis. *Reprod Med Biol* 13, 203-215.
- Ishizaki, T., Uehata, M., Tamechika, I., Keel, J., Nonomura, K., Maekawa, M. and Narumiya, S., 2000. Pharmacological properties of Y-27632, a specific inhibitor of rho-associated kinases. *Mol Pharmacol* 57, 976-83.
- Iwamatsu, T., 2004. Stages of normal development in the medaka *Oryzias latipes*. *Mech Dev* 121, 605-18.
- Johnson, A.D., Bachvarova, R.F., Drum, M. and Masi, T., 2001. Expression of axolotl DAZL RNA, a marker of germ plasm: widespread maternal RNA and onset of expression in germ cells approaching the gonad. *Dev Biol* 234, 402-15.

- Karashima, T., Sugimoto, A. and Yamamoto, M., 2000. *Caenorhabditis elegans* homologue of the human azoospermia factor DAZ is required for oogenesis but not for spermatogenesis. *Development* 127, 1069-79.
- Kawabata, M., Imamura, T. and Miyazono, K., 1998. Signal transduction by bone morphogenetic proteins. *Cytokine Growth Factor Rev* 9, 49-61.
- Kawakami, Y., Goto-Kazeto, R., Saito, T., Fujimoto, T., Higaki, S., Takahashi, Y., Arai, K. and Yamaha, E., 2010. Generation of germ-line chimera zebrafish using primordial germ cells isolated from cultured blastomeres and cryopreserved embryoids. *Int J Dev Biol* 54, 1493-501.
- Kawasaki, T., Saito, K., Sakai, C., Shinya, M. and Sakai, N., 2012. Production of zebrafish offspring from cultured spermatogonial stem cells. *Genes Cells* 17, 316-25.
- Kimble, J. and Page, D.C., 2007. The mysteries of sexual identity. The germ cell's perspective. *Science* 316, 400-1.
- Kobayashi, T., Kajiura-Kobayashi, H. and Nagahama, Y., 2000. Differential expression of vasa homologue gene in the germ cells during oogenesis and spermatogenesis in a teleost fish, tilapia, *Oreochromis niloticus*. *Mech Dev* 99, 139-42.
- Kosaka, K., Kawakami, K., Sakamoto, H. and Inoue, K., 2007. Spatiotemporal localization of germ plasm RNAs during zebrafish oogenesis. *Mech Dev* 124, 279-89.
- Kuo, P.L., Wang, S.T., Lin, Y.M., Lin, Y.H., Teng, Y.N. and Hsu, C.C., 2004. Expression profiles of the DAZ gene family in human testis with and without spermatogenic failure. *Fertil Steril* 81, 1034-40.
- Leeb, M. and Wutz, A., 2011. Derivation of haploid embryonic stem cells from mouse embryos. *Nature* 479, 131-4.
- Li, M., Hong, N., Gui, J. and Hong, Y., 2012. Medaka piwi is essential for primordial germ cell migration. *Curr Mol Med* 12, 1040-9.
- Li, M., Hong, N., Xu, H., Yi, M., Li, C., Gui, J. and Hong, Y., 2009. Medaka vasa is required for migration but not survival of primordial germ cells. *Mech Dev* 126, 366-81.
- Li, M., Shen, Q., Wong, F.M., Xu, H., Hong, N., Zeng, L., Liu, L., Wei, Q. and Hong, Y., 2011a. Germ cell sex prior to meiosis in the rainbow trout. *Protein Cell* 2, 48-54.
- Li, M., Shen, Q., Xu, H., Wong, F.M., Cui, J., Li, Z., Hong, N., Wang, L., Zhao, H., Ma, B. and Hong, Y., 2011b. Differential conservation and divergence of fertility genes boule and dazl in the rainbow trout. *PLoS One* 6, e15910.
- Li, Z., Bhat, N., Manali, D., Wang, D., Hong, N., Yi, M., Ge, R. and Hong, Y., 2011c. Medaka cleavage embryos are capable of generating ES-like cell cultures. *Int J Biol Sci* 7, 418-25.
- Li, Z., Li, M., Hong, N., Yi, M. and Hong, Y., 2014. Formation and cultivation of medaka primordial germ cells. *Cell Tissue Res* 357, 71-81.
- Linder, P., Lasko, P.F., Ashburner, M., Leroy, P., Nielsen, P.J., Nishi, K., Schnier, J. and Slonimski, P.P., 1989. Birth of the D-E-A-D box. *Nature* 337, 121-2.
- Maegawa, S., Yasuda, K. and Inoue, K., 1999. Maternal mRNA localization of zebrafish DAZ-like gene. *Mech Dev* 81, 223-6.
- Mardanpour, P., Guan, K., Nolte, J., Lee, J.H., Hasenfuss, G., Engel, W. and Nayernia, K., 2008. Potency of germ cells and its relevance for regenerative medicine. *J Anat* 213, 26-9.
- Martello, G. and Smith, A., 2014. The nature of embryonic stem cells. *Annu Rev Cell Dev Biol* 30, 647-75.
- Martin, G.R., 1981. Isolation of a pluripotent cell line from early mouse embryos cultured in medium conditioned by teratocarcinoma stem cells. *Proc Natl Acad Sci U S A* 78, 7634-8.
- Mitchell, R.T., Cowan, G., Morris, K.D., Anderson, R.A., Fraser, H.M., McKenzie, K.J., Wallace, W.H., Kelnar, C.J., Saunders, P.T. and Sharpe, R.M., 2008. Germ cell differentiation in the marmoset (*Callithrix jacchus*) during fetal and neonatal life closely parallels that in the human. *Hum Reprod* 23, 2755-65.
- Mota Filho, A.C., Silva, H.V., Nunes, T.G., de Souza, M.B., de Freitas, L.A., de Araujo, A.A. and da Silva, L.D., 2014. Cryopreservation of canine epididymal sperm using ACP-106c and TRIS. *Cryobiology* 69, 17-21.

- Oktaý, K. and Bedoschi, G., 2014. Oocyte Cryopreservation for Fertility Preservation in Postpubertal Female Children at Risk for Premature Ovarian Failure Due to Accelerated Follicle Loss in Turner Syndrome or Cancer Treatments. *J Pediatr Adolesc Gynecol*.
- Otori, M., Karashima, T. and Yamamoto, M., 2006. The *Caenorhabditis elegans* homologue of deleted in azoospermia is involved in the sperm/oocyte switch. *Mol Biol Cell* 17, 3147-55.
- Panda, R.P., Barman, H.K. and Mohapatra, C., 2011. Isolation of enriched carp spermatogonial stem cells from *Labeo rohita* testis for in vitro propagation. *Theriogenology* 76, 241-51.
- Peng, J.X., Xie, J.L., Zhou, L., Hong, Y.H. and Gui, J.F., 2009. Evolutionary conservation of *Dazl* genomic organization and its continuous and dynamic distribution throughout germline development in gynogenetic gibel carp. *J Exp Zool B Mol Dev Evol* 312, 855-71.
- Perez-Staples, D., Weldon, C.W., Radhakrishnan, P., Prenter, J. and Taylor, P.W., 2010. Control of copula duration and sperm storage by female Queensland fruit flies. *J Insect Physiol* 56, 1755-62.
- Rao, F., Wang, T., Li, M., Li, Z., Hong, N., Zhao, H., Yan, Y., Lu, W., Chen, T., Wang, W., Lim, M., Yuan, Y., Liu, L., Zeng, L., Wei, Q., Guan, G., Li, C. and Hong, Y., 2011. Medaka tert produces multiple variants with differential expression during differentiation in vitro and in vivo. *Int J Biol Sci* 7, 426-39.
- Reijo, R., Seligman, J., Dinulos, M.B., Jaffe, T., Brown, L.G., Disteche, C.M. and Page, D.C., 1996. Mouse autosomal homolog of *DAZ*, a candidate male sterility gene in humans, is expressed in male germ cells before and after puberty. *Genomics* 35, 346-52.
- Resnick, J.L., Bixler, L.S., Cheng, L. and Donovan, P.J., 1992. Long-term proliferation of mouse primordial germ cells in culture. *Nature* 359, 550-1.
- Rodriguez-Wallberg, K.A. and Oktaý, K., 2012. Recent advances in oocyte and ovarian tissue cryopreservation and transplantation. *Best Pract Res Clin Obstet Gynaecol* 26, 391-405.
- Ruggiu, M., Speed, R., Taggart, M., McKay, S.J., Kilanowski, F., Saunders, P., Dorin, J. and Cooke, H.J., 1997. The mouse *Dazla* gene encodes a cytoplasmic protein essential for gametogenesis. *Nature* 389, 73-7.
- Sawatari, E., Shikina, S., Takeuchi, T. and Yoshizaki, G., 2007. A novel transforming growth factor-beta superfamily member expressed in gonadal somatic cells enhances primordial germ cell and spermatogonial proliferation in rainbow trout (*Oncorhynchus mykiss*). *Dev Biol* 301, 266-75.
- Saxena, R., Brown, L.G., Hawkins, T., Alagappan, R.K., Skaletsky, H., Reeve, M.P., Reijo, R., Rozen, S., Dinulos, M.B., Disteche, C.M. and Page, D.C., 1996. The *DAZ* gene cluster on the human Y chromosome arose from an autosomal gene that was transposed, repeatedly amplified and pruned. *Nat Genet* 14, 292-9.
- Schrans-Stassen, B.H., Saunders, P.T., Cooke, H.J. and de Rooij, D.G., 2001. Nature of the spermatogenic arrest in *Dazl* <sup>-/-</sup> mice. *Biol Reprod* 65, 771-6.
- Seboun, E., Barbaux, S., Bourgeron, T., Nishi, S., Agulnik, A., Egashira, M., Nikkawa, N., Bishop, C., Fellous, M., McElreavey, K. and Kasahara, M., 1997. Gene sequence, localization, and evolutionary conservation of *DAZLA*, a candidate male sterility gene. *Genomics* 41, 227-35.
- Seifert, A.W., Bouldin, C.M., Choi, K.S., Harfe, B.D. and Cohn, M.J., 2009. Multiphasic and tissue-specific roles of sonic hedgehog in cloacal septation and external genitalia development. *Development* 136, 3949-57.
- ten Dijke, P., Fu, J., Schaap, P. and Roelen, B.A., 2003. Signal transduction of bone morphogenetic proteins in osteoblast differentiation. *J Bone Joint Surg Am* 85-A Suppl 3, 34-8.
- Thomson, J.A., Itskovitz-Eldor, J., Shapiro, S.S., Waknitz, M.A., Swiergiel, J.J., Marshall, V.S. and Jones, J.M., 1998. Embryonic stem cell lines derived from human blastocysts. *Science* 282, 1145-7.
- Vangompel, M.J. and Xu, E.Y., 2011. The roles of the *DAZ* family in spermatogenesis: More than just translation? *Spermatogenesis* 1, 36-46.
- Venables, J.P. and Eperon, I., 1999. The roles of RNA-binding proteins in spermatogenesis and male infertility. *Curr Opin Genet Dev* 9, 346-54.
- Versieren, K., Van der Jeught, M., O'Leary, T., Duggal, G., Gerris, J., Chuva de Sousa Lopes, S., Heindryckx, B. and De Sutter, P., 2012. Effect of small molecule supplements during in vitro culture of mouse



- zygotes and parthenogenetic embryos on hypoblast formation and stem cell derivation. *Stem Cell Rev* 8, 1088-97.
- Wakamatsu, Y., Ozato, K. and Sasado, T., 1994. Establishment of a pluripotent cell line derived from a medaka (*Oryzias latipes*) blastula embryo. *Mol Mar Biol Biotechnol* 3, 185-91.
- Wakayama, S., Hikichi, T., Suetsugu, R., Sakaide, Y., Bui, H.T., Mizutani, E. and Wakayama, T., 2007. Efficient establishment of mouse embryonic stem cell lines from single blastomeres and polar bodies. *Stem Cells* 25, 986-93.
- Watanabe, K., Ueno, M., Kamiya, D., Nishiyama, A., Matsumura, M., Wataya, T., Takahashi, J.B., Nishikawa, S., Nishikawa, S., Muguruma, K. and Sasai, Y., 2007. A ROCK inhibitor permits survival of dissociated human embryonic stem cells. *Nat Biotechnol* 25, 681-6.
- Wittbrodt, J., Shima, A. and Schartl, M., 2002. Medaka--a model organism from the far East. *Nat Rev Genet* 3, 53-64.
- Wobus, A.M. and Boheler, K.R., 2005. Embryonic stem cells: prospects for developmental biology and cell therapy. *Physiol Rev* 85, 635-78.
- Wong, T.T., Tesfamichael, A. and Collodi, P., 2013. Production of zebrafish offspring from cultured female germline stem cells. *PLoS One* 8, e62660.
- Wylie, C., 1999. Germ cells. *Cell* 96, 165-74.
- Xu, E.Y., Moore, F.L. and Pera, R.A., 2001. A gene family required for human germ cell development evolved from an ancient meiotic gene conserved in metazoans. *Proc Natl Acad Sci U S A* 98, 7414-9.
- Xu, H., Li, M., Gui, J. and Hong, Y., 2007. Cloning and expression of medaka *dazl* during embryogenesis and gametogenesis. *Gene Expr Patterns* 7, 332-8.
- Xu, H., Li, Z., Li, M., Wang, L. and Hong, Y., 2009. Boule is present in fish and bisexually expressed in adult and embryonic germ cells of medaka. *PLoS One* 4, e6097.
- Yajima, M. and Wessel, G.M., 2011. The multiple hats of Vasa: its functions in the germline and in cell cycle progression. *Mol Reprod Dev* 78, 861-7.
- Yen, P.H., 2004. Putative biological functions of the DAZ family. *Int J Androl* 27, 125-9.
- Yi, M., Hong, N. and Hong, Y., 2009. Generation of medaka fish haploid embryonic stem cells. *Science* 326, 430-3.
- Yi, M., Hong, N. and Hong, Y., 2010. Derivation and characterization of haploid embryonic stem cell cultures in medaka fish. *Nat Protoc* 5, 1418-30.
- Ying, Q.L., Wray, J., Nichols, J., Batlle-Morera, L., Doble, B., Woodgett, J., Cohen, P. and Smith, A., 2008. The ground state of embryonic stem cell self-renewal. *Nature* 453, 519-23.
- Yoshida, K., Taga, T., Saito, M., Suematsu, S., Kumanogoh, A., Tanaka, T., Fujiwara, H., Hirata, M., Yamagami, T., Nakahata, T., Hirabayashi, T., Yoneda, Y., Tanaka, K., Wang, W.Z., Mori, C., Shiota, K., Yoshida, N. and Kishimoto, T., 1996. Targeted disruption of gp130, a common signal transducer for the interleukin 6 family of cytokines, leads to myocardial and hematological disorders. *Proc Natl Acad Sci U S A* 93, 407-11.
- Yu, I.J., 2014. Canine sperm cryopreservation using glucose in glycerol-free Tris. *Cryo Letters* 35, 101-7.
- Zhang, L., Valdez, J.M., Zhang, B., Wei, L., Chang, J. and Xin, L., 2011. ROCK inhibitor Y-27632 suppresses dissociation-induced apoptosis of murine prostate stem/progenitor cells and increases their cloning efficiency. *PLoS One* 6, e18271.

**Website pages:** <http://www.aquaticcommunity.com/tilapia/tilapia.php>

## Appendix

### 1. Table S1. Primers used for gene cloning and probe synthesis

Name	Sequence
Tboule f	5'-ATGGCTAAGGAAGCGGCGAG-3'
Tboule r	5'-AACACAGGTGGCTGAACAGAAAC-3'
Tdazl f	5'-ATGAAAGAAAGGGTCTCTCGG-3'
Tdazl r	5'-GTTTGAGGCACGGAATGAGAGGCGAG-3'
Tvasa f	5'-GTCGAGGAAGAATCTCATCT-3'
Tvasa r	5'-ACTTGCTGACGTTTCTCTTT-3'
Tβ-actin f	5'-GGCATCACACCTTCTACAACGA-3'
Tβ-actin r	5'-ACGCTCTGTCAGGATCTTCA-3'

### 2. Chromogenic *in situ* hybridization for *vasa* RNA expression

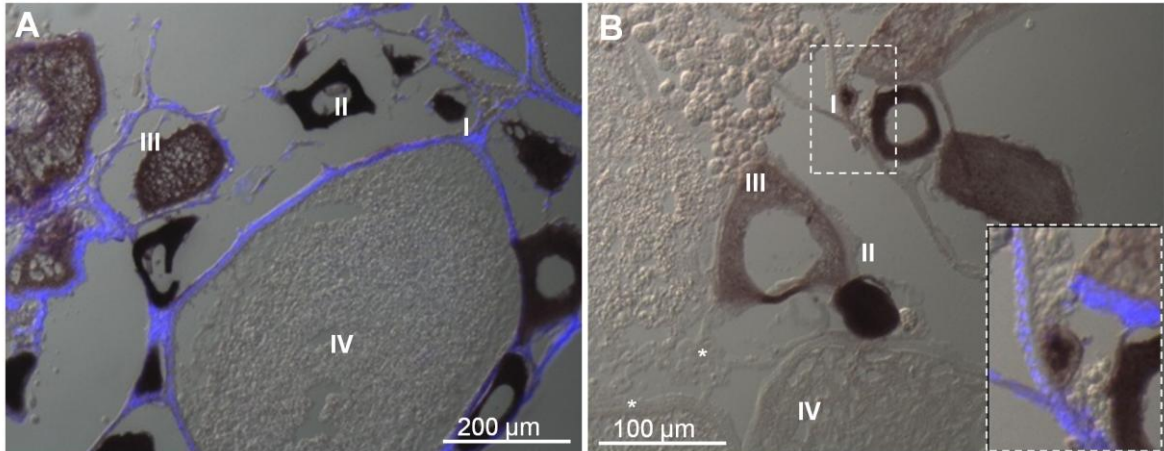


**Figure S2. *vasa* RNA expression in ovary** (A) CISH on ovary sections to show stages of oogenesis and *vasa* RNA distribution in oocytes. (B) Section at higher magnification to show stage I oocyte and the inset to show framed area with sub cellular signal distribution. *vasa* RNA is concentrated in pre-vitellogenic oocytes but widely dispersed in advanced oocytes at stage III and IV.

### 3. Proliferation of hES cells after cryopreservation and thawing.

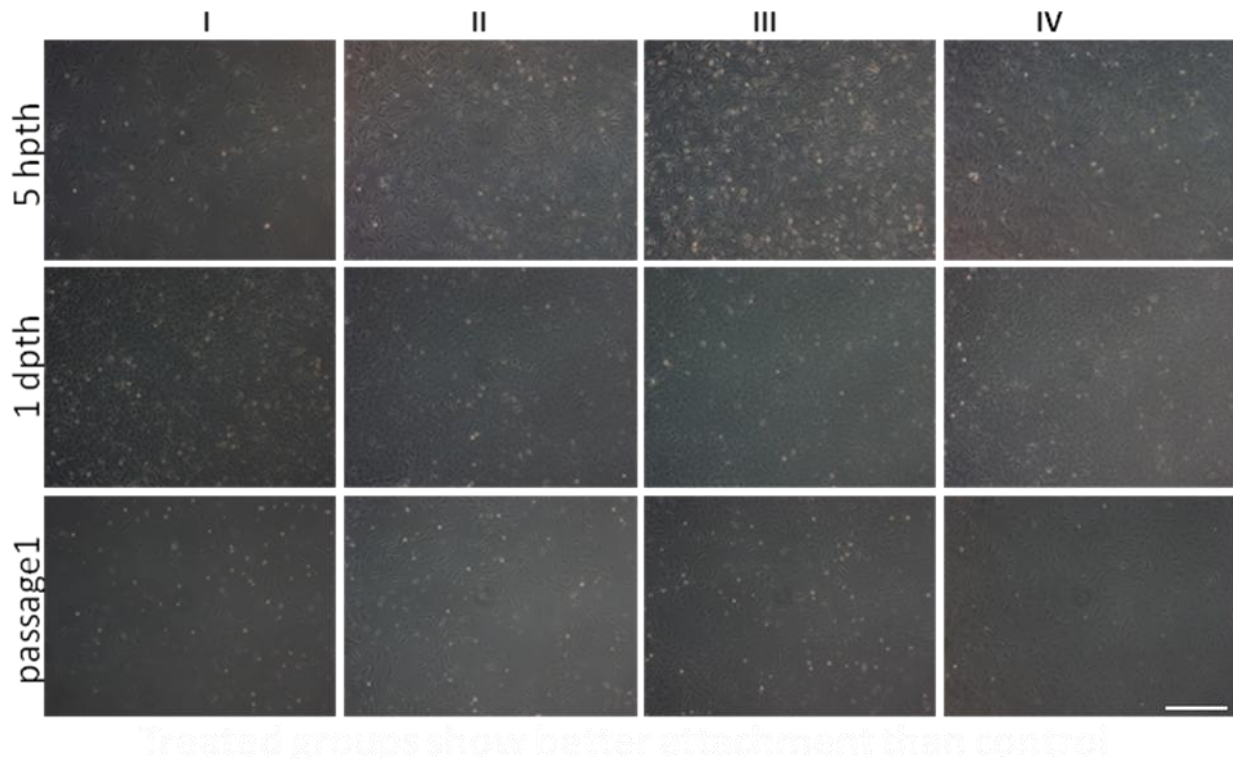


**Figure S3: Proliferation efficiency of medaka haploid ES cells after cryopreservation.** Phase contrast images of medaka haploid ES cells. Group I is (untreated) control and Y-27632 (10  $\mu$ M) in pretreatment for 24h before freezing (group II), freezing medium (group III), post thawing medium (group IV). Treated groups show better attachment than control group at 5hpth (hour post thawing). The difference in cell attachment was even obvious after a passage. Scale bars 100  $\mu$ m.

#### 4. Clonal expansion of medaka hES cells

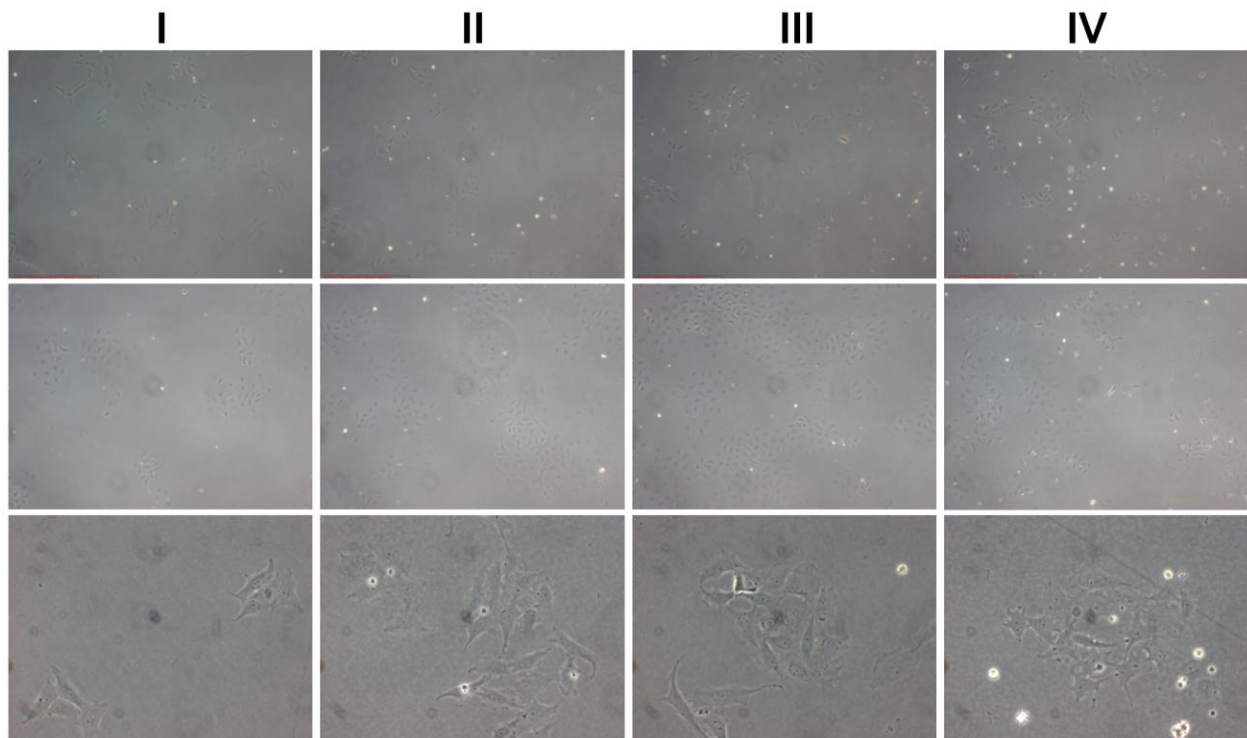


**Figure S4. Clonal expansion of cryopreserved medaka hES cells.** Phase contrast images of recovered cells seeded for colony formation in 10 cm dish. Colonies were formed after 5-6 dpc. Group I: (untreated) control, Group II: pretreatment with Y-27632 (10  $\mu$ m) for 24 h before freezing, Group III: Y-27632 (10  $\mu$ m) in freezing medium, Group IV: Y-27632 (10  $\mu$ m) in post thawing medium. Colonies in treated groups are larger than the colonies in untreated control group and the expansion speed is also higher than untreated group.

## 5. Effect of Y-27632 and apoptosis inhibitors on PGC culture

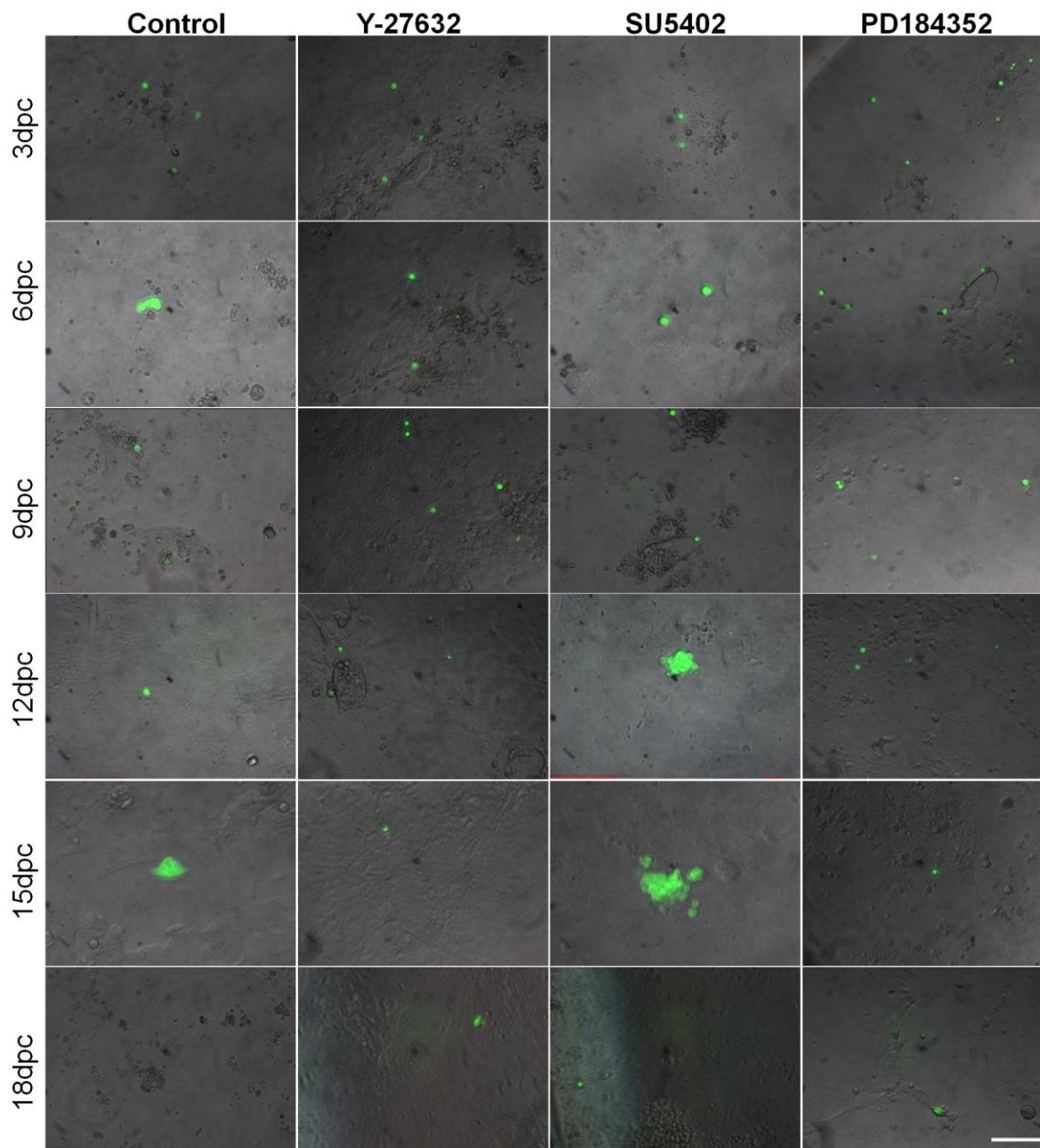


**Figure S5. Phase contrast images of PGCs.** Y-27632 (ROCK inhibitor), SU5402 (FGFR inhibitor) and PD184352 (MEK inhibitor) and control. PGCs are identified by their GFP (green fluorescent protein) expression, round and larger size than somatic non-fluorescent cells. PGCs are attached to somatic cells. There was increase in the number of PGCs in inhibitor treated blastula embryonic cell cultures than control. The difference is obvious during initial 9 days (All the time points are shown). Scale bar 100  $\mu$ m.

## 6. Effect of Y-27632 and other apoptosis inhibitors on PGC culture

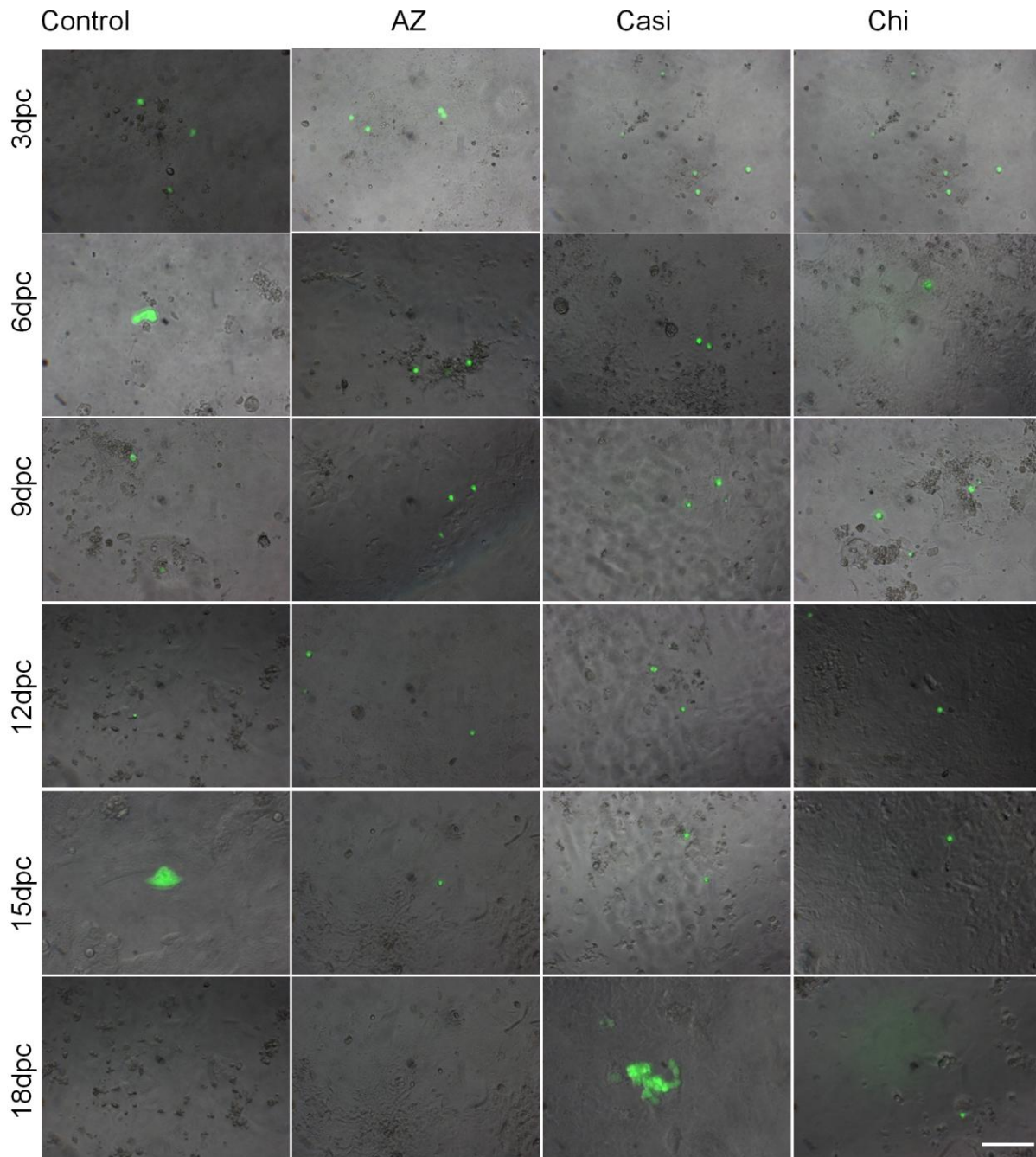


**Figure S6. Phase contrast images of PGCs.** AZ (GSK3 inhibitor), Casi (Caspase inhibitor) and Chi (Cyclopamine Hedgehog inhibitor) and control. PGCs are identified by their GFP expression, round and bigger than non-fluorescent somatic cells. PGCs are attached to somatic cells. There was increase in the number of PGCs in inhibitor treated blastula cell cultures than control. The difference is obvious during initial 9 days. Scale bar 100  $\mu$ m

## 7. Effect of Y-27632 and other apoptosis inhibitors on PGC culture

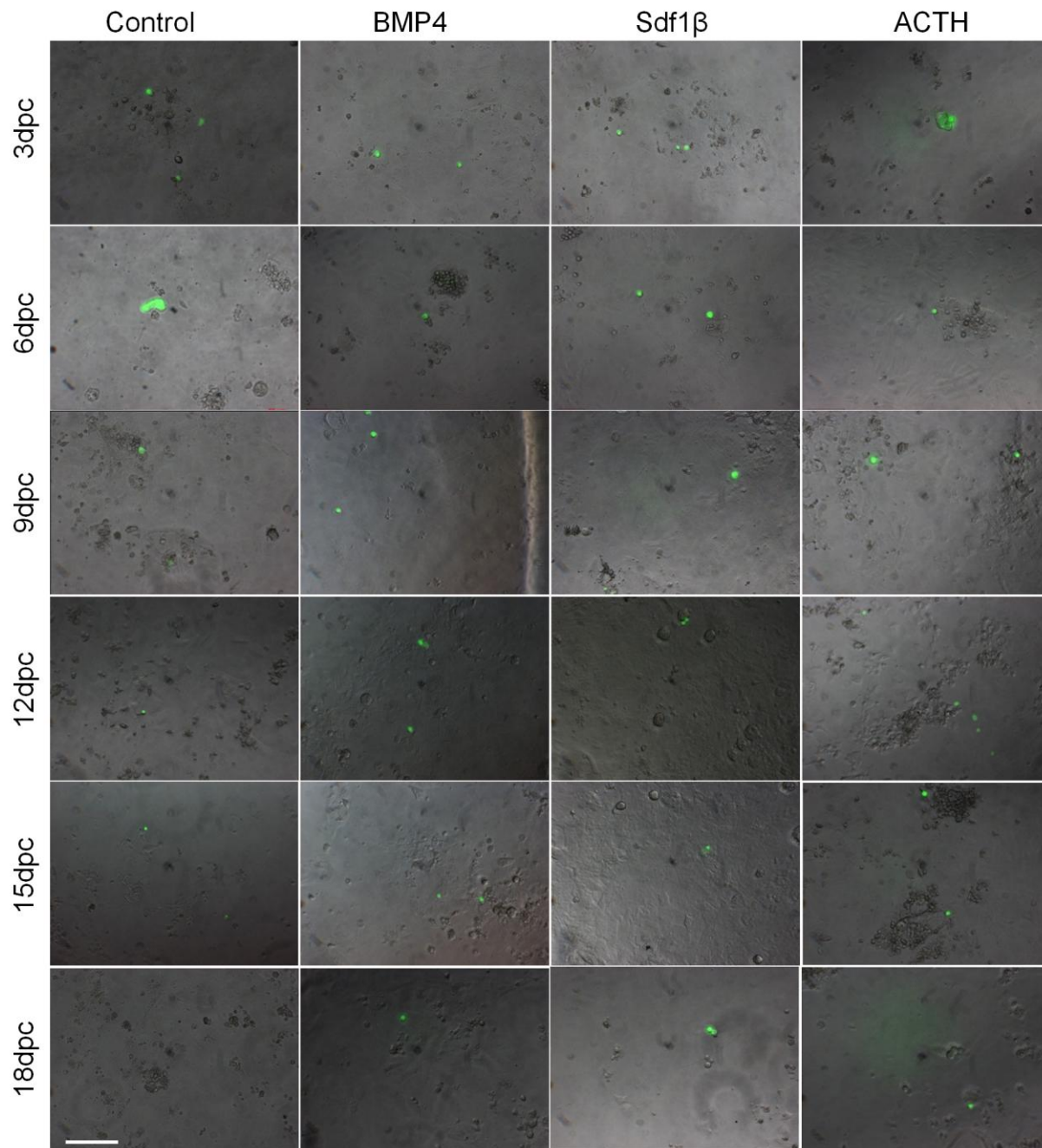


**Figure S7. Phase contrast images of PGCs.** BMP4 (Bone Morphogenetic Protein 4), Sdf1 $\beta$  (Stromal derived factor 1  $\beta$ ), ACTH (Adrenocorticotrophic hormone) together with control. PGCs are identified by their GFP expression, round and bigger than somatic non-fluorescent cells. PGCs are attached to somatic cells. There was increase in the number of PGCs in treated blastula cultures than in control. The difference is obvious during initial 9 days. Scale bar 100  $\mu$ m

## 8. Effect of Y-27632 with other apoptosis inhibitors on PGC culture

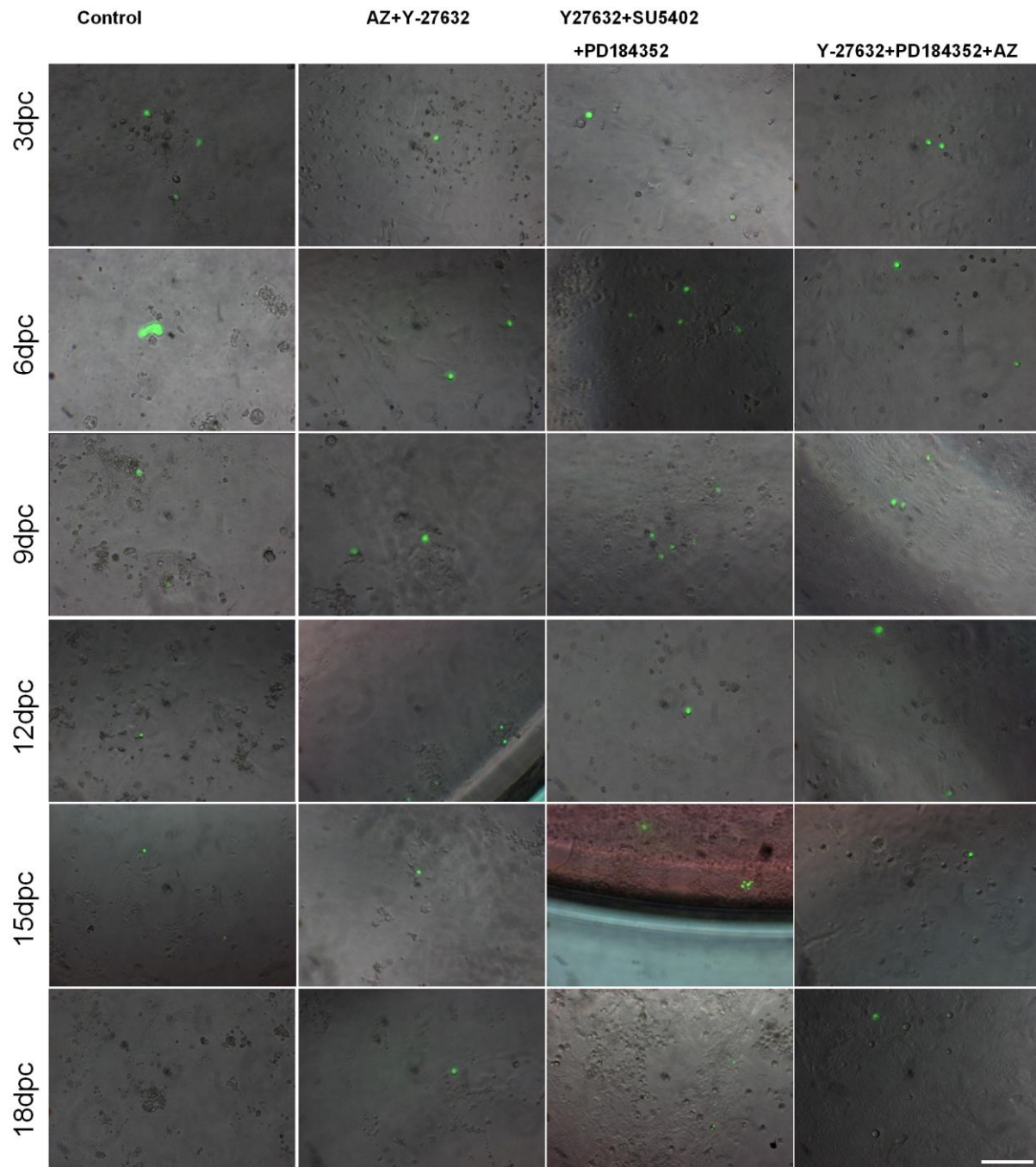


**Figure S8. Phase contrast images of PGCs.** Effect of Y-27632 with other apoptotic inhibitors on PGC culture are shown at different time points. Combinations of the inhibitors used are AZ+Y-27632, Y-27632+SU5402+PD184352, Y-27632+PD184352+AZ. PGCs are identified by their GFP expression, round and bigger size than somatic non-fluorescent cells. PGCs are attached to somatic cells. There was increase in the number of PGCs in inhibitor treated blastula embryonic cells than in control. The difference is obvious during initial 9 days. Scale bar 100  $\mu$ m.



## 9. Effect of Y-27632 other apoptosis inhibitors on PGC culture

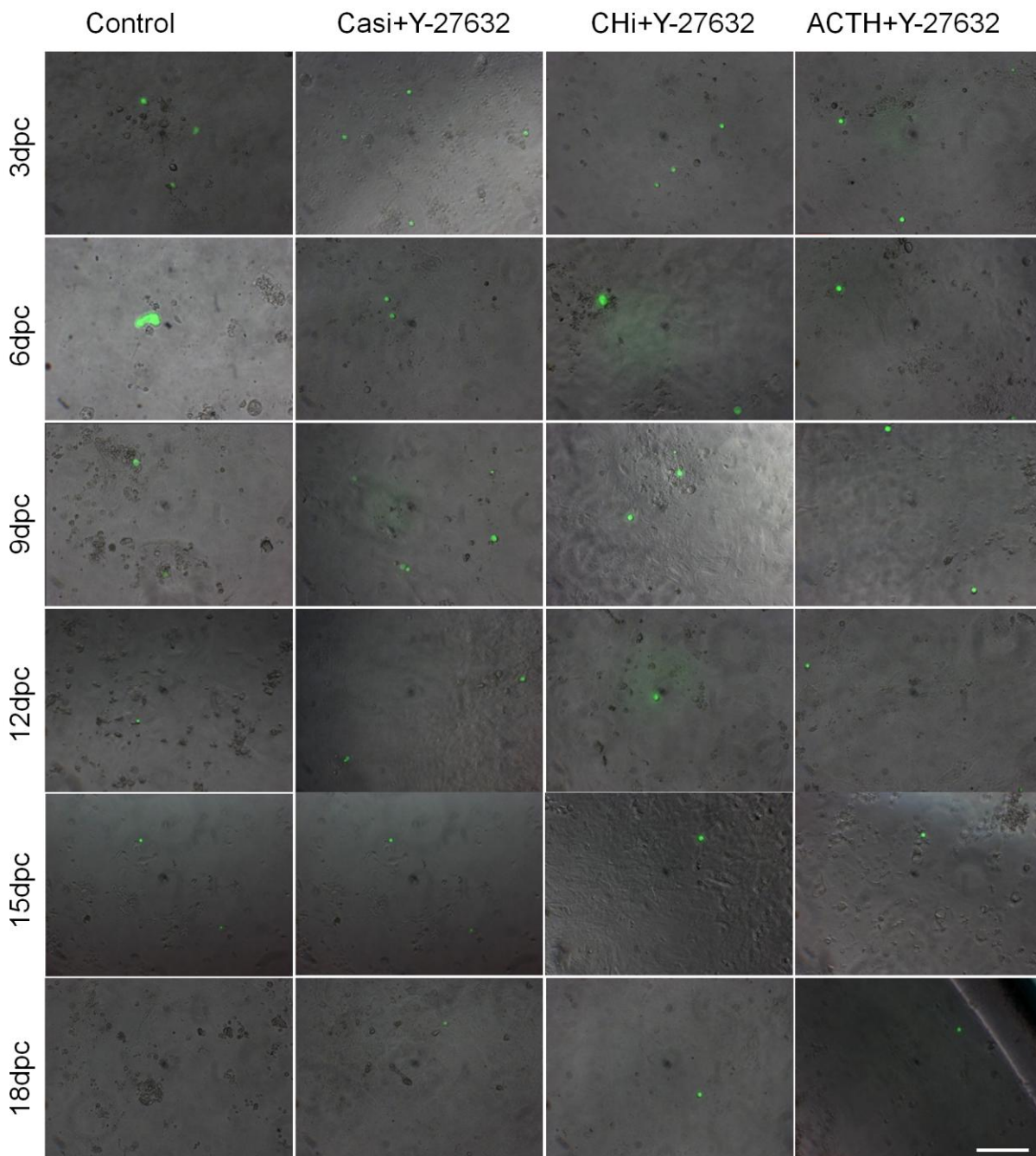


**Figure S9. Phase contrast images of PGCs.** Effects of ROCK inhibitor other apoptotic inhibitors on PGC culture are shown at different time points. Combinations are; Casi+Y-27632, CHi+Y-27632, ACTH+Y-27632. PGCs are identified by their GFP expression, round and bigger size than somatic non-fluorescent cells. PGCs are attached to somatic cells. There was increase in the number of PGCs in inhibitor treated blastula embryonic cells than in control. The difference is obvious during initial 9 days. Scale bar 100  $\mu$ m.

## 10. Effect of Y-27632 and growth factors on PGC culture

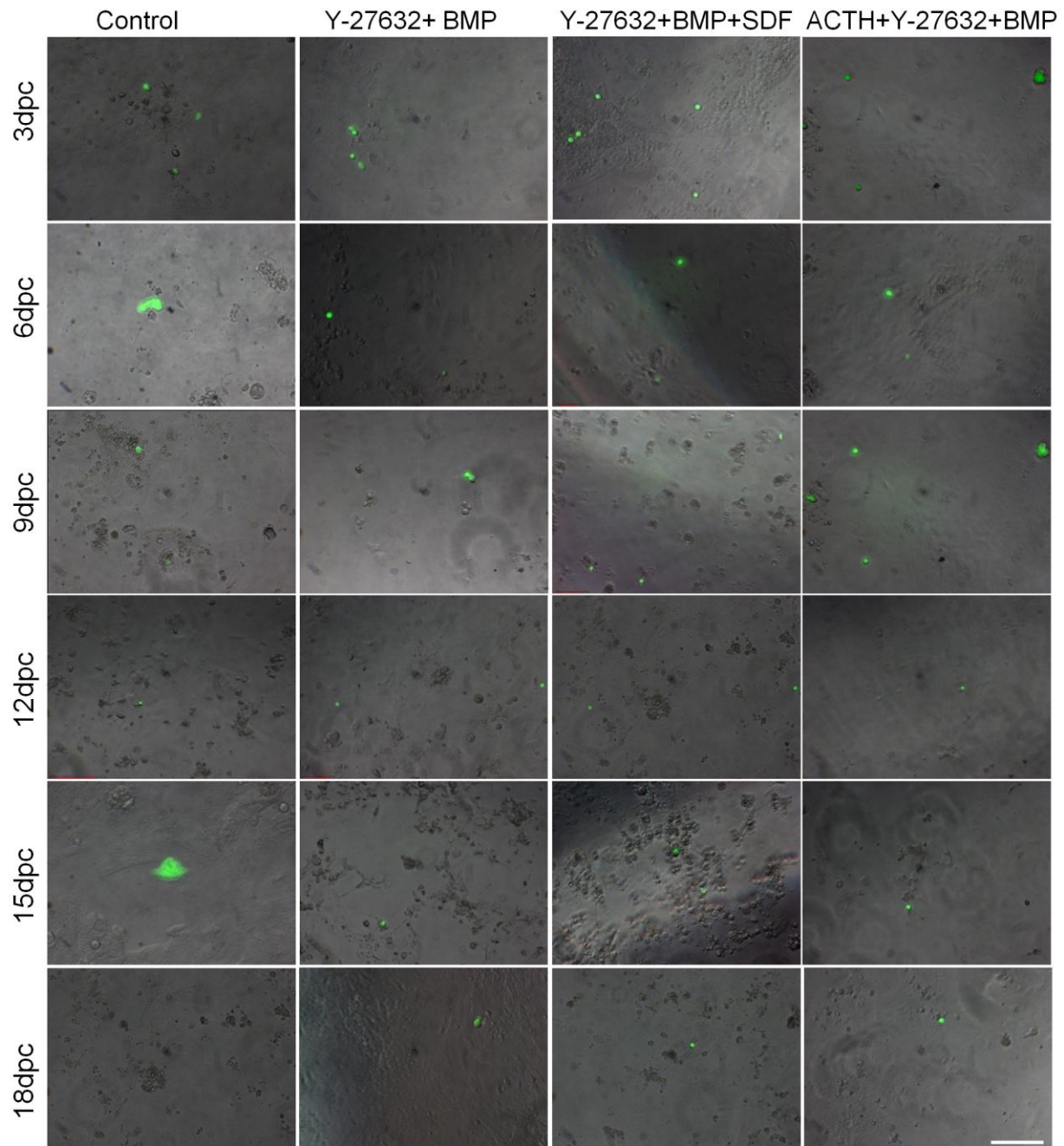


**Figure S10. Phase contrast images of PGCs.** Effect of Y-27632 with growth factors on PGC culture. Combinations are Y-27632+BMP4, Y-27632+BMP4+Sdf1 $\beta$ , ACTH+Y-27632+BMP4. PGCs are identified by their GFP expression, round and larger size than somatic non-fluorescent cells. PGCs are attached to somatic cells. There was increase in the number of PGCs in inhibitor treated cell culture than in control. The difference is obvious during initial 9 days (all time points are shown). Scale bar 100  $\mu$ m

## 11. NCBI links of proteins used for homology and phylogenetic analysis

### Boule

*Homo sapiens*: <https://www.ncbi.nlm.nih.gov/protein/EAW70173>

*Oryzias latipes*: [https://www.ncbi.nlm.nih.gov/protein/NP\\_001157989.1](https://www.ncbi.nlm.nih.gov/protein/NP_001157989.1)

*Bos taurus*: <https://www.ncbi.nlm.nih.gov/protein/ABS89140>

*Drosophila melanogaster*: [https://www.ncbi.nlm.nih.gov/protein/NP\\_729457.1](https://www.ncbi.nlm.nih.gov/protein/NP_729457.1)

*Mus musculus*: [https://www.ncbi.nlm.nih.gov/protein/NP\\_083543](https://www.ncbi.nlm.nih.gov/protein/NP_083543)

*Ornithorhynchus anatinus*: [https://www.ncbi.nlm.nih.gov/protein/XP\\_001512796.1](https://www.ncbi.nlm.nih.gov/protein/XP_001512796.1)

*Oncorhynchus mykiss*: <https://www.ncbi.nlm.nih.gov/protein/ADW41783>

*Gallus gallus*: [https://www.ncbi.nlm.nih.gov/protein/XP\\_421917.4](https://www.ncbi.nlm.nih.gov/protein/XP_421917.4)

### Dazl

*Carassius gibelio*: <https://www.ncbi.nlm.nih.gov/protein/225580744>

*Danio rerio*: <https://www.ncbi.nlm.nih.gov/protein/CAK04305.1?report=genpept>

*Oncorhynchus mykiss*: <https://www.ncbi.nlm.nih.gov/protein/ADW41782>

*Oryzias latipes*: <https://www.ncbi.nlm.nih.gov/protein/AAX94053>

*Homo sapiens*: [https://www.ncbi.nlm.nih.gov/protein/NP\\_001342](https://www.ncbi.nlm.nih.gov/protein/NP_001342)

*Mus musculus*: [https://www.ncbi.nlm.nih.gov/protein/NP\\_034151](https://www.ncbi.nlm.nih.gov/protein/NP_034151)

*Gallus gallus*: [https://www.ncbi.nlm.nih.gov/protein/NP\\_989549.1](https://www.ncbi.nlm.nih.gov/protein/NP_989549.1)

### Vasa

*Oncorhynchus mykiss*: [https://www.ncbi.nlm.nih.gov/protein/NP\\_001117665](https://www.ncbi.nlm.nih.gov/protein/NP_001117665)

*Oryzias latipes*: [https://www.ncbi.nlm.nih.gov/protein/NP\\_001098146](https://www.ncbi.nlm.nih.gov/protein/NP_001098146)

*Danio rerio*: <https://www.ncbi.nlm.nih.gov/protein/AAI29276>

*Gallus gallus*: <https://www.ncbi.nlm.nih.gov/protein/BAB12337>

*Bos Taurus*: <https://www.ncbi.nlm.nih.gov/protein/AFU08144>

*Homo sapiens*: <https://www.ncbi.nlm.nih.gov/protein/Q9NQI0>

*Mus musculus*: <https://www.ncbi.nlm.nih.gov/protein/Q61496>